

UNIVERSITI TEKNOLOGI MALAYSIA

BORANG PENGESAHAN  
LAPORAN AKHIR PENYELIDIKAN

TAJUK PROJEK : **THE STUDY ON THE DEVELOPMENT OF SATURATION  
PROFILE IN SOIL** \_\_\_\_\_

Saya     **NURLY GOFAR**    

Mengaku membenarkan **Laporan Akhir Penyelidikan** ini disimpan di Perpustakaan Universiti Teknologi Malaysia dengan syarat-syarat kegunaan seperti berikut :

1. Laporan Akhir Penyelidikan ini adalah hakmilik Universiti Teknologi Malaysia.
2. Perpustakaan Universiti Teknologi Malaysia dibenarkan membuat salinan untuk tujuan rujukan sahaja.
3. Perpustakaan dibenarkan membuat penjualan salinan Laporan Akhir Penyelidikan ini bagi kategori TIDAK TERHAD.
4. \* Sila tandakan (✓)

SULIT

(Mengandungi maklumat yang berdarjah keselamatan atau Kepentingan Malaysia seperti yang termaktub di dalam AKTA RAHSIA RASMI 1972).

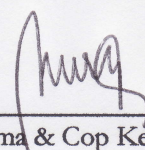
TERHAD

(Mengandungi maklumat TERHAD yang telah ditentukan oleh Organisasi/badan di mana penyelidikan dijalankan).

TIDAK  
TERHAD

TANDATANGAN KETUA PENYELIDIK

**DR. NURLY GOFAR**  
Associate Professor (DS53)  
Department of Geotechnics & Transportation  
Faculty of Civil Engineering  
Universiti Teknologi Malaysia

  
\_\_\_\_\_  
Nama & Cop Ketua Penyelidik

Tarikh : 30 NOVEMBER 2009

**CATATAN :** \* Jika Laporan Akhir Penyelidikan ini SULIT atau TERHAD, sila lampirkan surat daripada pihak berkuasa/organisasi berkenaan dengan menyatakan sekali sebab dan tempoh laporan ini perlu dikelaskan sebagai SULIT dan TERHAD.

**THE STUDY ON THE DEVELOPMENT OF SATURATION PROFILE IN  
SOIL**

**(KAJIAN MENGENAI PERKEMBANGAN PROFIL KETEPUAN DALAM  
TANAH)**

**NURLY GOFAR  
KHAIRUL ANUAR KASSIM  
AZMAN KASSIM  
LEE MIN LEE**

**FAKULTI KEJURUTERAAN AWAM  
UNIVERSITI TEKNOLOGI MALAYSIA**

**2009**

## **ACKNOWLEDGEMENT**

First and foremost, our sincere gratitude goes to Universiti Teknologi Malaysia for funding the research through Fundamental Research Grant Scheme (FRGS) Vot 78239. This research would not be accomplished without the financial aids provided.

The research was shaped through interaction with many academicians. For this, we are deeply grateful to Professor Dr. Harianto Rahardjo, Dr. David Toll, Professor Dr. Roslan Zainal Abidin, Professor Dr. Faisal Ali, Professor Dr. Mohd Amin Mohd Sam, and Mr. Low Tian Huat for sharing their valuable experiences.

We extend our gratitude to all the technical staffs of Department of Geotechnics and Transportation, Faculty of Civil Engineering, for their assistance in laboratory and field works. In particular, we thank fellow Master and Undergraduate students include Mohamed Elbyhagi, Wisam, Maiziz, Amir, Sim Kay Huei, Tan She Hooi, Yang Eik Hien, Elango, and Nadasan, for their involvement in part of this research. Besides, we sincerely appreciate the help of staffs of Research Management Center (RMC) in making this research a success.

## ABSTRACT

This study was carried out to investigate the mechanisms involved in the development of saturation profiles in soil. A series of numerical simulations and laboratory tests were conducted to monitor the saturation profiles in four types of soil under various rainfall conditions. In addition, two sloping sites were monitored for a period of one year to provide field verification for the findings. The understanding in saturation profile is essential to predict the shear strength of soil, particularly for slope stability problem. The study showed that the saturation profile in soil is greatly affected by the soil permeability and rainfall pattern. The effect of rainfall pattern on the saturation profile of high permeable soil is relatively insignificant. Conversely, the saturation profile in less permeable soil could be significantly altered when the soil is subjected to a prolonged rainfall. A chart is developed in the present study to determine the critical rainfall duration and intensity, as well as the resultant minimum suction value. The analysis result from the developed chart show good agreement with the field monitoring data. It is believed that the findings from the present study could lead to a better understanding of saturation profile in soil, and subsequently contribute efforts in mitigating rainfall-induced slope failure.

## ABSTRAK

Kajian ini dijalankan untuk mengkaji mekanisme yang terlibat dalam perkembangan profil ketepuan dalam tanah. Satu siri simulasi numerikal dan ujian makmal telah dijalankan untuk memantau profil ketepuan empat jenis tanah dalam pelbagai keadaan hujan. Selain itu, dua cerun di tapak telah dimantau selama setahun untuk memberi pembuktian di tapak. Kefahaman dalam profil ketepuan adalah penting untuk meramal kekuatan tanah terutamanya bagi masalah kestabilan cerun. Kajian ini menunjukkan profil ketepuan tanah amat dipengaruhi oleh ketelapan tanah dan corak hujan. Kesan corak hujan terhadap profil ketepuan tanah yang berketelapan tinggi adalah kurang nyata. Sebaliknya, profil ketepuan dalam tanah yang berketelapan rendah berubah dengan banyak apabila tanah terdedah kepada hujan yang berpanjangan. Satu carta telah dihasilkan dalam kajian ini untuk menentukan tempoh dan keamatan hujan kritikal, dan juga nilai *suction* minimum yang terhasil. Hasil analisis daripada carta tersebut menunjukkan kesamaan dengan data pemantauan tapak. Adalah diharapkan bahawa penemuan daripada kajian ini dapat memberi kefahaman yang lebih mendalam mengenai profil ketepuan tanah, dan seterusnya memberi sumbangan dalam pencegahan tanah runtuh akibat hujan.

## TABLE OF CONTENTS

<b>CHAPTER</b>	<b>TITLE</b>	<b>PAGE</b>
	<b>TITLE OF PROJECT</b>	i
	<b>ACKNOWLEDGEMENT</b>	ii
	<b>ABSTRACT</b>	iii
	<b>ABSTRAK</b>	iv
	<b>TABLE OF CONTENTS</b>	v
	<b>LIST OF TABLES</b>	ix
	<b>LIST OF FIGURES</b>	x
	<b>LIST OF SYMBOLS</b>	xiv
	<b>LIST OF APPENDICES</b>	xvi
<b>1</b>	<b>INTRODUCTION</b>	1
	1.1 Background of the Study	1
	1.2 Objectives	3
	1.3 Scope of the Study	4
	1.4 Significance of the Study	5
<b>2</b>	<b>LITERATURE REVIEW</b>	6
	2.1 Introduction	6
	2.2 Hydraulic Properties of Soil	6
	2.2.1 Soil Water Characteristic Curve (SWCC)	7
	2.2.2 Hydraulic Conductivity Function	8
	2.3 Rainfall Infiltration Model	10
	2.4 Wetting Front and Redistribution	13
	2.5 Correlation between Rainfall Pattern, Soil Suction and Slope Stability	16
	2.5.1 The Role of Suction on Shear Strength and	17

	Stability of Unsaturated Soil Slope	
	2.5.1.1 Shear Strength of Unsaturated Soil	17
	2.5.1.2 Stability Analysis of Unsaturated Soil	20
	Slope	
	2.5.2 Effect of Rainfall Pattern on Suction	22
	Distribution and Slope Stability	
2.6	Soil Column for Infiltration Analysis	25
2.7	Numerical Simulation for Seepage and Slope Stability	28
	Analyses	
2.8	Concluding Remarks	31
<b>3</b>	<b>METHODOLOGY</b>	<b>33</b>
3.1	Introduction	33
3.2	Statistical Analysis of Extreme Rainfall	35
3.3	Numerical Simulation	38
	3.3.1 Geometry of the slope	38
	3.3.2 Finite Element Mesh Design	39
	3.3.3 Slope Stability Analysis Approach	42
	3.3.4 Numerical Simulation Design	43
	3.3.4.1 Parametric Study	43
	3.3.4.2 Critical Rainfall Pattern Analysis	44
3.4	Laboratory Soil Column Tests	48
	3.4.1 Soil Column	50
	3.4.2 Water Flow System	50
	3.4.3 Instrumentations	53
	3.4.4 Data Acquisition System	55
	3.4.5 Experimental Design	57
3.5	Field Study	58
	3.5.1 Instrumentations	60

	3.5.1.1 Installation of Tensiometers	61
	3.5.1.2 Installation of Rain Gauge	62
	3.5.1.3 Installation and Calibration of Runoff Collector	62
	3.5.2 Field Monitoring	65
3.6	Concluding Remarks	65
<b>4</b>	<b>PRELIMINARY DATA</b>	66
4.1	Introduction	66
4.2	Extreme Rainfall Distribution	66
	4.2.1 Assumption of Surface Runoff	68
4.3	Soil Properties	70
4.4	Concluding Remarks	77
<b>5</b>	<b>RESULTS AND DISCUSSIONS</b>	78
5.1	Introduction	78
5.2	Numerical Simulations	78
	5.2.1 Parametric Study	79
	5.2.1.1 Influence of Initial Condition on Suction Distribution	79
	5.2.1.2 Influence of Rainfall Intensity on Suction Distribution	84
	5.2.1.3 Influence of Rainfall Duration on Suction Distribution	86
	5.2.1.4 Influence of Slope Inclination on Suction Distribution	89
	5.2.2 Critical Rainfall Pattern Analysis	92
5.3	Laboratory Soil Column Tests	100
	5.3.1 Initial Condition of Soil Column Tests	100

	5.3.2	Relationships between Infiltration and Runoff	101
	5.3.3	Saturation Profiles	104
	5.3.4	Suction Redistributions	107
	5.4	Field Study	108
	5.4.1	Overall Trend of Suction Distributions	109
	5.4.2	Response of Suction Distribution to Single Rainfall Pattern	112
	5.5	Concluding Remarks	117
<b>6</b>		<b>CONCLUSIONS AND SUGGESTIONS</b>	121
	6.1	Introduction	121
	6.2	Conclusions	121
	6.2.1	Extreme Rainfall Characteristics for the Malaysian Peninsular	122
	6.2.2	Relationships between Rainfall, Runoff and Infiltration Rate	122
	6.2.3	Effect of Soil Permeability on Suction Distribution and Redistribution	123
	6.2.4	A Chart for Preliminary Evaluation of Rainfall-Induced Slope Instability	124
	6.3	Suggestions for Future Researches	124
		<b>REFERENCES</b>	126
		Appendix A-D	136-175
		List of Related Publications	176

**LIST OF TABLES**

<b>TABLE NO.</b>	<b>TITLE</b>	<b>PAGE</b>
3.1	Experimental design for infiltration tests	58
4.1	Ten-year return period extreme rainfalls for five selected locations in the Malaysian Peninsular	67
4.2	Rainfall and runoff data recorded from July 2007 to August 2007	69
4.3	Physical properties of soils used in the study	72
4.4	Mineral constituents obtained from XRD test	74
4.5	Mineral compositions obtained from mineralogy test	74
4.6	SWCC parameters of soils used in the study	76
5.1	Critical duration of antecedent rainfall for different locations and depths of slip plane	99
5.2	Contrasting responses of suction distribution to rainfall infiltration for a coarse-grained soil slope and a fine-grained soil slope	117

## LIST OF FIGURES

FIGURE NO.	TITLE	PAGE
2.1	Typical absorption and desorption SWCC (Zhan and Ng, 2004)	7
2.2	Typical suction-dependent hydraulic conductivity function	9
2.3	Relationship between rainfall and infiltration	12
2.4	Development of wetting front	14
2.5	Volumetric water content and suction in the development of wetting front	15
2.6	Redistribution of soil moisture for (a) $L_f < L_{cr}$ and (b) $L_f > L_{cr}$	16
2.7	Unsaturated soil strength properties	20
2.8	Soil element of typical infinite unsaturated soil slope	21
2.9	Schematic diagram of soil column developed by Yang <i>et al.</i> (2004)	27
3.1	Research framework	34
3.2	Five selected locations in the Malaysian Peninsular	36
3.3	Geometry of the infinite slope for numerical simulation	39
3.4	Element meshes and boundary conditions of the numerical model	41
3.5	Techniques used to assign slip surface plane parallel to ground surface	42

3.6	Parametric study design for various initial conditions	45
3.7	Parametric study design for various rainfall intensities	46
3.8	Parametric study design for various rainfall durations	46
3.9	Parametric study design for various slope inclinations	47
3.10	Simulation scheme for determining critical antecedent rainfall	48
3.11	Three-dimensional diagram of the laboratory model setup Photograph of the laboratory model setup	49
3.12	Components of the soil column model	49
3.13	(a) An assembled tensiometer-transducer, (b) Gypsum block	51
3.14	Cross-sectional view of the tensiometer connector	53
3.15	(a) Photograph, (b) Three-dimensional diagram, and (c) Cross-sectional view of the gypsum block connector	54
3.16	(a) Photograph, (b) Three-dimensional diagram, and (c) Cross-sectional view of the gypsum block connector	55
3.17	Data acquisition system	57
3.18	Location map of the study areas	59
3.19	Contours of study areas: (a) Balai Cerapan (b) Kolej 12	60
3.20	Photographs of study areas: (a) Balai Cerapan (b) Kolej 12	60
3.21	Runoff collector installed at research plot	64
3.22	Dimensions and components of runoff collector	64
4.1	IDF curves for five selected locations in the Malaysian Peninsular	67
4.2	Output of non-linear regression analysis for the relationship between rainfall and runoff	70

4.3	Particle size distribution of soils used in the study	71
4.4	SEM images of (a) sand-gravel, (b) silty gravel, (c) sandy silt, and (d) silt (kaolin)	73
4.5	SWCC of soils used in the study	75
4.6	Hydraulic Conductivity function predicted by Van Genuchten's method (1980)	76
5.1	Influence of initial condition on suction distribution as the result of short and intense rainfall for (a) sand-gravel, (b) silty gravel, (c) sandy silt, and (d) silt (kaolin)	80
5.2	Influence of initial condition on suction distribution as the result of prolonged rainfall for (a) sand-gravel, (b) silty gravel, (c) sandy silt, and (d) silt (kaolin)	81
5.3	Drying paths of suction for (a) sand-gravel, (b) silty gravel, (c) sandy silt, and (d) silt (kaolin)	82
5.4	Estimation of initial condition from SWCC	83
5.5	Initial conditions for the four types of soil	84
5.6	Influence of rainfall intensity on the suction distribution for (a) sand-gravel, (b) silty gravel, (c) sandy silt, and (d) silt (kaolin)	85
5.7	Influence of rainfall duration on suction distribution for (a) sand-gravel, (b) silty gravel, (c) sandy silt, and (d) silt (kaolin)	87
5.8	An idealized infiltration model	88
5.9	Influence of slope inclination on suction distribution as the result of short and intense rainfall for (a) sand-gravel, (b) silty gravel, (c) sandy silt, and (d) silt (kaolin)	90
5.10	Influence of slope inclination on suction distribution as the result of long and less intense rainfall for (a) sand-gravel, (b) silty gravel, (c) sandy silt, and (d) silt (kaolin)	91

5.11	Rainfall infiltration components on a sloping surface	92
5.12	Suction distributions as the result of various extreme antecedent rainfalls for (a) sand-gravel, (b) silty gravel, (c) sandy silt, and (d) silt (kaolin)	93
5.13	Variation in factor of safety as the result of various extreme antecedent rainfalls at the slip planes of (a) 1m, (b) 3m, and (c) 5m depth	94
5.14	Proposed chart to predict critical antecedent rainfall and critical suction value of a soil slope	98
5.15	The setup of soil column models for (a) sand-gravel, (b) silty gravel, (c) sandy silt, and (d) silt (kaolin)	101
5.16	Relationships between rainfall and surface runoff for (a) silty gravel, (b) sandy silt, and (c) silt (kaolin)	102
5.17	Cracks formed at the surface of silt (kaolin)	103
5.18	Saturation profiles in (a) sand-gravel, (b) silty gravel, (c) sandy silt, and (d) silt (kaolin)	105
5.19	Suction redistributions in (a) sand-gravel, (b) silty gravel, (c) sandy silt, and (d) silt (kaolin)	108
5.20	Rainfall and suction distributions monitored for 12 months at Balai Cerapan site	110
5.21	Rainfall and suction distributions monitored for 12 months at Kolej 12 site	111
5.22	Suction distributions as the result of (a) Rainfall pattern A, (b) Rainfall pattern B, and (c) Rainfall pattern C at Balai Cerapan site	114
5.23	Suction distributions as the result of (a) Rainfall pattern D, and (b) Rainfall pattern E at Kolej 12 site	116

## LIST OF SYMBOLS

$A_{ev}$	-	Air entry value
$c'$	-	Effective cohesion
$h$	-	Hydraulic head
$I$	-	Rainfall intensity
$I_{cr}$	-	Critical rainfall intensity
$k$	-	Water coefficient of permeability
$k_{sat}$	-	Saturated permeability
$L_a$	-	Wetting front depth as the result of antecedent rainfall
$L_{cr}$	-	Critical wetting front depth
$L_f$	-	Wetting front depth
$m_w$	-	Slope of soil water characteristic curve (SWCC)
$P$	-	Rainfall amount
$q$	-	Rainfall unit flux
$Q$	-	Rainfall total flux
$R$	-	Rainfall return period
$R_f$	-	Surface Runoff
${}^R I_t$	-	Average rainfall intensity for a particular return period
$S_r$	-	Degree of saturation
$S_x$	-	Standard deviation of annual maximum rainfall intensities
$t$	-	Time
$t_p$	-	Time when surface runoff start to occur
$u_a$	-	Pore-air pressure
$u_w$	-	Pore-water pressure
$(u_a - u_w)$	-	Matric suction

$W$	-	Total weight of soil
$W_{ev}$	-	Water entry value
$X$	-	Extreme rainfall intensity for a particular rainfall duration
$\bar{X}$	-	Mean of annual maximum rainfall intensities
$Y$	-	Gumbel's reduced variate
$\bar{Y}$	-	Mean of Gumbel's reduced variates
$z$	-	Elevation head
$\beta$	-	Slope inclination angle
$\chi$	-	Parameter related to the soil degree of saturation
$\phi'$	-	Effective friction angle
$\phi^b$	-	Unsaturated friction angle
$\gamma_d$	-	Unit weight of dry soil
$\gamma_w$	-	Unit weight of water = 9.81kN/m <sup>3</sup>
$\theta$	-	Volumetric water content
$\theta_a$	-	Average volumetric water content in the wetted zone
$\theta_i$	-	Initial volumetric water content
$\theta_r$	-	Residual volumetric water content
$\theta_s$	-	Volumetric water content at saturation of desorption curve
$\theta'_s$	-	Volumetric water content at saturation of absorption curve
$\sigma$	-	Total normal stress
$\sigma'$	-	Effective normal stress
$\sigma_y$	-	Standard deviation of Gumbel's reduced variates
$\tau_f$	-	Shear stress at failure
$\psi$	-	Suction
$\psi_{min}$	-	Minimum Suction value
$\psi_T$	-	Total suction

**LIST OF APPENDICES**

<b>APPENDIX</b>	<b>TITLE</b>	<b>PAGE</b>
A	Example of Statistical Extreme Rainfall Analysis for Johor Bahru	136
	Program for CR10X Data Logger	
B	Calibration Result of Runoff Collector	147
C	Field Monitoring Data	155
D		157

## **CHAPTER 1**

### **INTRODUCTION**

#### **1.1 Background of the Study**

Rainfall-induced slope failure is one of the most severe disasters in tropical regions causing major loss of life and property. Generally, the high occurrences of the slope failures in these regions can be attributed to two major factors: intense and frequent downpours, and natural characteristics of residual soil.

Conventionally, most of the cut slopes were designed based on the assumption of saturated soil behavior. However, recent studies discovered that the design and construction of saturated soil slope cannot be applied successfully for the slopes under unsaturated conditions (Brand 1984, Fourie 1996, Raharjo et al., 2001, Tsaparas et al. 2002, and others). The increasing acceptance of unsaturated soil mechanic has highlighted the need to correlate the slope failure with rainfall and the soil behavior in order to understand the mechanism of rainfall-induced slope failures.

The correlation between rainfall and slope failures has been studied extensively over the past few decades. For example, Ng et al. (1999) performed a numerical simulation to study the effect of rainfall infiltration on suction in an unsaturated slope, hence on slope stability. They found that the responses of suction

and the groundwater table to the rainfall infiltration are mainly governed by the ratio of  $q/k_{sat}$  and  $k_{sat}/m_w$ , where  $q$  is the infiltration flux,  $k_{sat}$  is saturated permeability, and  $m_w$  is the slope of the soil water characteristic curve (SWCC), as well as the initial suctions and boundary conditions. Collins and Znidarcic (2004) did an analytical analysis to develop a methodology for predicting the depth and the relative time of failure for slopes subjected to infiltration. Extensive studies on the causation of rainfall-induced slope failures in different parts of the world have been conducted, for example by Brand et al. (1984) in Hong Kong and Rahardjo et al. (1996-2001) in Singapore. In fact, hundreds of articles written on this topic based on case studies from different geographical region have suggested different conclusions on the threshold rainfall condition for the slope failures.

The process of rainfall infiltration through soil could induce seepage problem, increase in soil moisture content, and groundwater fluctuation. As rainfall water infiltrates into the soil, it flows through the unsaturated zone of soil, until it reaches the groundwater table. Estimating the seepage path and fluctuation of groundwater table is another complex problem due to the variations in soil properties. The saturation profile is governed by several mechanisms which should be treated as an integrated problem. However, existing methods treated each mechanism separately. Most of the methods were developed based on laboratory and field test, each of them has its own limitation in term of sample size and the extent of the study area. Furthermore, most of the methods involve numbers of parameters which are difficult to estimate precisely. Even the existing software has treated the different mechanism separately, instead of taking it as an integrated problem.

Transient analysis carried out based on numerical modeling of the advancement of wetting front in soil profiles can be used to bridge the different mechanism. This research will look into each variable affecting the mechanism such as rainfall pattern, interface boundary conditions, soil types and soil properties,

and the hydraulic condition, as well as the effect of the mechanism itself on the shear strength characteristics of the soil. The ability to combine those mechanisms into a comprehensive analysis will enhance the understanding of the effect of changing in moisture content on the slope stability.

## 1.2 Objectives

The focus of this study is to model the flow of water through unsaturated soil. The study is also aimed at identifying the real mechanism of slope failure induced by rainfall; thus appropriate preventive measures can be developed. The study embarks on the following objectives:

- i. To identify the extreme rainfall characteristics for five selected locations in the Malaysian Peninsular.
- ii. To evaluate the relationship between rainfall, runoff, and infiltration rate.
- iii. To investigate the effect of soil permeability on the suction distribution and redistribution under various rainfall pattern (rainfall duration and rainfall intensity).
- iv. To produce a chart for preliminary evaluation of rainfall-induced slope failure in Peninsular Malaysia

### 1.3 Scope of the Study

The study focuses mainly on three research approaches, namely numerical simulation, laboratory modeling, and field monitoring.

The numerical simulations were performed by utilizing an imaginary infinite slope model. As such, the analysis can be regarded as one-dimensional analysis. The rainfall patterns assigned on the slope model were obtained from the extreme rainfalls in Johor Bahru. The behaviours of four types of homogeneous soil (i.e. sand-gravel, silty gravel, sandy silt, and silt) under various rainfall conditions were investigated.

The laboratory modeling was performed to provide experimental evidences for the results of numerical simulation. A soil column model was fabricated to simulate the one-dimensional model employed in the numerical simulation. Monitoring instruments with automated data acquisition system were installed on the model to allow continuous pore-water pressure measurements.

In addition, two instrumented slopes were monitored for a period of one year. The suction variation and runoff under actual field condition were measured to further verify the findings from the present study.

Due to the constraints of the experimental apparatus and research scope, the study was exposed to certain assumptions and limitations: (1) The ideal environment in the laboratory with controlled precipitation and room temperature was assumed to be representative of the actual climate condition. (2) The infiltration rate was derived from the difference between rainfall and runoff rate. Other surface losses was assumed to be negligible. (3) The study was valid for one

dimensional analysis, thus only the vertical flow was concerned. (4) The soil materials used in the numerical simulation and laboratory modeling are assumed to be homogeneous. It is believed that these limitations could be overcome through inferences of the results from multiple methodologies adopted in this study.

#### **1.4 Significance of the Study**

With regards to the importance of this research, the findings may be viewed as a coupled fundamental-application research. The benefits that would be gained from the study may include the following:

- i. Understanding of the saturation profile for different combinations of soil types, boundary conditions, and rainfall patterns.
- ii. Developing a chart for preliminary evaluation of rainfall-induced slope instability.

## **CHAPTER 2**

### **LITERATURE STUDY**

#### **2.1 Introduction**

This chapter provides the basic and clinical researches on the topic of saturation profile in soil. Considerable literatures relevant to the topic are available. Most of the literatures were directed towards determining the saturation profile under certain rainfall condition, development of wetting front, and studies on the hydraulic properties of unsaturated soils, and case studies from different parts of the world. The numerical simulations and laboratory soil column tests carried out by previous researchers are also reviewed in the latter part of this chapter.

#### **2.2 Hydraulic Properties of Soil**

The hydraulic properties of soil can be attributed to water retention characteristic (soil water characteristic curve) and water coefficient of permeability (hydraulic conductivity function).

### 2.2.1 Soil Water Characteristic Curve (SWCC)

The soil water characteristic curve (SWCC), also referred to as the soil moisture retention curve, depicts the relationship between soil water content and soil water pressure potential. A typical adsorption and desorption SWCC are shown in Figure 2.1.

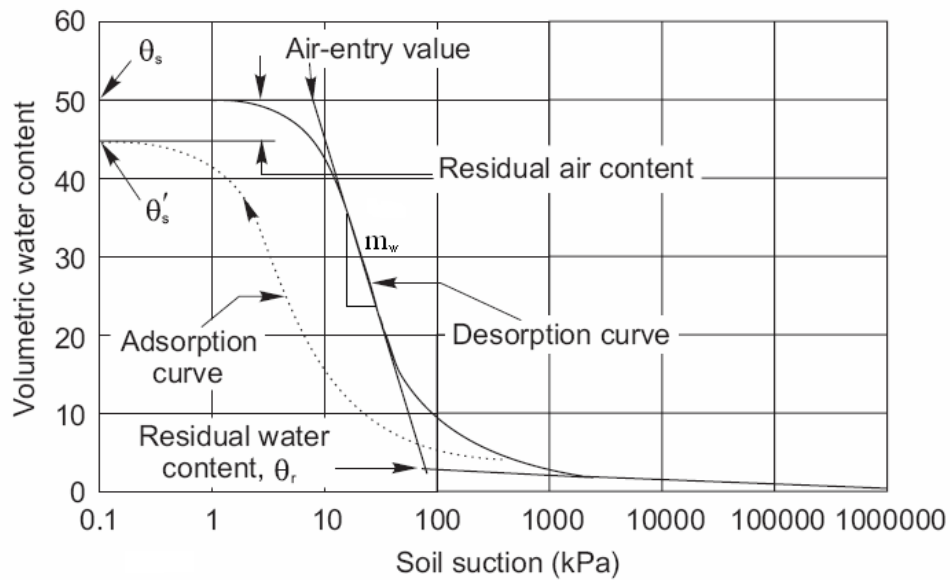


**Figure 2.1** Typical absorption and desorption SWCC (Zhan and Ng, 2004)

As observed in Figure 2.1, the volumetric water content at saturation of desorption curve ( $\theta_s$ ) is greater than that of adsorption curve ( $\theta'_s$ ). The difference between  $\theta_s$  and  $\theta'_s$ , defined as the residual air content, is caused by the entrapped air in the soil during absorption process. There are two characteristic points in a SWCC, namely air entry value ( $A_{ev}$ ) and residual water content ( $\theta_r$ ) (Zhan and Ng, 2004). The  $A_{ev}$  indicates the maximum suction required to dissipate the entrapped air from the soil. Before the suction exceeds  $A_{ev}$ , the soil is saturated or nearly saturated, hence the behaviour of the soil is similar to that of saturated soil with a compressible fluid due to the existence of occluded air bubbles. On the other end of the curve, very little water exists in the soil when the soil suction is greater than  $\theta_r$ .

The effect of water content on the behaviour of soil is thus negligible. As the result, the soil at these two unsaturated stages is not the main concern for the behaviour of unsaturated soil (Bao *et al.*, 1998). What is of greater concern is the SWCC between  $A_{ev}$  and  $\theta_r$ , in which both air and water phases are continuous or partially continuous, and the soil properties are strongly related to its water content or negative pore-water pressure (Zhan and Ng, 2004). The rate of changes in negative pore-water pressure corresponding to volumetric water content is represented by the slope of SWCC ( $m_w$ ).

A wide-array of methods can be used to obtain the SWCC, depending on the desired path (absorption or desorption) and the range of matric suction. Laboratory SWCC test can be conducted by using pressure plate test (for suction less than 1500 kPa), salt solution method (for suction greater than 1500 kPa), and capillary rise open tube method (for absorption SWCC), while field SWCC can be obtained by taking the field measurements of water content and suction by moisture probe and tensiometer, simultaneously. Alternatively, the SWCC can be predicted by using empirical relationships, as proposed by several researchers included Fredlund and Xing (1994), Agus *et al.* (2001) and Gitirana and Fredlund (2004).

### **2.2.2 Hydraulic Conductivity Function**

The water coefficient of permeability ( $k$ ) represents the soil's ability to transmit and drain water. This, in turn, indicates the ability of the soil to change matric suction as a result of environmental changes (Fredlund and Rahardjo, 1993). Water coefficient of permeability of saturated soil is a function of void ratio ( $e$ ) only. For unsaturated soil, the water coefficient of permeability is a function of void ratio ( $e$ ) and volumetric water content ( $\theta$ ). This relationship is commonly expressed by a

suction-dependent hydraulic conductivity function, as illustrated in Figure 2.2.

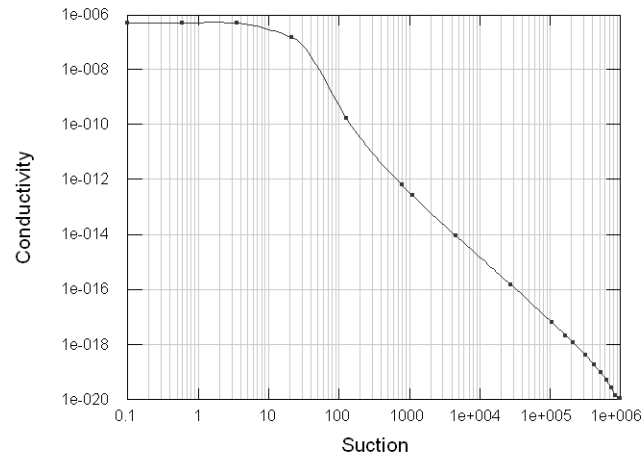


**Figure 2.2** Typical suction-dependent hydraulic conductivity function

The hydraulic conductivity function of unsaturated soil can be obtained through direct or indirect measurement. The direct measurement of unsaturated flow behaviour that commonly conducted by using Instantaneous Profile Method (IPM) is not encouraged in practice since the test requires elaborate equipment and qualified personnel, which proves time consuming and expensive (Brisson *et al.*, 2002). The duration of the test increases as the water content in the soil decreases (Leong and Rahardjo, 1997).

The indirect prediction methods for hydraulic conductivity function have been proposed by several researchers. Van Genuchten (1980) developed a close form equation to estimate unsaturated hydraulic conductivity through three independent parameters obtained by fitting the proposed soil water retention model to experimental data. The unsaturated hydraulic conductivity was predicted well in four out of five study cases. Fredlund *et al.* (1994) and Gribb *et al.* (2004) suggested that hydraulic conductivity function can be estimated through saturated permeability and SWCC by using fitting method. Leong and Rahardjo (1997) compared the hydraulic conductivity function estimated from several empirical equations, macroscopic models and statistical models. They concluded that the use



The infiltration rate ( $I_f$ ) is the rate at which water enter the soil surface. The Green-Ampt model predicts:

$$I_f = k_w \frac{S + L_f}{L_f} \quad (2.2)$$

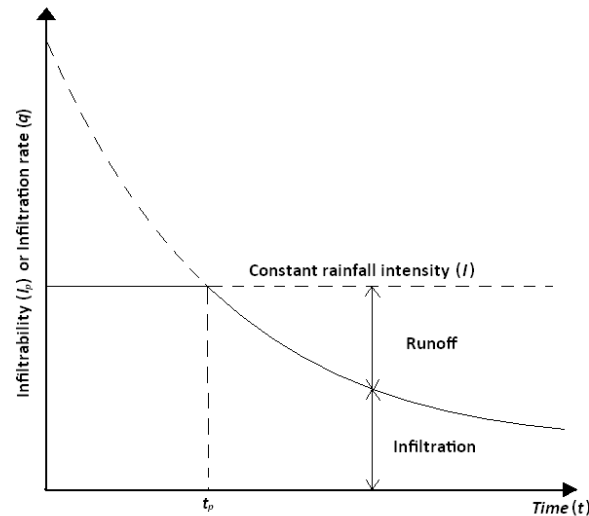
In Green and Ampt's model of infiltration, water from precipitation is assumed to enter the soil as a sharp wetting front. The soil above the front is assumed to be saturated. The soil below of the front is assumed at some uniform initial moisture. This model gives a very reasonable prediction even when compared with other more rigorous approaches based on unsaturated flow (Bouwer, 1966). Other researchers such as Mein and Larson (1973), Neuman (1976), Loáiciga and Huang (2007) have produced a similar infiltration equation with some modifications.

Figure 2.3 shows the relationship between rainfall and infiltration. Initially the infiltrability ( $I_p$ ) is greater than the rainfall intensity ( $I$ ). Thus, the infiltration rate ( $I_f$ ) is limited by the  $I$ . After a period of constant rainfall, the  $I_p$  decreases over time to a rate of less than  $I$ . At this stage, the  $I_f$  is controlled by the  $I_p$ , and surface runoff takes place. Horton (1933) found that when there is plenty of water available for infiltration, the infiltration rate follows the limiting function of  $I_p$ , until a constant rate known as infiltration capacity is reached. Freeze and Cherry (1979) found that the infiltration capacity is equal to the saturated permeability of soil ( $k_{sat}$ ). This finding was supported by Mein and Larson (1973) who found that the infiltration rate is initially exceeded the saturated permeability of soil, but drops to a value identical to the saturated permeability when the soil becomes fully saturated.

One of the often heard questions is how long after a constant rainfall intensity will initiate the generation of surface runoff. As shown in Figure 2.3,  $t_p$  is the time

when surface runoff start to occur. Mein and Larsson (1973) found that  $t_p$  can be predicted from an empirical equation as follows:

$$t_p = \frac{S\mu k_w}{I(I - k_w)} \quad (2.3)$$



**Figure 2.3** Relationship between rainfall and infiltration

In actual condition, the infiltration-runoff system sustains much more complexity than those expressions in a simple physical or empirical model. The infiltration rate could be affected by the distribution of rainfall, soil initial condition, rearrangement of soil particles due to the impact of raindrops, swelling of clayey soils, activities of worms and other soil fauna etc. (Bouwer 1966). The simulation of infiltration process as result of a rainfall event is still possible. However, the threshold rainfall for a slope failure could be a combination of a number of rainfall events or a prolonged antecedent rainfall. Under such circumstances, the simulation of rainfall infiltration could be extremely time consuming if not impossible. Ng *et al.* (2003) who carried out their studies on the rainfall-induced slope failure in Hong Kong suggested that, on average, 40% of rainfall considered as surface loss.

Rahardjo *et al.* (2004) made another assumption in Singapore by suggesting 60% of rainfall contributed to the surface loss. Despite of the fact that such correlation could be vague, it is still an acceptable assumption in practice.

## 2.4 Wetting Front and Redistribution

Wetting front and redistribution are two important phenomena in the saturation profile of unsaturated soil. As mentioned earlier, the conceptual model based on a sharp wetting front approach was first developed by Green and Ampt (1911). The studies in wetting front have been extended by numerous researchers, with the likes of Lumb (1962), Bouwer (1966), Mein and Farrel (1974), Pradel and Raad (1993), Kim *et al.* (2006), and Wang *et al.* (2003). Recent studies attempted to correlate the wetting front with the redistribution in order to provide a more comprehensive explanation to the soil moisture movement after the infiltration processes (Youngs, 1958; Jury *et al.*, 2003; Wang *et al.*, 2003).

As illustrated in Figure 2.4, the wetting front depth ( $L_f$ ) under uniform amount of rainfall infiltration ( $P$ ) can be approximated to:

$$L_f = \frac{P}{\theta_a - \theta_i} \quad (2.4)$$

Where  $\theta_a$  is the average moisture content in the wetted zone, and  $\theta_i$  is the initial moisture content (Wang *et al.*, 2003).

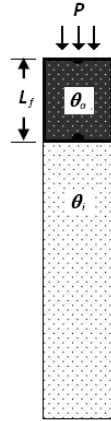


**Figure 2.4** Development of wetting front

From the absorption and desorption SWCC shown in Figure 2.5, Wang *et al.* (2003) found that the soil below the wetting front initially takes up moisture following an absorption curve OA until the suction reaches the water entry value ( $W_{ev}$ ) at the wetting front. Subsequently, the volumetric water content increases abruptly to  $\theta'_s$ . Above the wetting front (soil near the ground surface), water drains out from the soil following the desorption curve BO. When the suction reaches the air-entry value ( $A_{ev}$ ), the major pores begin to empty. The difference between the  $W_{ev}$  and  $A_{ev}$  indicates the ability of a porous medium to entrap a zone of higher water content behind the wetting front (Glass *et al.*, 1989). Considering the inclination angle of slope ( $\beta$ ), Wang *et al.* (2003) revised this special moisture retention ability and proposed a term known as the critical wetting front depth ( $L_{cr}$ ):

$$L_{cr} = \frac{W_{ev} - A_{ev}}{\cos \beta} \quad (2.5)$$

The term of critical wetting front depth was given because it is the limit for the redistribution and unstable flow to take place. In other words, when  $L_f < L_{cr}$ , the downward flux is not possible and the corresponding suction redistribution will be as shown in Figure 2.6a. Otherwise ( $L_f > L_{cr}$ ), downward flow continues after water

input stops due to excessive amount of infiltration and the corresponding suction redistribution is as illustrated in Figure 2.6b. It can be inferred from recent studies that with this type of redistribution pattern, a threshold water-entry pressure at the wetting front is required for the water to enter the unwetted zone (Liu *et al.*, 1993; Geiger and Durnford, 2000).

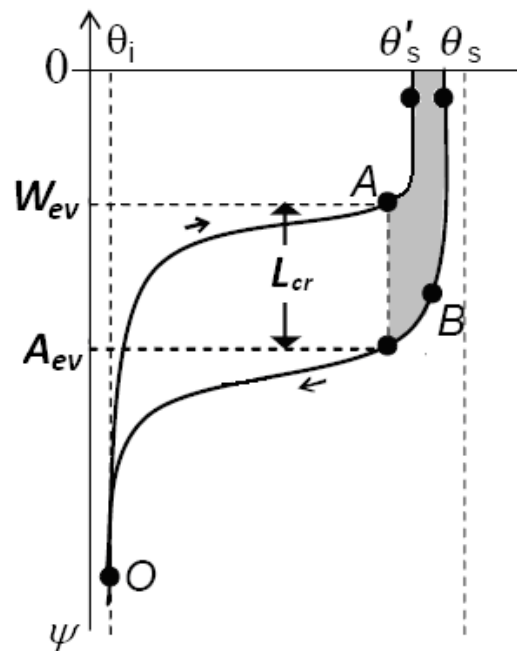


**Figure 2.5** Volumetric water content and suction in the development of wetting front

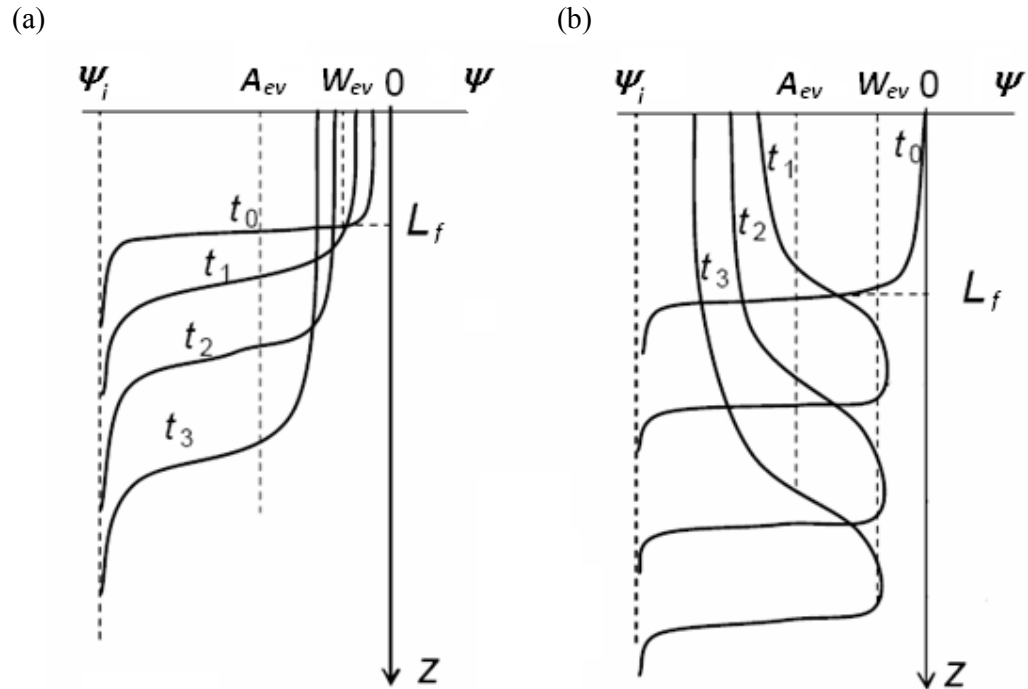


**Figure 2.6** Redistribution of soil moisture for (a)  $L_f < L_{cr}$  and (b)  $L_f > L_{cr}$

## 2.5 Correlation between Rainfall Pattern, Soil Suction and Slope Stability

The suction distribution of soil is greatly affected by the rainfall pattern (Li *et al.*, 2005). A rainfall pattern can be attributed to the rainfall intensity ( $I$ ), rainfall duration ( $t$ ), frequency of rainfall occurrences, and antecedent rainfall. In addition, the response of suction distribution to the rainfall pattern is also governed by other controlling factors such as soil permeability and initial suction condition. The variation in suction in turn would alter the shear strength of soil, and subsequently affect the stability of soil slope. In this section, the relationships between rainfall pattern, suction distribution, and slope stability are discussed in detail to provide a more comprehensive understanding in the mechanism of rainfall-induced slope failure.

## 2.5.1 The Role of Suction on Shear Strength and Stability of Unsaturated Soil Slope

Most natural soil deposits encountered in engineering practice are often unsaturated or only partially saturated (Chen *et. al.*, 2004). In unsaturated soil, the pore-water pressure will turn up as negative value or referred as matric suction. A better understanding of the role of negative pore-water pressures in increasing the shear strength of the soil has been developed, i.e. since the publication of book “*Soil Mechanics for Unsaturated Soils*” by Fredlund and Rahardjo (1993). Even though the inclusion of matric suction parameter into the slope stability analysis may cause more intricate solution, for certain situation where groundwater table is deep, the matric suction can no longer be ignored.

### 2.5.1.1 Shear Strength of Unsaturated Soil

The shear strength of soil is an important parameter for the slope stability analysis since the factor of safety of a slope is assessed by the ratio of the resistance force (quantified by the shear strength of the soil) to the mobilized force. The shear strength computed from the conventional Mohr-Coulomb failure criterion and effective stress concept (Terzaghi, 1936) is defined as:

$$\tau_f = c' + \sigma' \tan \phi' \quad (2.6)$$

Where,

- $\tau_f$  = shear stress at failure
- $c'$  = effective cohesion
- $\sigma'$  = effective normal stress

$\phi'$  = effective friction angle

For unsaturated soil, the water phase occupies only parts of the pore volume, while the remainder is covered by air (Cai and Ugai, 2004). Therefore, the main difference between shear strength of saturated soils and unsaturated soils is the definition for effective normal stress. The effective normal stress of saturated soils is commonly expressed in the form of equation as follows:

$$\sigma' = \sigma - u_w \quad (2.7)$$

Where  $\sigma$  is the total normal stress.

Evidence has shown that only a single-valued effective stress [i.e.,  $(\sigma - u_w)$ ] is required to describe the mechanical behaviour of saturated soil. However, the single-valued effective stress could not be applied in unsaturated soil as the behaviour of unsaturated soil is much more complicated than that of saturated soils.

Several attempts to estimate the effective stress and shear strength for unsaturated soils have been proposed by the researchers. Bishop (1959) proposed an equation for the effective stress of unsaturated soils which has gained widespread reference.

$$\sigma' = (\sigma - u_a) + \chi(u_a - u_w) \quad (2.8)$$

Where,  $\chi$  is a parameter related to the degree of saturation.

The  $\chi$  parameter with the value between zero (dry soil) and unity (saturated soils) can be obtained experimentally based on the degree of saturation ( $S_r$ ). Similar form of equation has been proposed by Aitchison (1961) and Jennings (1961). Jenning and Burland (1962) were the first to suggest that Bishop's equation did not provide adequate relationship between volume change and effective stress of the soil. Subsequently, there were attempts to separate the single-valued effective stress into two independent stress state variables in order to eliminate the need for inclusion of soil properties in the stress state description.

Fredlund *et al.* (1978) proposed an equation that include a parameter known as unsaturated friction angle ( $\phi^b$ ). The  $\phi^b$  depicts the increment rate of shear strength with a change in negative pore-water pressure. The equation has been widely accepted, even until today:

$$\tau_f = c' + (\sigma - u_a) \tan \phi' + (u_a - u_w) \tan \phi^b \quad (2.9)$$

The unsaturated friction angle ( $\phi^b$ ) can be obtained by performing a series of triaxial compression tests under various matric suction conditions. Measurement of unsaturated friction angle ( $\phi^b$ ) requires modification to the standard triaxial test apparatus through which the pore-air pressure control and transducer are installed to measure the matric suction ( $u_a - u_w$ ). Figure 2.7 shows the unsaturated friction angle ( $\phi^b$ ) obtained from the Mohr circle diagram. Commonly, the unsaturated friction angle ( $\phi^b$ ) range from  $15^\circ$  to  $20^\circ$  (GEO-SLOPE International Ltd., 2004a). Rahardjo *et al.* (2004) found that  $\phi^b$  remains constant and can be approximated to  $\phi'$  within low matric suction range.

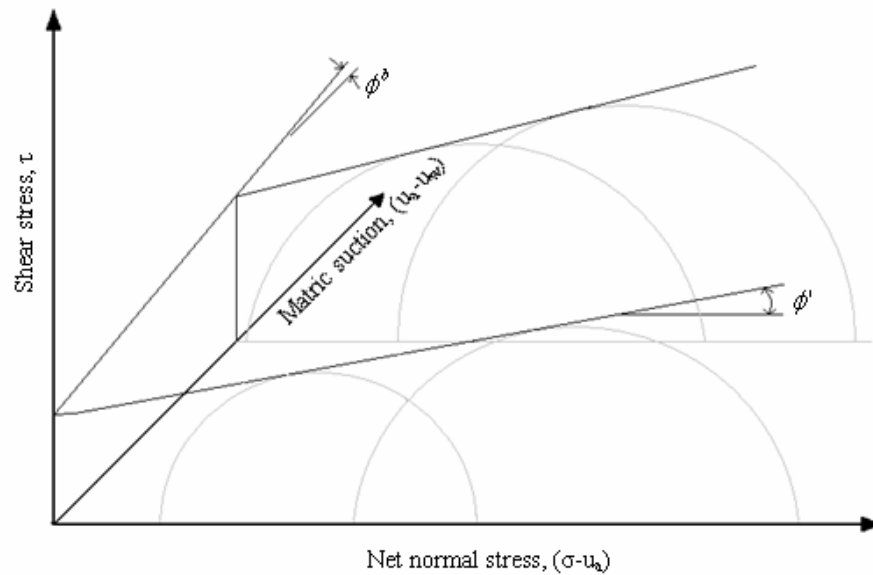


**Figure 2.7** Unsaturated soil strength properties

### 2.5.1.2 Stability Analysis of Unsaturated Soil Slope

The stability of a slope can be assessed by using several methods such as the methods of Janbu (1954), Bishop (1955), Morgenstern and Price (1965) etc. The major differences between these methods are the assumptions on the horizontal force and the equilibrium state (force equilibrium or moment equilibrium). The appropriateness of an analysis method is also greatly influenced by the potential failure mode of the slope (translational or rotational). Since the initial failures for most of the unsaturated soil slopes have small depth-to-length ratios and form the failure planes parallel to the slope surface, the use of infinite slope analysis for stability evaluation is thus justified (Collins and Znidarcic, 2004).

Figure 2.8 shows the soil element of a typical slice of an infinite slope in unsaturated condition with the width of  $l$ . The factor of safety (FOS) of the slope is

calculated using a modified Mohr-Coulomb failure criterion (Fredlund *et al.*, 1978):

$$FOS = \frac{c' + \sigma \tan \phi' + (u_a - u_w) \tan \phi^b}{W \sin \beta \cos \beta} \quad (2.10)$$

Where  $W$  is the total weight of soil. By assuming that  $\phi^b = \phi'$  and the pore-air pressure ( $u_a$ ) is at atmospheric, Equation 2.10 can be rewritten as:

$$FOS = \frac{c' + (\sigma - u_w) \tan \phi'}{W \sin \beta \cos \beta} \quad (2.11)$$

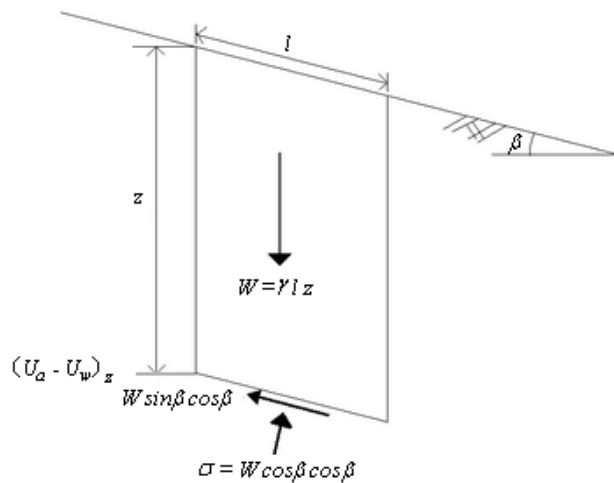


**Figure 2.8** Soil element of typical infinite unsaturated soil slope

From Equation 2.11, it is evidenced that other than the contributing factors such as soil strength properties, soil mass, and slope geometry, the factor of safety of a slope can be altered by the changes in negative pore-water pressure or suction, which in turn is greatly influenced by the triggering factor of rainfall infiltration. These relationships reveal the importance of the studies in rainfall pattern and suction distribution to correlate with the slope instability problem.

### 2.5.2 Effect of Rainfall Pattern on Suction Distribution and Slope Stability

The effect of rainfall intensity on the stability of slope has been studied by numerous researchers (Ng and Shi, 1998; Kasim *et al.*, 1998; Ng *et al.*, 1999, Gasmo *et al.*, 2000; Rahardjo *et al.*, 2001 etc). Kasim *et al.* (1998) performed a numerical simulation to investigate the influence of hydraulic properties of soil on the steady-state suction distributions in horizontal and inclined unsaturated soil layer. The study showed that the ratio of rainfall unit flux to saturated permeability (i.e.,  $q/k_{sat}$ ) and the air-entry value of the soil are the dominant factors affecting the steady-state suction distributions.

Ng and Shi (1998) and Ng *et al.* (1999) accounted for more parameters in their numerical studies on the effects of rain infiltration on suction in unsaturated slopes and hence on slope stability. The parameters considered in their study included intensity and duration of rainfall, saturated permeability, the presence of an impeding layer and conditions of surface cover. They found that the responses of suction and the groundwater table to the rainfall infiltration are mainly governed by the ratio of  $q/k_{sat}$  and  $k_{sat}/m_w$ , as well as the initial condition and boundary condition.

Previous studies on rainfall-induced slope failure (e.g. Lumb, 1975; Ng and Shi, 1998; Tsaparas *et al.*, 2002) have focused on the role of antecedent rainfall other than the influence of a single rainstorm event for the initiation of slope failure. Ayalew (1999) conducted a study through an observation of slope failure incidents in Hong Kong. He found that there were a few occasions where the slope experienced a rainfall with the intensity is identical to the intensity of triggering rainstorm, but no slope failures has occurred. Therefore, he rose up a question to the role of major rainfall in causing the slope failure. Besides, Ayalew (1999) found that more landslides generally occur in September than in July, despite July being wetter; and as many failures occur in October as in June, despite the amount of rainfall in

October is almost negligible. The phenomenon indicates that there could be some time delay between a rainfall event and its effect on the stability of a slope. Whether this is due to the antecedent rainfall leading to a build up of moisture within the soil, or whether it is a reflection of the movement of water in some form of wetting front, is still not clear.

Lumb (1975) suggested that rainfall-induced slope failure should be related to the duration and intensity of antecedent rainfall (up to fifteen days prior to the failure event), in addition to the intensity of triggering rainstorm. These findings have been contested by Brand (1984), who pointed out that Lumb's work was based on daily rainfall data at the Hong Kong Royal Observatory, not from the data collected local to the landslide locations. Brand used both 1-hour and 24-hour rainfall data recorded from the rain gauges installed near the landslides, and found that antecedent rainfall had no significant effect on major landslide events in Hong Kong, although he conceded that three to four days antecedent rainfall does seem significant to minor landslides. Brand's data indicated that major events were resulted from the short duration, high intensity rainfall events. Most of the severe landslides occur when rainfall exceeded 70 mm/hr. A significant number of failures could be expected in Hong Kong if the rainfall exceeded 100 mm/day.

The findings from Brand were contested by Ng and Shi (1998) who carried out a numerical investigation on the slope instability as result of rainfall in Hong Kong. They found that single threshold rainfall did not provide a reliable warning of land movement, and that a critical rainfall duration preceding the failure, of between three to seven days, was also applicable to failure events. From the foregoing findings, it is evidenced that the duration of antecedent rainfall to be considered in a slope stability analysis is still a matter of debate.

Rahardjo *et al.* (2001) carried out a case study in Singapore by considering 5-day antecedent rainfall in the slope stability analysis. They analyzed four actual rainfall patterns with the amounts of rainfall were identical to the storm event that has actually triggered the slope failure. They concluded that both triggering rainfall and antecedent rainfall have significant influence on the initiation of slope failure. The triggering rainfall alone cannot be used as the determinant for slope failure. However, the soil characteristics were not accounted in their study.

Tsaparas *et al.* (2002) used Seep/W to perform seepage analysis for an unsaturated soil slope and determine the factor of safety by integrating the seepage results in the Slope/W. They considered the effect of antecedent rainfall, and found in general that prolonged antecedent rainfall would significantly alter the pore water pressure conditions prior to the main rainfall event. The effect of rainfall on the stability of slope was controlled by the duration of the rainfall event, in which the longer the rainfall duration, the lower the factor of safety of the slope. Antecedent rainfall had some impact, especially when continuous, as previously noted. Soil slope with lower saturated permeability tended to be more stable, since higher permeability permitted deeper and more rapid penetration of the wetting front, leading to greater loss of suction.

Tsaparas *et al.*'s findings were supported by Cai and Ugai (2004) who found that the slope with low permeability should fail after sufficient duration of rainfall even if the rainfall was with a low intensity. For slope with comparatively high permeability, the slope failures possibly took place under the rainfall with a shorter duration and a greater intensity. However, their findings have not yet been verified with the field or laboratory evidences.

Zêzere *et al.* (2005) studied the landslides event in Portugal for the past 50 years. They concluded that one to fifteen days rainfalls are categorized as intense

and short rainfall which responsible to the shallow landslide. On the other hand, one to three months prolonged rainfalls are the main factor causing the deep-seated slope failure. It should be noted that the study was carried out in the European region in which the climate and the soil properties could be a huge factor affecting the conclusion of the study.

In Malaysia, Roslan and Mohd (2005) suggested that seven days of rainfall should be considered in the slope stability analysis. The energies associated to the rainfalls were applied in the Universal Soil Loss Equation (USLE). However, their studies were more emphasizing on the soil erosion or erosion-induced slope failures which might not be applicable in the case of rainfall-induced slope failure.

In summary, despite of the fact that abundant numerical, field and laboratory studies can be traced, the rainfall pattern that should be accounted in the stability analysis of a slope is still a matter of debate. Experiences from different regions of the world have resulted in different conclusions as to the significance of antecedent rainfall for slope instability. Therefore, the mechanism of rainfall-induced slope failure should be treated as a localized problem. In Malaysia, there are still very limited studies conducted by employing the local rainfall data. Furthermore, the permeability of soil appears to be another controlling factor that could greatly affect the mechanism of rainfall-induced slope failure.

## **2.6 Soil Column for Infiltration Analysis**

Soil column has been used by several researchers to model the infiltration mechanism. Stormont and Anderson (1999) used a soil column apparatus to study the infiltration behavior of layered soils. The apparatus consists of an acrylic

cylinder of 203 mm in diameter and 800mm in height. Nahlawi *et al.* (2007) carried out an infiltration experiment to study the one-dimensional unsaturated hydraulic behaviour of a layered soil-geotextile system. Their infiltration experiments were conducted in a clear Perspex cylinder of 138.7 mm in diameter and 1,600 mm in height. The column assembly comprises four-part cylindrical sections, with each section having a 400 mm height. Other published works on infiltration testing using one-dimensional soil column include Rousseau and Pietro (2004), Jason and Joel (2004) and Hincapié *et al.* (2007). Their studies mainly focused on the investigation of the transportation of contaminants, chemical solutes and leachate in soil.

The modeling of infiltration mechanism by the soil column infiltration test can be traced from the studies conducted by Yang *et al.* (2004b) and Yang *et al.* (2006). Yang *et al.* (2006) investigated the effect of rainfall intensity and duration on infiltration mechanism through a large scale soil column apparatus, and provide experimental evidence for soil water redistribution and hysteresis. The details and the performance of the apparatus are described by Yang *et al.* (2004b).

Figure 2.9 shows the schematic diagram of the soil column apparatus developed by Yang *et al.* (2004b). The soil column was made of acrylic and supported by a steel frame. The soil column was 1.5m in height with the internal diameter of 190mm. Two types of instruments were installed on the soil column model, i.e. tensiometer for suction measurement, and TDR for volumetric water content measurement. The measurements were logged automatically into a data logger. Water circulation system was installed to circulate the water discharged during the tests.

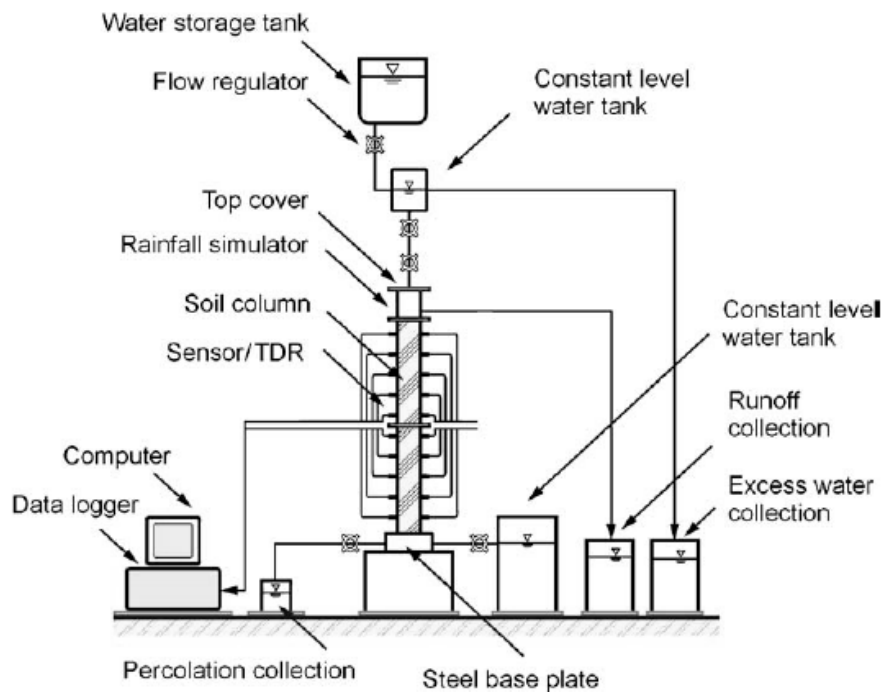


**Figure 2.9** Schematic diagram of soil column developed by Yang *et al.* (2004)

A few criteria should be considered in the design of soil column model to accommodate the requirements of specific research, i.e. the dimension, the material and the boundary conditions of the model. Generally, it is recommended that the diameter of the soil column is ten times greater than the soil particle size in order to minimize the boundary effect on the test results. Lim *et al.* (1996) measured the pore-water pressure changes during rainfall in a slope in Singapore and concluded that the pore-water pressure changes occurred within the depths of 1.5m. It is thus essential to use a soil column with sufficient length and dimensions for pore-water pressure monitoring. Besides, the boundary conditions of the soil column should also be properly defined to represent the desired condition.

## 2.7 Numerical Simulation for Seepage and Slope Stability Analyses

From the past few decades, the numerical modeling technique has been increasingly applied in the seepage and slope stability analysis owing to the rapid development in the computing power and commercial software. In this section, some of the pronounced published works using numerical simulation are cited.

Ng and Shi (1998) performed a parametric study to investigate the effect of rainfall infiltration on a typical unsaturated hillside with a steep cut slope in Hong Kong. Their study was performed by using the finite element program Seep/W, with the rainfall modeled through the application of a specified infiltration rate (equal to the rainfall data) on the boundary surface. The resultant pore water pressures were then applied in a conventional limit equilibrium analysis to calculate the factors of safety. By using the infiltration rate equal to the rainfall data, their results on the pore-water pressure distribution seems to have over-estimated.

Chapuis *et al.* (2001) considered a number of both saturated and saturated-unsaturated problems, while assessing the validity of the numerical codes. They carried out the numerical analysis by using Seep/W. Two significant points were noted from their work. Firstly, they show that numerical convergence problems may occur due to large elements used in the model. This clearly reinforces the point that non-linear numerical analysis can be highly influenced by the size and geometry of the elements used, and that care must be taken to investigate the sensitivity of an analysis to the proportions of the mesh used to solve it. There were certainly no published rules or guidelines to determine the size and density of the mesh elements. GEO-SLOPE International Ltd. (2004b) suggested that the density of the mesh should be designed such that every single element is visible when the model is zoomed at 100%. Secondly, Chapuis *et al.* (2001) did consider an analysis featuring infiltration into a slope with a fissured clay surface layer over

less permeable clay. As modeled directly, very high pore pressures are generated in the fissured clay layer as the infiltration is forced into this layer, but the water is unable to penetrate into the less permeable clay beneath. This is presented as an illustration of a weakness in a numerical code generating an inaccurate result. Chapuis *et al.* (2001) suggested that this particular problem could be dealt with by adding a surface, highly permeable gravel layer, which more readily allows lateral flow, thus preventing the build up of pore pressures.

Ng *et al.* (2001) used a finite element program, FEMWATER to perform a three-dimensional analysis of rainfall infiltration on a cut slope in Hong Kong. They investigated the effect of rainfall intensity on the pore water pressure distribution of soil. In order to account for the amount of rainwater that taken off as runoff and evapotranspiration, Ng *et al.* did not reproduce this effect directly, but rather simulate it indirectly with a '60% of rainfall as infiltration' assumption.

Rahardjo *et al.* (2001) used Seep/W to compute the changes in pore-water pressure as result of various rainfall patterns. In order to simulate a groundwater fluctuation condition, the left and right boundaries below the groundwater table were specified as constant total head, while zero total flux boundaries were assigned above the groundwater table.

Generating the initial condition of pore-water pressure as identical as possible to the in-situ condition is always a difficult task in numerical modeling. Rahardjo *et al.* (2001) performed a steady state analysis to produce a hydrostatic condition. Subsequently, a transient analysis was used to establish an initial pore-water pressure profile by applying low unit flux to the slope surface for a long duration. The value of the applied net flux on the slope surface was determined by trial and error until the required initial pore-water pressure condition was achieved.

Tsaparas *et al.* (2002) used Seep/W to perform seepage analysis in an unsaturated soil slope, and subsequently determined the factor of safety by using Slope/W. They simulated a high rainfall relative to the saturated permeability which resulted in only shallow wetting front because most of the rain water became run-off. This was done by re-setting the surface pore water pressure to 0 kPa which indicated that ponding is not allowed on the soil surface.

Cai and Ugai (2004) carried out a finite element analysis of transient water flow through unsaturated-saturated soils to investigate the effects of hydraulic characteristics, initial relative degree of saturation, methods to consider boundary condition, rainfall intensity and duration on the pore-water pressure in slope. Shear strength reduction technique was adopted in the slope stability analysis using a software package known as SLOPE@FE. They found that the higher the initial volumetric moisture content, the faster the water pressure increase in the slopes that subjected to rainfall. This point can be explained with the suction dependent hydraulic conductivity in unsaturated soil. As shown in hydraulic conductivity function, higher suction (lower volumetric water content as shown in SWCC curve) in soil will lead to lower hydraulic conductivity, and vice versa.

Babu and Murthy (2005) performed a reliability analysis of unsaturated soil slope by using finite element program developed by Döll (1997). They found that reliability theory can be used by means of evaluating the effects of various parameters on the stability of an unsaturated soil slope. The matric suction ( $u_a - u_w$ ) and unsaturated friction angle ( $\phi^b$ ) were found to be the critical random variables in the slope reliability assessment.

## 2.8 Concluding Remarks

In this chapter, the basic theories and the clinical researches relevant to the topic of rainfall-induced slope failure were discussed in details. Besides, the published works related to the statistical prediction of extreme rainfall, soil column model, and numerical simulation techniques were reviewed to provide supportive information for the methodologies employed in the present study.

Despite of the fact that the theory of unsaturated soil mechanic has been well established, the application of unsaturated soil mechanic in the slope stability analysis is still very limited. Apparently, the designer found that it is too risky to apply such approach that exposed to so many uncertainties. There are several factors that may govern the mechanism of rainfall-induced slope failure, such as rainfall intensity, rainfall duration, antecedent rainfall, soils strength properties, slope geometry, and hydraulic properties of soils etc. Which factors are dominating the mechanism is still unclear. It is questions such as this that provoked this study to be carried out.

Several research gaps have been identified from the existing literatures to form the basis for much of the research works carried out in the present study. Firstly, the rainfall infiltration characteristic of soil, particularly on slope is still unclear. The problem is mainly caused by the high temporal and spatial variability in both rainfall pattern and soil behaviour.

Secondly, the critical rainfall pattern for the rainfall-induced slope failure is still a matter of debate. The major uncertainties associated with the critical rainfall pattern include the critical rainfall duration that should be considered in a slope stability analysis, and the relative role of major rainfall and antecedent rainfall for the

initiation of slope failure. Furthermore, the minimum suction corresponding to the critical rainfall pattern is yet to be identified.

Thirdly, the studies on the topic of rainfall-induced slope failure are still very limited in Malaysia. As mentioned earlier, the rainfall-induced slope failure problem should be treated as a localized problem, in which experiences from different regions of the world would result in different conclusions. Thus, it is necessary to study the mechanism of rainfall-induced slope failure based on the extreme rainfall analyzed from the local historical rainfall data.

Fourthly, the permeability of soil is found to be one of the main controlling factors affecting the mechanism of rainfall-induced slope failure. Most of the previous studies were conducted numerically and analytically. It is thus essential to provide the laboratory and field evidences for verification purpose.

Lastly, the application of unsaturated soil mechanic and the integration of extreme rainfall into the slope stability analysis have yet to become a common practice, in view of large number of parameters and uncertainties involved in the analysis. A simplified analysis is required for the preliminary stability evaluation before a detailed investigation is implemented.

## **CHAPTER 3**

### **METHODOLOGY**

#### **3.1 Introduction**

The main objective of this research is to investigate the mechanisms involved in the development of saturation profile. To achieve the objective, five phases of research activities were undertaken, i.e. research initialization, preliminary preparation, experiments, analysis, and generalization. In general, the research was shaped through three approaches, namely numerical simulation, laboratory modelling, and field monitoring. Figure 3.1 shows the flow chart of the research activities.

The study was initiated by critically reviewing published works related to the topic of rainfall-induced slope failure in order to develop a strong background of the research. The knowledge on the state of the art of the research topic was gained through consultation with several well-known experts such as Professor Harianto Rahardjo from Nanyang Technological University Singapore, Dr. David Toll from University of Durham, Professor Faisal Ali from University of Malaya, Professor Roslan Zainal Abidin from University Technology Mara, and Mr. Law Tien Huat from Mohd. Asby Consultant Sdn. Bhd. Problem statement and hypothesis were formed based on the literature reviews and the professional opinions from experts.

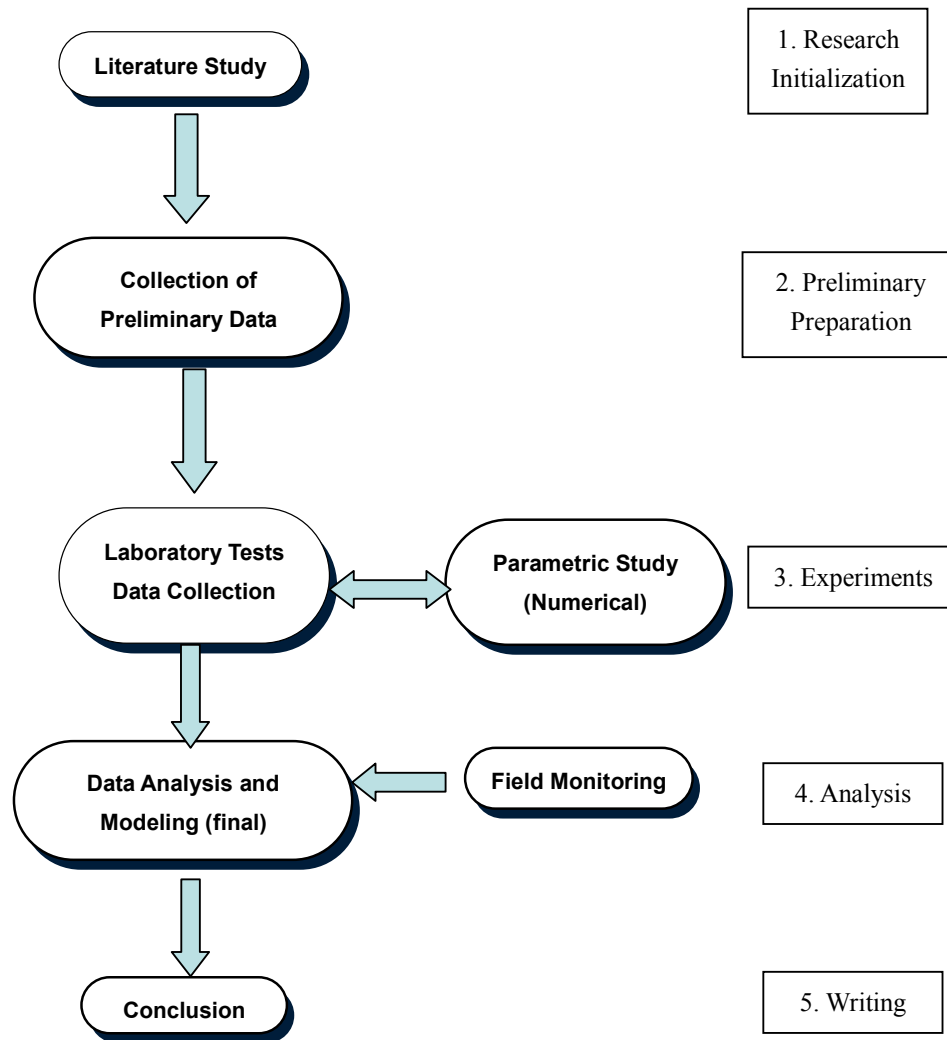


**Figure 3.1** Research framework

The second stage of the research involves the preliminary preparation of experimental apparatus. Numerical analysis was performed to facilitate the preliminary design of the laboratory model. The sketch of the laboratory model was then fabricated.

Investigation on the dominant factors affecting saturation profile, and the threshold rainfall patterns for different types of soil were carried out during the third stage of research through numerical simulation. A series of laboratory experiments

on a physical soil column model were performed to provide laboratory evidence for the results of numerical simulation.

In the analysis stage, the data obtained from the laboratory tests were analyzed and compared with the results of numerical simulation. Subsequently, discussions were made to explain the dominant factors affecting the saturation profile and its correlation with slope stability. Field monitoring results were also acquired to further verify the findings.

The last stage of the study involved report writing and documentation of research findings.

### 3.2 Statistical Analysis of Extreme Rainfall

The IDF curve for the analysis of rainfall-induced slope instability should cover a wide range of duration (i.e. from one hour to thirty days) because the water flow in soil is governed by the soil's hydraulic conductivity, which ranges from  $1 \times 10^{-4}$  m/s to  $1 \times 10^{-11}$  m/s. An equation was developed by Department of Irrigation and Drainage (2001) to relate the average rainfall intensity ( ${}^R I_t$  in mm/hr) for a particular return period ( $R$ ) with the rainfall duration ( $t$  in min):

$$\ln({}^R I_t) = a + b \ln(t) + c(\ln(t))^2 + d(\ln(t))^3 \quad (3.1)$$

Where  $a$ ,  $b$ ,  $c$  and  $d$  are fitting constants dependant on geographical location. The equation and fitting constants, however, are only valid for the IDF curve within 1-day duration (i.e. 1-hour to 24-hour). Therefore, a statistical extreme rainfall analysis should be performed to plot the IDF curve with longer duration (i.e. 1-day to

30-day). The extreme rainfalls for five selected locations in the Malaysian Peninsular (Figure 3.2) were analyzed by using the method of Gumbel (1954). The selection of locations was based on geographical reason.



**Figure 3.2** Five selected locations in the Malaysian Peninsular

Thirty years historical daily rainfall data of the five selected locations were acquired from the Department of Irrigation and Drainage (DID) Ampang, Malaysia. The annual maximum rainfall intensities corresponding to the durations ranging from one to thirty days were then identified from the historical daily rainfall data. Subsequently, the extreme intensities of rainfall ( $X$ ) were linearly related to the

reduced variate in the Gumbel's distribution ( $Y$ ), as follows:

$$X = \mu + \frac{1}{\alpha} Y \quad (3.2)$$

whereas

$$\frac{1}{\alpha} = \frac{S_x}{\sigma_y} \quad \text{and} \quad (3.3)$$

$$\mu = \bar{X} - \frac{\bar{Y}}{\alpha} \quad (3.4)$$

Where  $\mu$  and  $\alpha$  are parameters characterized by rainfall duration,  $\bar{X}$  and  $S_x$  are the mean and standard deviation of annual maximum rainfall intensities while  $\bar{Y}$  and  $\sigma_y$  are the mean and standard deviation of Gumbel's reduced variates (Chow, 1988; Lam and Leung, 1995). The Gumbel's reduced variate is a function of return period ( $R$ ) and expressed by:

$$Y = -Ln [-Ln (1 - 1/R)] \quad (3.5)$$

In the present study, the IDF curves of ten-year return period was developed because it is recommended by the Geotechnical Manual for Slope in Hong Kong (GCO, 1984) and has been used as common design practice for slopes in Malaysia (Liew, 2005; Gue and Tan, 2002). An example of calculations to obtain the IDF curve for Johor Bahru is presented in Apendix A.

### **3.3 Numerical Simulation**

In this section, the details of the numerical simulation are presented. The transient seepage analysis was performed by Seep/W (GEO-SLOPE International Ltd., 2004b) while the slope stability analysis was carried out by Slope/W (GEO-SLOPE International Ltd., 2004a).

#### **3.3.1 Geometry of the slope**

An idealized infinite slope model was simulated as shown in Figure 3.3. The infinite slope analysis was adopted for two reasons: (1) the infinite slope makes it attractive in describing the physical process of failure initiation (Sung and Seung, 2002), and (2) the simulation of infinite slope, regarded as an one-dimensional analysis, allows the results to be effectively verified through laboratory soil column tests. Despite of the fact that the infinite slope analysis cannot completely represent the actual condition of all the slopes in Malaysia, it should not significantly affect the relative factor of safety computed in this study.

The numerical model represents an imaginary slope stood at an inclination of  $21^\circ$ . The model was 20 m in length, with the additional 1 m-length elements at both left and right edges specified as infinite elements. By setting the pole position at the center of the model, the horizontal distance between the pole and the infinite element was approximately 10m. Seep/W will duplicate this distance (10m) in the infinite elements, hence a total length of 40 m was actually simulated for the model.

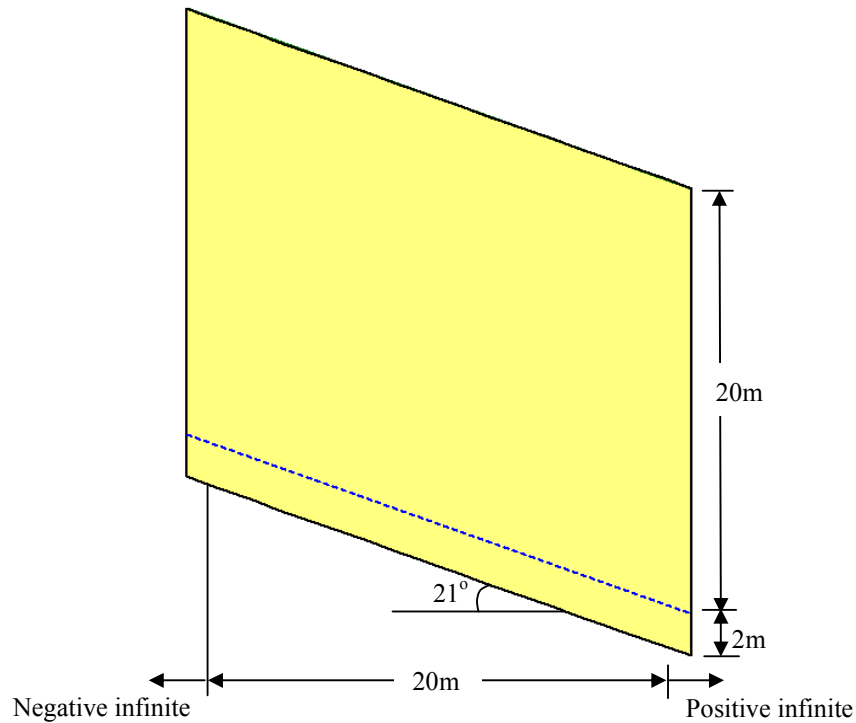


**Figure 3.3** Geometry of the infinite slope for numerical simulation

Four types of soil (i.e. sand-gravel, silty gravel, sandy silt, and silt) were employed in the numerical analysis to simulate four different soils with respect to the hydraulic properties. Most of the soil properties assigned in the numerical analysis (i.e. saturated permeability, SWCC, shear strength parameters, and unit weight) were determined from laboratory tests. The hydraulic conductivity function was predicted by using Van Genuchten (1993)'s method which was integrated in the Seep/W.

### 3.3.2 Finite Element Mesh Design

Two-dimensional finite element code, Seep/W, was used to model flows under saturated and transient unsaturated conditions. The mesh comprised 1265

nodes and 1188 quadrilateral elements. Insufficient mesh elements could result in the discontinuity of the generated flow path. Conversely, overly dense mesh element would result in lengthy computation time. Furthermore, numerical difficulties associated with convergence might occur at the area near to the ground surface where the pore-water pressures change rapidly during infiltration. Tsaparas *et al.* (2002) found that the use of finer elements near the soil surface could overcome the problem effectively. Thus, very fine first order quadrilateral elements ( $0.25 \times 1$  m) were designed for the ground surface to a depth of 5m. Larger quadrilateral elements ( $0.5 \times 1$  m) were used below 5m depth. Four-noded elements were assigned to the entire mesh, except for the infinite elements on the left and right edges in which eight-noded quadrilaterals were required to form a decay function. Figure 3.4 shows the element mesh designed for the numerical model to produce satisfactory result within a reasonable processing time.

Seep/W allows the adjustment of the tolerance between each iteration procedure. In other words, Seep/W would continue the iteration procedure at each time step until the desired tolerance was met. In this study, 50 iterations were assigned with the tolerance of the computed norm of the head vectors between two consecutive iterations was set at 0.1. The typical duration for each simulation was between 10 and 30 minutes on a Pentium 4 3.0 GHz processing unit, depending on the time step assigned in each simulation.

For the boundary conditions, the left and right edges above the water table were specified as a no flow boundary ( $Q = 0$ ), while the edges below the water table were assigned as head boundary equal to the elevation of the water table. These boundary conditions might not simulate the actual conditions in a soil slope, but should give reasonable pore-water pressure distribution if the horizontal boundary is set at a sufficient distance to avoid saturation of the slope model due to the rise of the water table. On the exposed sloping surface, infiltration due to rainfall was

modeled by applying a unit flux ( $q$ ) with a no ponding option to the slope with varying intensity. The bedrock located at 22 m from the ground surface was assumed to be an impermeable layer.

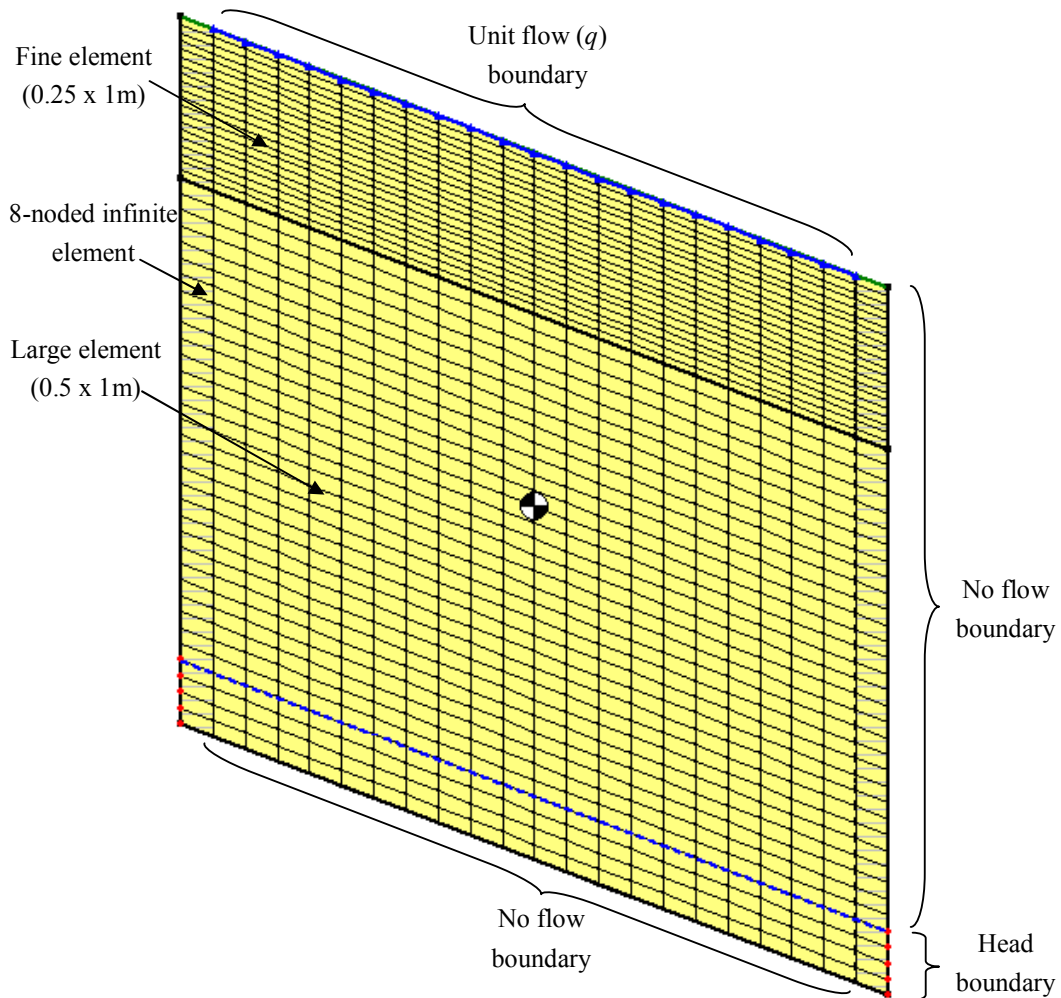


**Figure 3.4** Element meshes and boundary conditions of the numerical model

A hydrostatic initial condition was established at the beginning of the transient seepage analysis. The water table was assigned at 20 m below the ground surface that would certainly produce an unrealistically high negative pore-water pressure (196.2 kPa) near the ground surface in conjunction with hydrostatic

condition. Therefore, a limiting negative pore-water pressure was imposed at the beginning of the analysis. The limiting value was determined from the parametric study which will be discussed in detail in the latter part of this report.

### 3.3.3 Slope Stability Analysis Approach

The pore-water pressure distribution computed from Seep/W during a transient state analysis was imported into Slope/W for the slope stability analysis. The General Limit Equilibrium method was adopted in the analysis. A fully specified slip plane, parallel to the sloping surface, was imposed at the desired depth with a tension crack was assigned along the slip surface, as shown in Figure 3.5. This step is necessary to prevent sharp entry and exit angles of the slip surface that may cause a convergence problem. In such manner, the slip surface will vertically exit the ground surface whenever the slip surface intersected with the tension crack line.

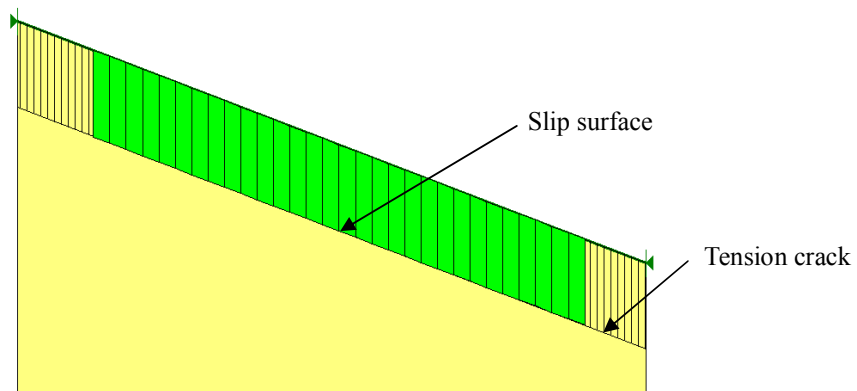


**Figure 3.5** Techniques used to assign slip surface plane parallel to ground surface

### 3.3.4 Numerical Simulation Design

The numerical simulation is divided into two parts, namely parametric study, and critical rainfall pattern analysis. The parametric study was performed to obtain an overview regarding the responses of sand-gravel, silty gravel, sandy silt and silt (kaolin) to different rainfall characteristics, while the critical rainfall pattern analysis was carried out to determine the critical rainfall pattern for the four types of soil at five selected locations.

#### 3.3.4.1 Parametric Study

Four variables were investigated in the parametric study, including initial condition, rainfall intensity, rainfall duration, and slope inclination angle, as illustrated in Figure 3.6, Figure 3.7, Figure 3.8 and Figure 3.9, respectively.

Firstly, the effect of initial condition on the suction distribution was investigated. The limiting suctions of 15kPa, 30kPa, 45kPa and 60kPa were imposed to the initial condition of each soil slope. Two types of rainfall pattern were considered in the analysis, i.e. short and intense 1-day major rainfall, and long and less intense 30-day antecedent rainfall. Subsequently, a limiting suction of 5kPa was assigned to the model to represent a very wet condition in the soil. The soil model was then left drying for 120 days to monitor the drying path of the soil suction. From the observation, an appropriate initial suction condition was suggested for each type of soil.

Secondly, the effect of rainfall intensity on the suction distribution was studied by applying the 1-day rainfalls of various intensities (from  $1 \times 10^{-7}$  m/s to

$5 \times 10^{-6}$  m/s) on the slope models consisting of the four types of soil.

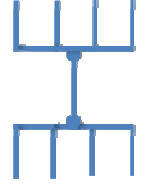
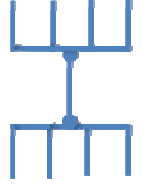
Thirdly, the effect of rainfall duration on the suction distribution of the four types of soil was investigated by applying a rainfall intensity of  $1 \times 10^{-7}$  m/s for various durations (i.e. 1-day, 2-day, 3-day, 5-day, 7-day, 14-day, and 30-day). The low-intensity rainfall was adopted to avoid fully saturation of the slope model.

Lastly, the effect of slope inclination on the suction distribution was studied. Two patterns of rainfall (1-day major rainfall, and 30-day antecedent rainfall) were applied in the numerical analysis. The slope inclination angles varies by  $0^\circ$ ,  $21^\circ$  (1V:2.5H),  $27^\circ$  (1V:2H),  $34^\circ$  (1V:1.5H), and  $45^\circ$  (1V:1H). A total of 128 combinations of numerical tests were performed in the parametric study.

#### **3.3.4.2 Critical Rainfall Pattern Analysis**

The numerical analysis was performed to determine the critical rainfall pattern for sand-gravel, silty gravel, sandy silt and silt (kaolin) at five selected locations. The extreme rainfalls ranging from one day to 30 days were assigned to the numerical models. Figure 3.10 summarizes the variables considered in this analysis. A total of 140 combinations of numerical tests were performed in this analysis.

**Parametric Study 1: Initial Condition**

Variable I: Initial Condition	Variable II: Soil Type	Constants	Objective
15 kPa 30 kPa 45 kPa 60 kPa	 <p>Sand-Gravel Silty Gravel Silty Silt Silt (Kaolin)</p>	<p>Rainfall intensity: <math>4.00 \times 10^{-6}</math> m/s                      Rainfall Duration: 1 day                      Slope angle: <math>21^\circ</math></p>	To study the effect of initial condition on the suction distribution of different types of soil as result of major rainfall
15 kPa 30 kPa 45 kPa 60 kPa	 <p>Sand-Gravel Silty Gravel Silty Silt Silt (Kaolin)</p>	<p>Rainfall intensity: <math>1.00 \times 10^{-7}</math> m/s                      Rainfall Duration: 30 days                      Slope angle: <math>21^\circ</math></p>	To study the effect of initial condition on the suction distribution of different types of soil as result of antecedent rainfall
	 <p>Sand-Gravel Silty Gravel Silty Silt Silt (Kaolin)</p>	<p>Rainfall intensity: 0 m/s                      Rainfall Duration: 0 days                      Slope angle: <math>21^\circ</math>                      Initial Condition: 5 kPa                      Drying Duration: 120 days</p>	To determine the appropriate initial condition for different types of soil

**Figure 3.6** Parametric study design for various initial conditions

**Parametric Study 2: Rainfall Intensity**

Variable I: Rainfall Intensity	Variable II: Soil Type	Constants	Objective
<ul style="list-style-type: none"> <li>1.00 × 10<sup>-7</sup> m/s</li> <li>1.00 × 10<sup>-6</sup> m/s</li> <li>2.00 × 10<sup>-6</sup> m/s</li> <li>3.00 × 10<sup>-6</sup> m/s</li> <li>4.00 × 10<sup>-6</sup> m/s</li> <li>5.00 × 10<sup>-6</sup> m/s</li> </ul>	<ul style="list-style-type: none"> <li>Sand-Gravel</li> <li>Silty Gravel</li> <li>Sandy Silt</li> <li>Silt (Kaolin)</li> </ul>	Rainfall Duration: 1 day Slope angle: 21° Initial Condition: As identified for each soil type	To study the effect of rainfall intensity on the suction distribution of different types of soil

**Figure 3.7** Parametric study design for various rainfall intensities

**Parametric Study 3: Rainfall Duration**

Variable I: Rainfall Duration	Variable II: Soil Type	Constants	Objective
<ul style="list-style-type: none"> <li>1 day</li> <li>2 days</li> <li>3 days</li> <li>5 days</li> <li>7 days</li> <li>14 days</li> <li>30 days</li> </ul>	<ul style="list-style-type: none"> <li>Sand-Gravel</li> <li>Silty Gravel</li> <li>Sandy Silt</li> <li>Silt (Kaolin)</li> </ul>	Rainfall intensity: 1.00 × 10 <sup>-7</sup> m/s Slope angle: 21° Initial Condition: As identified for each soil type	To study the effect of rainfall duration on the suction distribution of different types of soil

**Figure 3.8** Parametric study design for various rainfall durations

**Parametric Study 4: Slope Inclination**

Variable I: Slope Angle	Variable II: Soil Type	Constants	Objective
0° 21° 27° 34° 45°		Rainfall intensity: $4.00 \times 10^{-6}$ m/s Rainfall Duration: 1 day Initial Condition: As identified for each soil type	To study the effect of slope inclination angle on the suction distribution of different types of soil as result of major rainfall
0° 21° 27° 34° 45°		Rainfall intensity: $1.00 \times 10^{-7}$ m/s Rainfall Duration: 30 days Initial Condition: As identified for each soil type	To study the effect of slope inclination angle on the suction distribution of different types of soil as result of antecedent rainfall

**Figure 3.9** Parametric study design for various slope inclinations

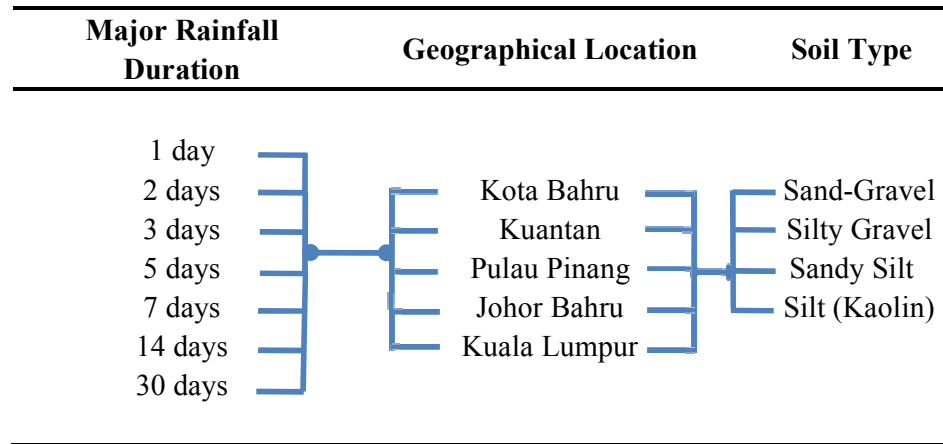


**Figure 3.10** Simulation scheme for determining critical antecedent rainfall

### 3.4 Laboratory Soil Column Tests

The soil column model designed for this study consisted of four main parts, i.e.: acrylic soil column, water flow system, instrumentation, and data acquisition system. A three-dimensional diagram of the soil column model is illustrated in Figure 3.11, while the photograph of the apparatus is shown in Figure 3.12.

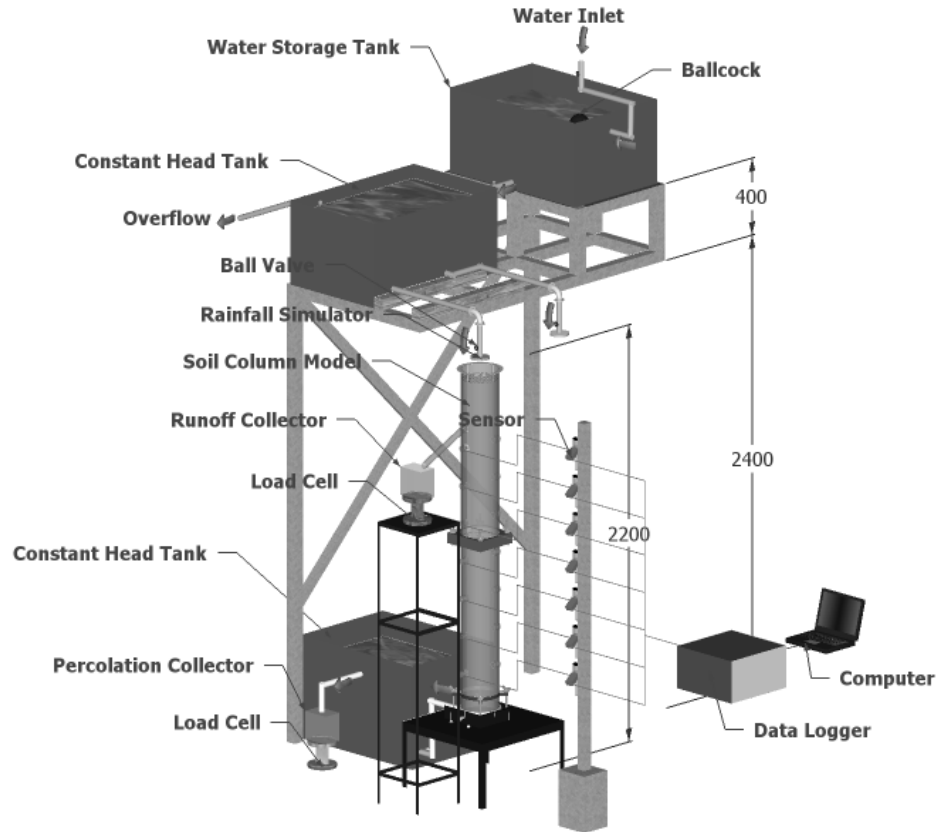


**Figure 3.11** Three-dimensional diagram of the laboratory model setup

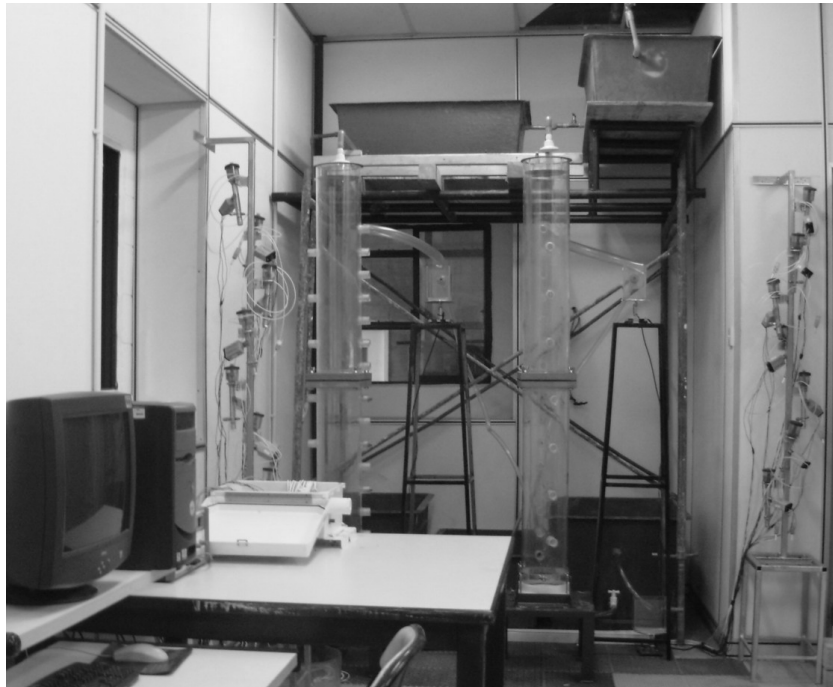


**Figure 3.12** Photograph of the laboratory model setup

### **3.4.1 Soil Column**

The soil column was made of acrylic transparent tube with a 5 mm-thick wall and 190-mm internal diameter. The soil column consisted of two separated tubes (900 mm high each) connected securely by clamp system and rubber O- ring. This arrangement was necessary for the ease of compaction and removal of soil sample.

Two types of threaded holes were fabricated on the soil column model wall. One type was used for the installation of tensiometer probes (ceramic cups), while the other was fabricated to install gypsum moisture block. Both threaded holes were spaced at 200 mm along the length of the soil column. The holes that were not in use during an experiment were sealed with threaded plugs.

Screw clamp system was employed to prevent water leakage at the joint between two separated cylinders, and the joint between the cylinder and base plate (Figure 3.13). An O-ring was placed in groove, and fastened with bolts and nuts. The silicon grease was used to improve the resistance to water leakage.

### **3.4.2 Water Flow System**

The water flow system of the infiltration column comprises three parts, i.e. inflow/rainfall control, overflow/runoff discharge, and percolation discharge (Figure 3.11)

The inflow/rainfall control consisted of a water storage tank, a constant head tank, a flow regulator (ball valve), and a rainfall distributor. The water storage tank

with storage capacity of 216 L was placed 2.8 m from the ground surface. The function of the water storage tank is to provide continuous water flow into the constant head tank. The constant head tank, which was placed immediately below the water storage tank, had a storage capacity of 216L and a constant head of 0.3 m. Water in the storage tank flowed into the constant head tank through a control valve. An overflow outlet was placed at the same level with the inlet flow of constant head tank to create the constant head condition during the test. Beneath the constant head tank was a flow regulator, by which simulated rainfall rate was precisely controlled. Note that this system could only produce flow rate greater than 5mL/min ( $q = 2.94 \times 10^{-6}$  m/s).

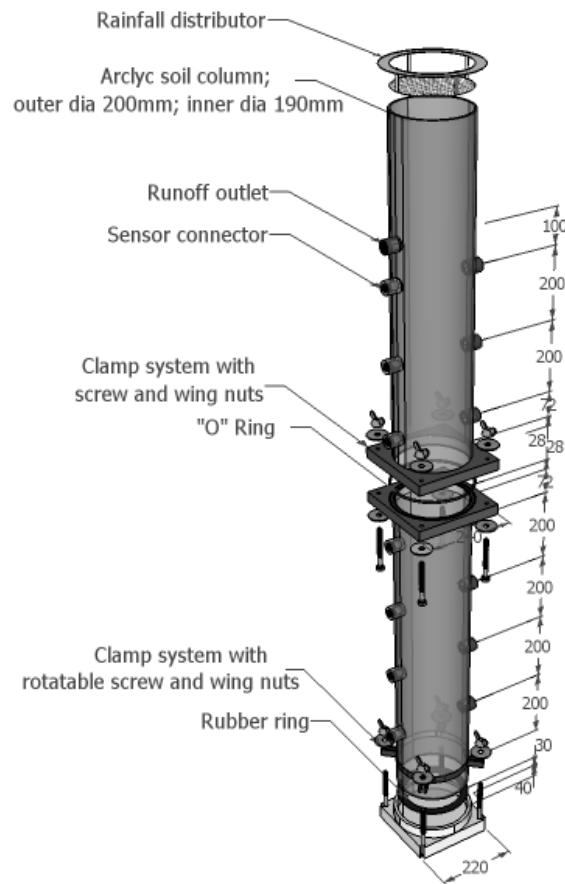


**Figure 3.13** Components of the soil column model

A perforated aluminum plate was placed on top of the soil column to avoid excessive raindrop energy that may cause erosion on the surface of soils. When a rainfall was applied, the water flowed through the holes of the plate and dripped onto a piece of filter paper that was placed in contact with the surface of the soil column. Through these arrangements, water was delivered to the soil surface in a relatively uniform pattern.

The second component of the water flow system is the overflow / runoff discharge. The overflow discharge system was used to create the no-ponding upper boundary condition for the soil column. The overflow was discharged as runoff through the outlet located at the soil surface. The runoff was then directed to a load cell that has the capacity of 2 kg, to quantify the runoff rate. Alternatively, the ponding condition can be created by sealing the runoff outlet with a threaded plug.

The last component of the water flow system is the outlet for the discharge of percolated flow. A constant head tank was placed on the floor to maintain the water table at the bottom of the soil column. This was intended to form a clear lower boundary condition. The constant head tank with large open area helped to produce a constant water table with a minimum fluctuation and to allow percolated water in the soil column to drain out freely. The constant head tank was connected to the soil column through a flexible tube. Gravels with the average size of 5mm and a filter paper were placed at the bottom of the soil column to avoid turbulent discharge flow. When water percolated through the soil column, the water flow into the constant head tank and drain out through an overflow outlet placed at the tank. The overflow was directed to a load cell to quantify the rate of percolated flow.

### 3.4.3 Instrumentations

Two types of soil suction measurement instruments were used in the study, i.e. tensiometer and gypsum block. The tensiometer (Soil Moisture Corp. Model 2100F) is equipped with pressure transducer (Soil Moisture Corp. Model 5301-B1). Attempts to measure soil suction higher than 70 kPa during calibration was unsuccessful. Therefore, the gypsum block (Soil Moisture Corp. model 5201F1L06 G-Block) with measurement capacity of 10 kPa to 1500 kPa was introduced. In this study, tensiometer was used to measure soil suction at low range of 0 kPa to 70 kPa (valid for most of the suctions measured in this study), whereas gypsum block was used to ensure that any suction higher than 70kPa could be traced during the process of setting up initial condition and redistribution. Figure 3.14a and 3.14b show an assembled tensiometer-transducer and gypsum block, respectively.

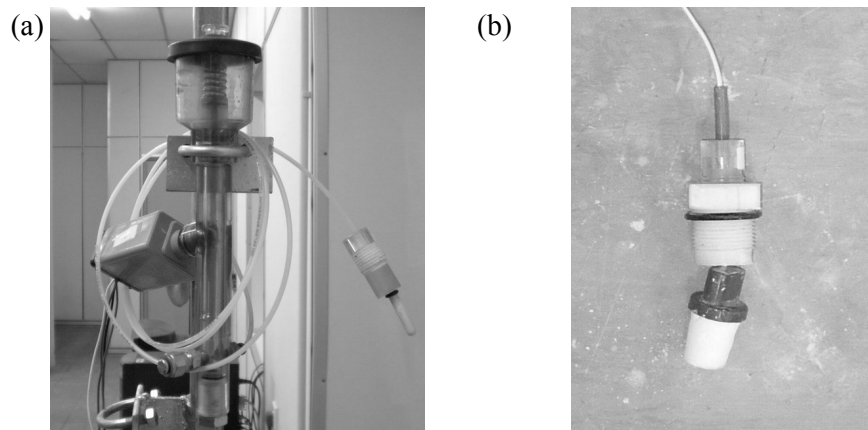


**Figure 3.14** (a) An assembled tensiometer-transducer, (b) Gypsum block

A ceramic cup was installed into the soil column through a predrilled hole after compacting the soil column. The method offers the advantages of protecting the ceramic cup from damage during soil compaction, but care should be taken to ensure that the ceramic cup was closely contacted with the soil particles. To mount the ceramic cup and the tube assembly on the wall of the acrylic column, holes with

threaded housing were fabricated on the column wall. A specially designed connector that fit well into the threaded housing, O-ring, and sealing tape were used to form a good seal at the connection. The details of the connector are shown in Figure 3.15.

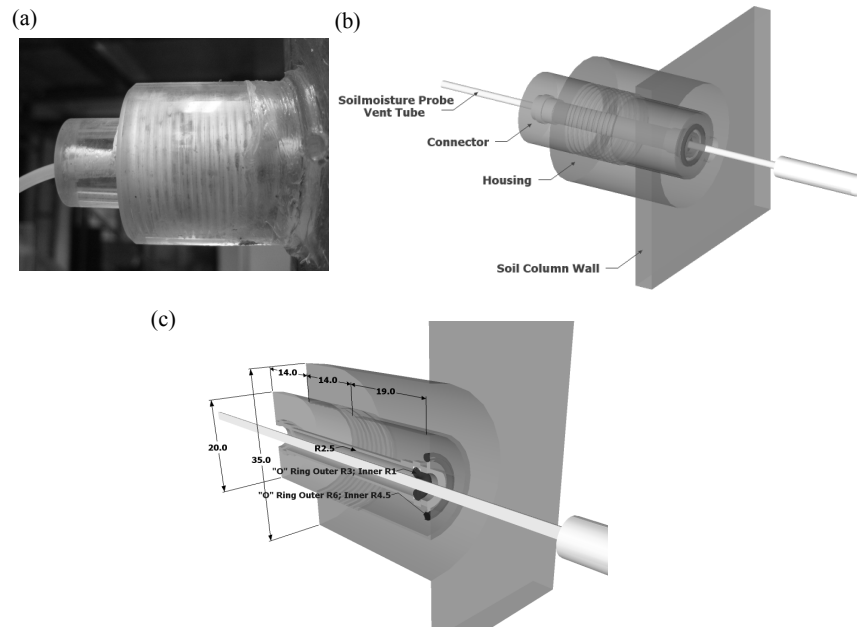


**Figure 3.15** (a) Photograph, (b) Three-dimensional diagram, and (c) Cross-sectional view of the tensiometer connector

The connection of gypsum block to soil column consisted of two parts (Figure 3.16). The first part was fitted into the housing, while the second part, facilitated by an “O” Ring, was used to seal the wire fitting to the connector. Since the gypsum block sensor was connected to the data logger via two wires, it was essential to use a wire fitting to provide a cylindrical shape for the ease of sealing. The silicon grout sealer was injected into the space in between the wire fitting and wires to provide a good seal.

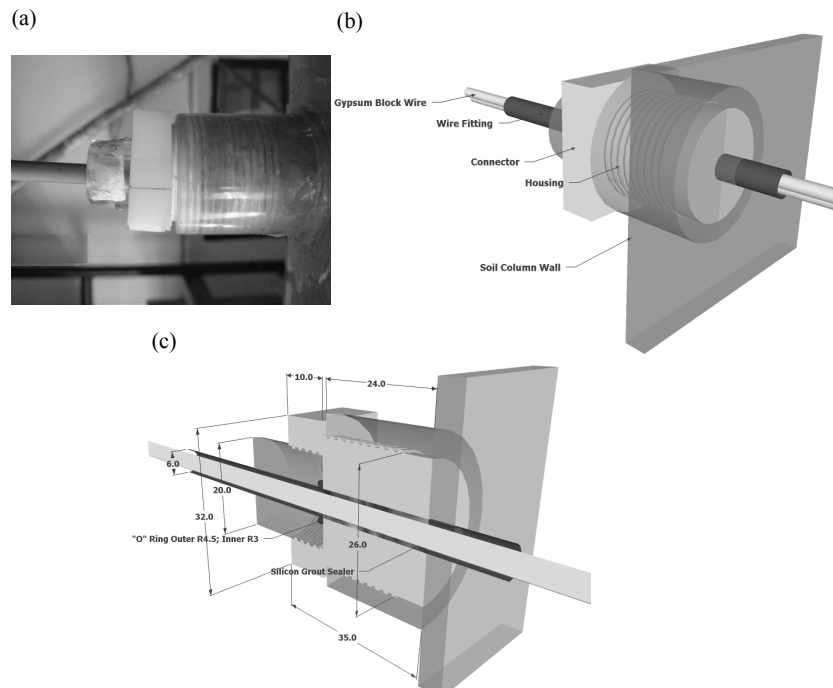


**Figure 3.16** (a) Photograph, (b) Three-dimensional diagram, and (c) Cross-sectional view of the gypsum block

### 3.4.4 Data Acquisition System

The data acquisition system used in the study comprises two units of data logger, a solid state relay, an external power supply, and a personal computer, as shown in Figure 3.17. The tensiometers and gypsum blocks were connected to the Campbell Scientific Data Logger, model CR10x (Campbell Scientific Inc.), while the load cells were connected to the GDS 8 Channel Serial Data Acquisition Pad.

The CR10x data logger consisted of two units of 32 single-ended channels multiplexer (model MUX AM416). A program was written to set up

communication and data collection between the data logger and instruments, as presented in Appendix B. Besides, a controlling software named PC208W version 2.3 was used to execute the data logger.

The CR10x data logger was powered up by an internal 12 V battery but the optimum power requirement for the tensiometer transducer system was 24 V. Therefore, the tensiometer transducer system was connected to an external 24 V power supply via a solid state relay. The functions of the solid state relay are to protect the data logger circuit and to switch on the power only when the triggering signal from data logger was received. These functions are essential to protect the tensiometer transducer system from over-heated due to long operating durations.

The GDS 8 Channel Serial Data Acquisition Pad is a data logger with eight channels of 16-bit data acquisition. The configuration of the data logger was originally designed to log the data for shearing machine. Some modifications have been made to allow the logging of four load cells concurrently. A controlling software named GDSLAB v2 was used to communicate with the GDS data logger.

The data from the data logger units were transferred to the personal computer periodically through the serial ports. The data stored in the personal computer were normally set in a format of pressure versus real time at a desired interval. An interval of 15-min was used in this study.

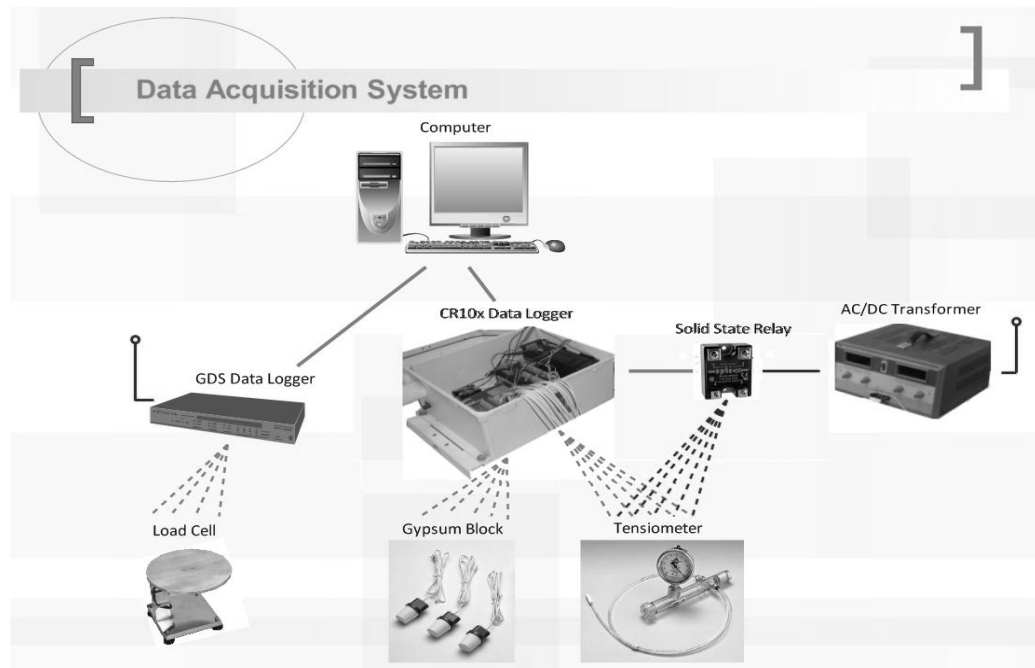


**Figure 3.17** Data acquisition system

### 3.4.5 Experimental Design

A total of 10 tests were carried out for different combinations of rainfall patterns and soil types. The initial conditions for sand, silty gravel and sandy silt were set at residual volumetric water content, while the initial condition for kaolin was simulated from the field measurement (Gofar *et al.*, 2007). These initial conditions were created by mixing the dry soil with the corresponding volumetric water content during the compaction. The description of each infiltration test is summarized in Table 3.1. Note that the ponding condition for tests no. 7 and 10 were created by maintaining a water level of 10 mm above the soil surface.

**Table 3.1:** Experimental design for infiltration tests

Test	Soil Type	Rainfall duration (hour)	Rainfall intensity (m/s)	Top Boundary Condition	Remark
1	Sand-Gravel	1	$1.84 \times 10^{-5}$	$q < k_{sat}$	
2	Sand-Gravel	24	$3.35 \times 10^{-6}$	$q < k_{sat}$	
3	Silty Gravel	1	$1.84 \times 10^{-5}$	$q > k_{sat}$	Runoff
4	Silty Gravel	24	$3.35 \times 10^{-6}$	$q < k_{sat}$	Runoff
5	Sandy Silt	1	$1.84 \times 10^{-5}$	$q > k_{sat}$	Runoff
6	Sandy Silt	24	$3.35 \times 10^{-6}$	$q > k_{sat}$	Runoff
7	Sandy Silt	120	-	Ponding	
8	Silt (Kaolin)	1	$1.84 \times 10^{-5}$	$q > k_{sat}$	Runoff
9	Silt (Kaolin)	24	$3.35 \times 10^{-6}$	$q > k_{sat}$	Runoff
10	Silt (Kaolin)	120	-	Ponding	

### 3.5 Field Study

Two study areas were selected for field monitoring purpose. The study areas were selected based on two criteria: (i) the study areas should consist of a coarse grained soil slope and a fine-grained soil slope to form the main variable in this study, and (ii) the locations of the two selected slopes should be in the vicinity of each other to ensure a uniform rainfall pattern between the two selected sites. These two criteria were essential to provide convenience in the comparison analysis.

Considering the prescribed criteria, two slopes located at Universiti Teknologi Malaysia (UTM) were selected for the monitoring purpose, namely Balai Cerapan and Kolej 12 (Figure 3.18). The Balai Cerapan slope consisted of soil that can be classified as silty gravel (coarse-grained soil). The study area poised a sloping angle of approximately  $21^\circ$  with an average length of 40m. The Kolej 12 was a sandy silt

(fine-grained soil) slope that inclined at an average angle of  $30^\circ$ . Both of the slopes were located at a distance of 2 km apart from each other. The contours and the photographs of the instrumented slopes are shown in Figure 3.19 and Figure 3.20, respectively.

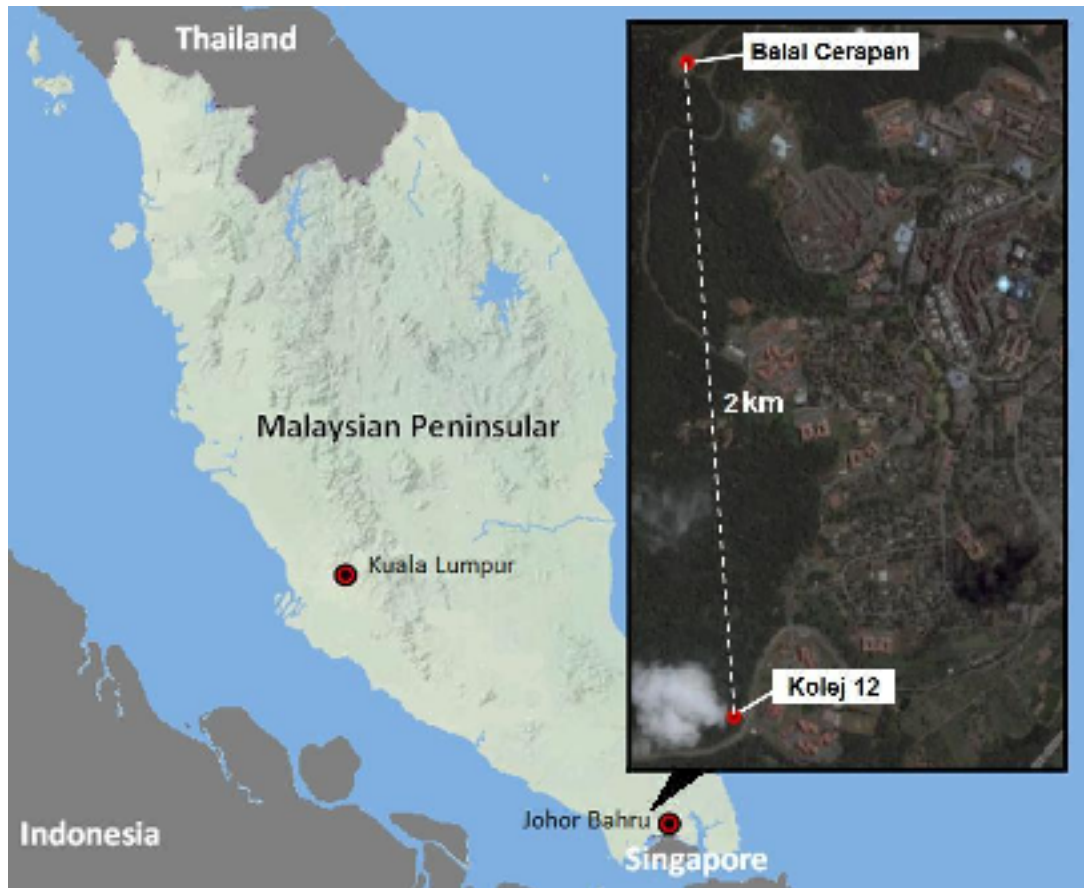


**Figure 3.18** Location map of the study areas

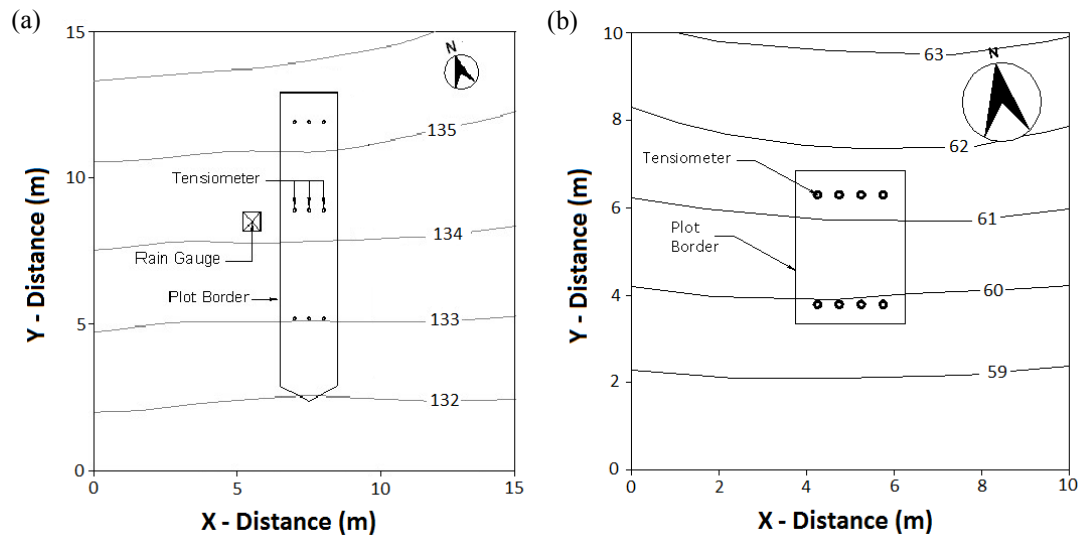


**Figure 3.19** Contours of study areas: (a) Balai Cerapan (b) Kolej 12

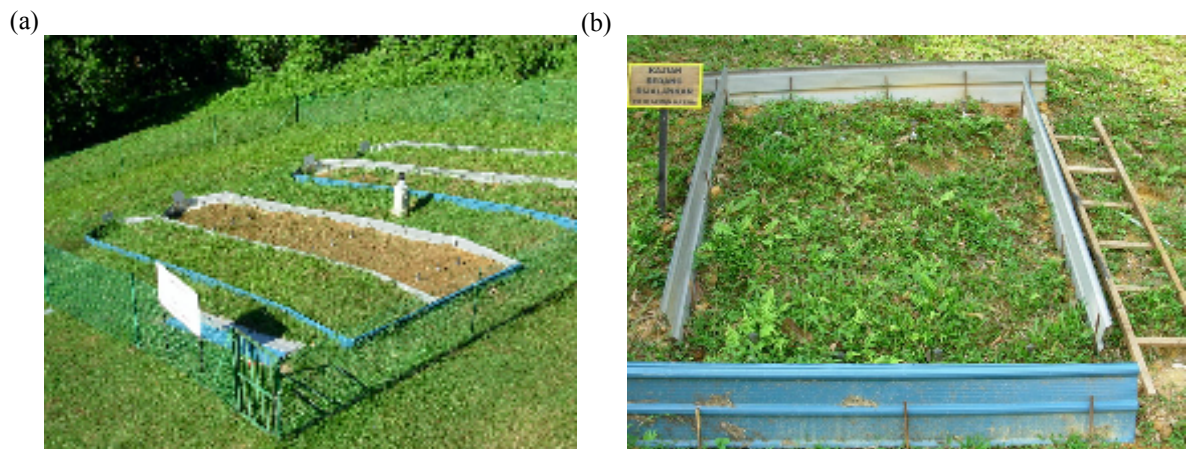


**Figure 3.20** Photographs of study areas: (a) Balai Cerapan (b) Kolej 12

### 3.5.1 Instrumentations

Three sets of measurement were collected to quantify the hydrological characteristics of the study site: (1) tensiometers to measure soil suction, (2) rain gauge to measure rainfall rate, and (3) runoff collector to measure runoff amount. In this section, the installation, measurement and calibration of each instrument are

described in details.

### **3.5.1.1 Installation of Tensiometers**

Jet-fill tensiometers (Soil Moisture Corp. model 2725) were installed at the study areas to measure the in-situ soil suction (Figure 2). The Jet-fill tensiometer was connected to a vacuum gauge that required the readings to be taken manually.

The tensiometers provided in different lengths i.e. 0.5m, 0.75m, 1m, 1.2m, and 1.5m. Prior to the installation, the ceramic cups of the tensiometers were soaked overnight in the de-aired water. De-aired distilled water was used to fill the tensiometer. The trapped air bubble in the tensiometer body and vacuum gauge was removed by using a vacuum pump. The tensiometers were then inserted into the pre-drilled holes with the top of the hole was sealed with original soil slurry to prevent direct infiltration of surface water. It should be noted that the size of the drilled hole must fit well to the diameter of the tensiometer body to ensure a good contact between the soil particles and the ceramic cup.

Upon the installation, the tensiometers were left for two days to stabilize the pore-water pressure measurement before any reading was taken. For the following two weeks period, the tensiometer readings were monitored to confirm that the soil suction measurements were in correct order before the actual field monitoring was taken place.

### **3.5.1.2 Installation of Rain Gauge**

A HOBO RG3-M tipping bucket rain gauge was installed at the study area of Balai Cerapan to measure the rainfall rate. Each tip of the rain gauge represented a 0.2mm depth of rainfall. The tipping bucket rain gauge was connected to a HOBO event data logger featured with 64,000 bytes nonvolatile data storage capacity. Generally, 8,000 data points, equivalent to the total rainfall amount of 1600mm, can be stored in the logger.

The rain gauge was sat on a concrete column to provide a plane base for a more accurate rainfall measurement. The bubble was adjusted to the center of the plug by adjusting the nuts mounted on the feet of the rain gauge. Prior to the data logging, the calibration was performed by placing a container filled with 373ml water at the top of the rain gauge. The water was allowed to drip through a pre-drilled needle sized hole at the bottom of the container. Successful field calibration of this sort should result in one hundred tips plus or minus two. A controlling software, Box-Car Pro 4.0 was used to communicate with the data logger. The logged data was retrieved periodically to a portable computer via an USB cable.

### **3.5.1.3 Installation and Calibration of Runoff Collector**

A runoff collector was placed at the lowest end of the sloping plot to quantify the runoff amount (Figure 3.21). The surface runoff, guided by the plot border, flowed into the runoff collector tank through a 50 mm-diameter pipe. The tank was designed to cater for 1-day extreme rainfall of 10 years return period at Johor Bahru. The dimensions and the components of the runoff collector are illustrated in Figure 3.22.

A removable wire mesh was installed immediately below the inlet pipe to filter sediment from runoff water. The runoff water was then directed to the bottom left corner of the tank through a sloping base. A 5 mm tube was used to guide the water flowed into the rain gauge. Through this arrangement, the water flow can be limited to a very low rate to avoid over flow at the rain gauge. The rain gauge was seated on a flat concrete base and partially covered with loose gravels to prevent the collapse of surrounding soil while providing the free-draining condition at the bottom of rain gauge.

The runoff collector was calibrated before the actual measurements were taken. The rain gauge used in the runoff collector system could only function effectively at a tipping rate lower than 100 tips per hour. However, the average flow rate into the rain gauge could be as high as 1500 tips per hour. Therefore, calibration tests were performed by pouring a known volume of water into the runoff collector tank. The amount of water recorded from the rain gauge was compared to the actual amount of water. The calibration graph of the runoff collector is shown in Appendix C. It was found that the rainfall amount measured from the rain gauge could be approximated to the actual rainfall amount by multiplying a constant of 3.63.



**Figure 3.21** Runoff collector installed at research plot

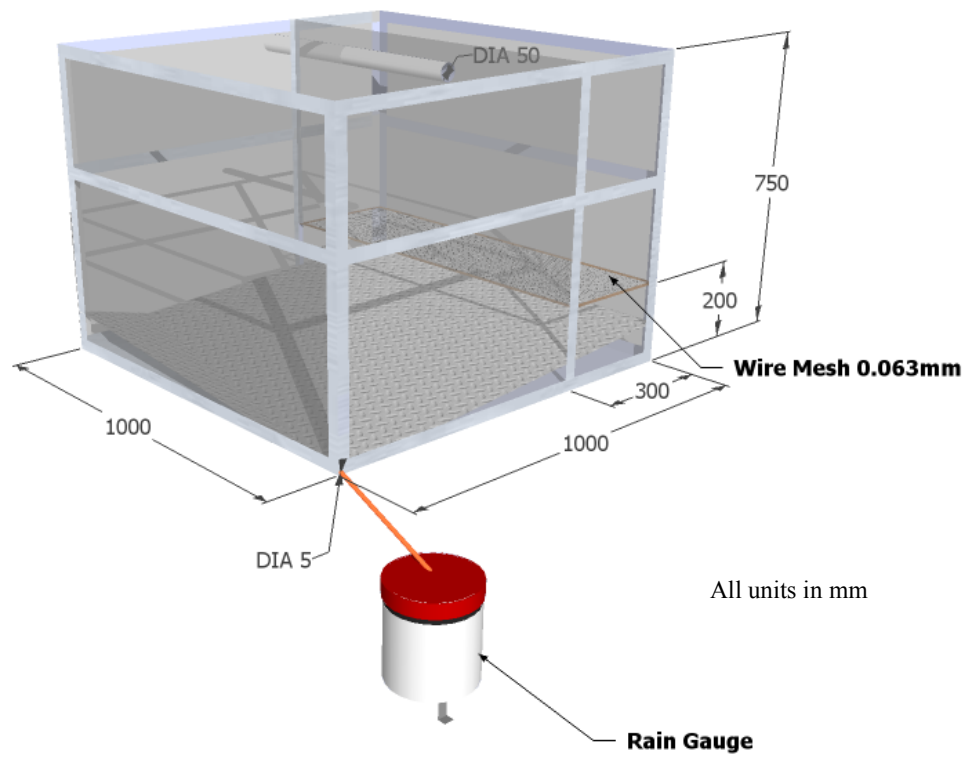


**Figure 3.22** Dimensions and components of runoff collector

### **3.5.2 Field Monitoring**

The field monitoring was carried out for a period of 12 months (from 12 September 2006 to 11 September 2007) at Balai Cerapan site, and six months (from July 2007 to January 2008) at Kolej 12 site. During the course of the monitoring period, the suction measurements were taken manually three times per day (morning, afternoon, and evening), while the measurements of rainfall were retrieved once in a month.

### **3.6 Concluding Remarks**

In conclusion, this chapter provides the detail descriptions of the research phases (i.e. research initialization, preliminary data collection, experiment and analysis, verification, and generalization), and research methodologies (i.e. numerical simulation, laboratory modeling, and field monitoring and study cases) employed in this study. The use of multiple methodologies permitted triangulation of data to improve the validity of the findings, and enable greater inferences from the results.

## **CHAPTER 4**

### **PRELIMINARY DATA**

#### **4.1 Introduction**

The preliminary data for the numerical and laboratory models are presented in this chapter. Generally, the data can be divided into two parts, i.e.: the extreme rainfall distribution computed from the statistical analysis, and the soil properties obtained from a series of laboratory tests.

#### **4.2 Extreme Rainfall Distribution**

The extreme rainfall distribution was obtained by utilizing both DID's (2001) equation and Gumbel's (1958) distribution. The ten-year return period extreme rainfalls for five selected locations in the Malaysian Peninsular are tabulated in Table 4.1, while the Intensity-Duration-Frequency (IDF) curve are illustrated in Figure 4.1.

**Table 4.1:** Ten-year return period extreme rainfalls for five selected locations in the Malaysian Peninsular

Location	Kuala Lumpur		Johor Bahru		Pulau Pinang		Kuantan		Kota Bharu	
	<i>P</i>	<i>I</i>	<i>P</i>	<i>I</i>	<i>P</i>	<i>I</i>	<i>P</i>	<i>I</i>	<i>P</i>	<i>I</i>
1 hour	84	83.9	88	88.4	93	92.8	93	93.3	94	94.5
2 hours	100	50.1	109	54.4	114	56.9	124	62.1	129	64.4
4 hours	114	28.6	130	32.5	132	33.1	162	40.4	175	43.7
8 hours	128	16.0	156	19.5	153	19.1	214	26.8	243	30.4
16 hours	146	9.1	197	12.3	184	11.5	301	18.8	346	21.6
1 day	159	6.6	218	9.1	222	9.3	368	15.3	413	17.2
2 days	201	4.2	253	5.3	301	6.3	516	10.7	541	11.3
3 days	228	3.2	287	4.0	351	4.9	619	8.6	628	8.7
5 days	272	2.3	336	2.8	413	3.4	743	6.2	729	6.1
7 days	323	1.9	368	2.2	461	2.7	856	5.1	807	4.8
14 days	496	1.5	453	1.3	604	1.8	1086	3.2	936	2.8
30 days	636	0.9	647	0.9	929	1.3	1355	1.9	1129	1.6

Note: *P* = Rainfall amount in unit mm; *I* = Rainfall intensity in unit mm/hour

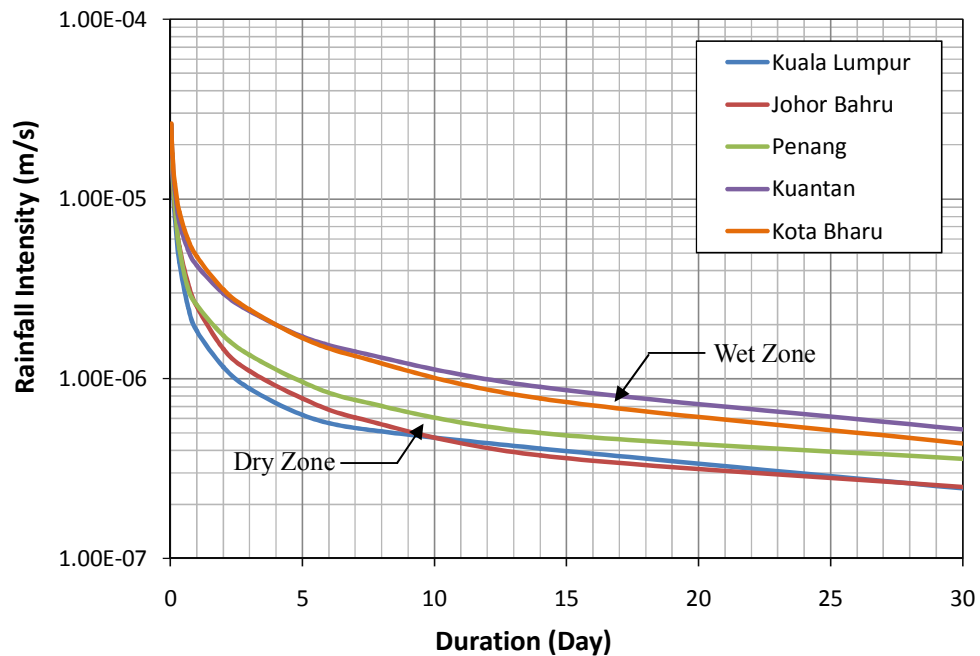


**Figure 4.1** IDF curves for five selected locations in the Malaysian Peninsular

Cities located on the east coast of the Peninsula (i.e. Kuantan and Kota Bharu) receive greater amounts of rainfall compared to cities on the west coast (i.e. Pulau Pinang, Johor Bahru and Kuala Lumpur) due to the geographical location and the direction of monsoon wind. Thus, it is adequate to categorize the rainfall distribution in the Malaysian Peninsular into two zones i.e. the wet zone on the east coast and the dry zone on the west coast.

#### **4.2.1 Assumption of Surface Runoff**

In the experiments, only 70% of the extreme rainfalls obtained from the IDF curve were applied as infiltration, while the remaining 30% was assumed to contribute as surface runoff. This assumption was deemed conservative compared to the previous studies by Ng *et al.* (2003) and Rahardjo *et al.* (2004) who assumed 60% and 40% of rainfall infiltration, respectively.

In order to further clarify this assumption, the runoff amounts for twenty rainfall events, occurred from July 2007 to August 2007, were collected at Balai Cerapan site by using a fabricated runoff collector. Despite of the fact that the infiltration characteristics are governed by several factors such as ground surface cover, slope angle, type of soil etc., only the rainfall pattern was considered in this study assuming other factors are negligible.

Table 4.2 presents the rainfall and runoff data recorded for 20 rainfall events. Generally, the runoff amount can be positively correlated with the rainfall amount and rainfall intensity. Since the runoff percentage was governed by two variables, a non-linear regression analysis was required to solve the equation. Figure 4.2 shows the output of the regression analysis. The relationship between the runoff

percentage ( $R_f$ ) with the rainfall intensity ( $i$ ) and total rainfall depth ( $P$ ) is expressed by an equation as follows:

$$R_f (\%) = 85.078 \left[ 1 - \frac{1}{1.00013246^{(13.944 \times I \times P)}} \right] \quad (4.1)$$

Under typical rainfall condition, most of the measured runoff amounts were within 30% of total rainfall. As for the case of intense rainfall (rainfall depth greater than 70mm), the runoff amount can be as high as 90% of total rainfall. Thus, the assumption of 30% of total rainfall contribute to the runoff should be deemed as a conservative assumption for the extreme rainfall assigned in the numerical simulation.

**Table 4.2:** Rainfall and runoff data recorded from July 2007 to August 2007

<b>Event</b>	<b>Duration</b> (min)	<b>Rainfall Depth</b> (mm)	<b>Rainfall Intensity</b> (mm/hr)	<b>Rainfall Amount</b> $\times 10^5$ (mm <sup>3</sup> )	<b>Runoff Amount</b> $\times 10^5$ (mm <sup>3</sup> )	<b>Runoff Percentage</b> (%)
1	10.8	1.2	6.67	24	0.27	1.13
2	75.3	10	7.97	200	27.49	13.74
3	34.6	12.6	21.85	252	35.54	14.10
4	117.1	33.2	17.01	664	487.84	73.47
5	92.3	11.6	7.54	232	76.30	32.89
6	152.5	6.6	2.60	132	5.28	4.00
7	34.7	9.4	16.25	188	38.18	20.31
8	198.4	38	11.49	760	510.86	67.22
10	20.7	6	17.39	120	4.40	3.67
11	63.6	1.8	1.70	36	0.20	0.56
12	68.9	1.4	1.22	28	0.07	0.24
13	69.1	2.8	2.43	56	0.00	0.00
14	77.9	4	3.08	80	2.03	2.54
15	264.1	16.4	3.73	328	32.70	9.97
16	103.4	12.2	7.08	244	10.63	4.36
17	62.7	75.4	72.15	1508	1360.82	90.24
18	103.6	9.4	5.44	188	4.47	2.38
19	161.8	16.6	6.16	332	0.00	0.00
20	72.7	27.8	22.94	556	213.67	38.43

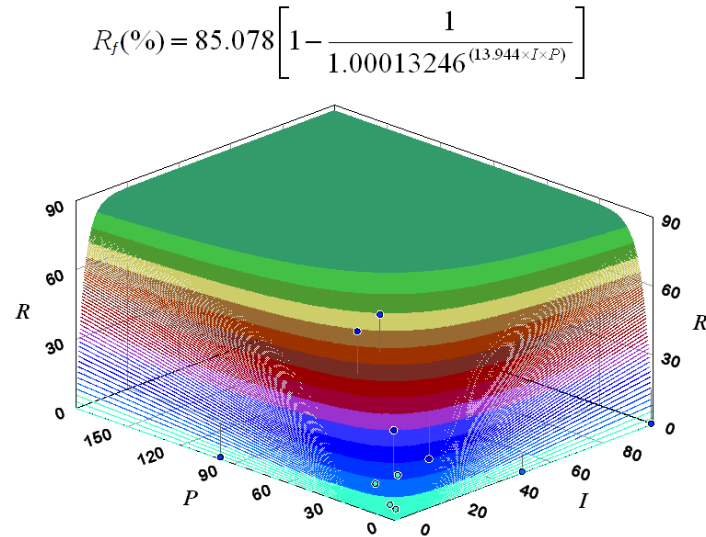


**Figure 4.2** Output of non-linear regression analysis for the relationship between rainfall and runoff

### 4.3 Soil Properties

Four types of soil (i.e. sand-gravel, silty gravel, sandy silt and silt) were employed in the experiments. Their physical properties were determined through the laboratory tests. Figure 4.3 shows the particle size distribution (PSD) of the soils used in this study, while Table 4.3 presents the properties of the soils, including particles composition, liquid limit (LL), plastic limit (PL), plasticity index (PI), soil classification according to British Soil Classification System (BSCS), specific gravity ( $G_s$ ), bulk density ( $\rho_b$ ), dry density ( $\rho_d$ ), maximum dry density (MDD), optimum moisture content (OMC), maximum relative density, saturated permeability ( $k_{sat}$ ), effective cohesion ( $c'$ ), and effective friction angle ( $\phi'$ ).

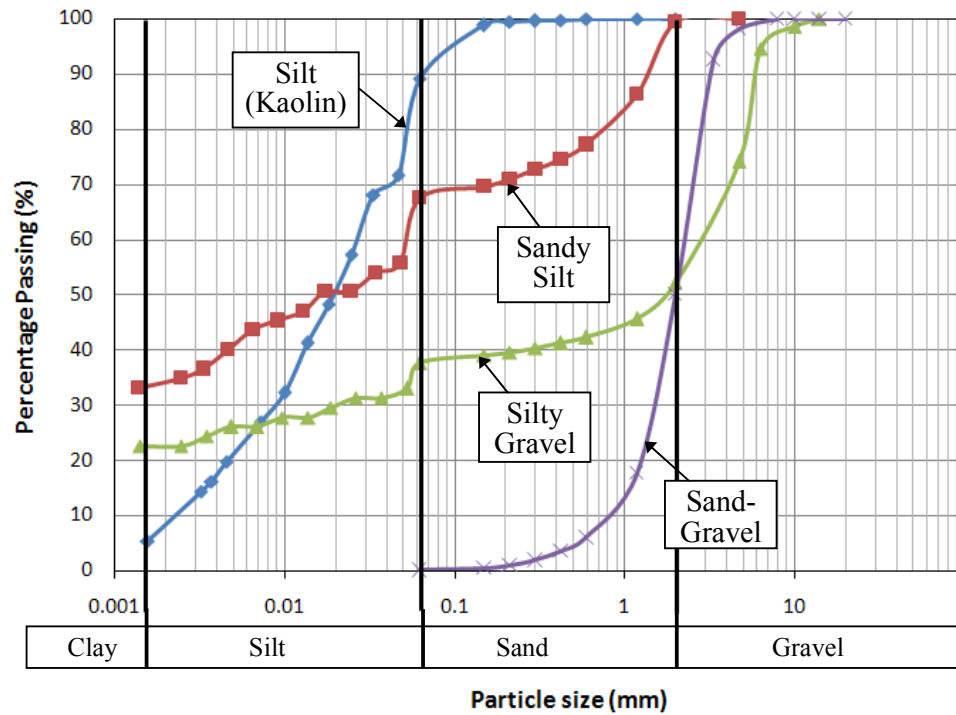


**Figure 4.3** Particle size distribution of soils used in the study

The sand-gravel used in the study was a natural hill sand that contained equal portions of sand and gravel, while the sandy silt and silty gravel were the soil obtained from the same origin, hereby exhibited similarity in some of the physical properties. The silt (kaolin) was coarse kaolin that contained large portion of silt particles.

The scanning electron micrograph (SEM) images of the soil samples are illustrated in Figure 4.4. Figure 4.4a shows that the particles of sand-gravel are irregularly shaped and the sizes are relatively large. The silty gravel (Figure 4.4b) and sandy silt (Figure 4.4c) consisted of wide range of particle sizes. The microstructure of the soils demonstrated some similarities as both soils were obtained from the same origin. Figure 4.4d shows that the particles sizes of silt (kaolin) are relatively fine and uniform.

**Table 4.3:** Physical properties of soils used in the study

	<b>Sand-Gravel</b>	<b>Silty Gravel</b>	<b>Sandy Silt</b>	<b>Silt (Kaolin)</b>
<b>Composition</b>				
Gravel (%)	50	48	0	0
Sand (%)	50	15	33	11
Silt (%)	0	20	34	81
Clay (%)	0	17	33	8
<b>LL (%)</b>	-	53.2	59.3	44.8
<b>PL (%)</b>	-	35.5	31.9	30.6
<b>PI</b>	-	17.7	27.4	14.2
<b>Soil Classification BSCS</b>	S-GP	GMH	MHS	MI
<b>G<sub>s</sub></b>	2.65	2.65	2.63	2.52
<b>ρ<sub>b</sub> (kg/m<sup>3</sup>)</b>	-	1805	-	-
<b>ρ<sub>d</sub> (kg/m<sup>3</sup>)</b>	-	1366	-	-
<b>MDD (kg/m<sup>3</sup>)</b>	-	-	1415	1587
<b>OMC (%)</b>	-	-	31.0	19.3
<b>Density @ e<sub>max</sub> (kg/m<sup>3</sup>)</b>	1856	-	-	-
<b>K<sub>sat</sub> (m/s)</b>	3.44 x 10 <sup>-4</sup>	3.68 x 10 <sup>-6</sup>	5.00 x 10 <sup>-7</sup>	6.78 x 10 <sup>-8</sup>
<b>CU Test</b>				
c' (kPa)	-	-	7.6	9.2
φ' (°)	-	-	32.1	17.6
<b>Direct Shear</b>				
c' (kPa)	1.2	3.3	-	-
φ' (°)	38.7	39.5	-	-

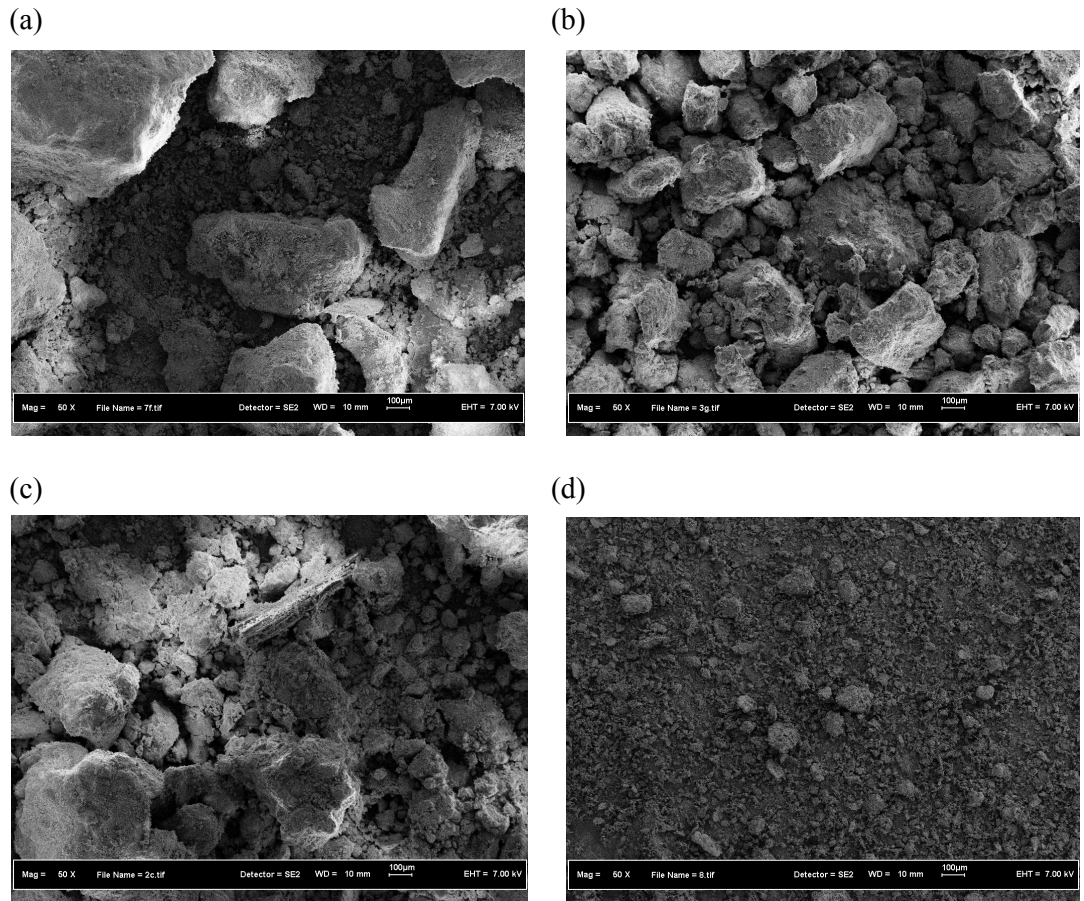


**Figure 4.4** SEM images of (a) sand-gravel, (b) silty gravel, (c) sandy silt, and (d) silt (kaolin)

The mineral constituents determined from XRD test are tabulated in Table 4.4, while the mineral composition of the soils obtained from the mineralogy test are summarized in Table 4.5. Generally, the results obtained from the chemical tests showed great agreement with the physical tests. For instance, the sand-gravel contained large portion of quartz mineral, while the silt (kaolin) consisted of large portion of kaolinite. The mineral constituents of sandy silt and silty gravel were found almost identical to each other.

**Table 4.4:** Mineral constituents obtained from XRD test

<b>Soil Type Mineral Constituents</b>	<b>Sand- Gravel</b>	<b>Silty Gravel</b>	<b>Sandy Silt</b>	<b>Silt (Kaolin)</b>
<b>Major Constituents</b>	Quartz, Feldspar, Iron Oxide	Gibbsite	Kaolinite, Smectite, Iron Oxide	Kaolinite, Quartz
<b>Minor Constituents</b>	-	Quartz, Kaolinite, Iron Oxide, Geothite, Smectite	Geothite, Quartz	-
<b>Trace Amounts</b>	Montmorillonite	Feldspar	-	Feldspar, Fluorite

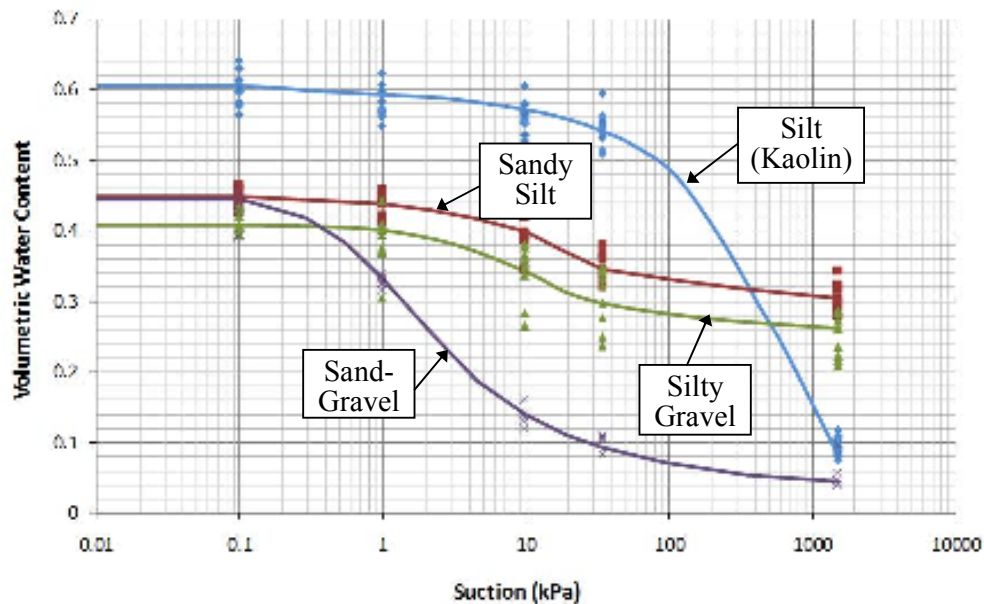
**Table 4.5:** Mineral compositions obtained from mineralogy test

<b>Soil Type Minerals</b>	<b>Sand- Gravel (%)</b>	<b>Silty Gravel (%)</b>	<b>Sandy Silt (%)</b>	<b>Silt (Kaolin) (%)</b>
<b>Clay minerals</b>	15.0	65.0	72.0	88.0
<b>Quartz</b>	76.0	8.5	15.5	10.0
<b>Feldspar</b>	8.5	19.0	11.0	1.5
<b>Iron-oxides</b>	Tr	7.5	1.5	0.5
<b>Rock fragments</b>	-	Tr	Tr	-
<b>Magnetite</b>	Tr	Tr	Tr	-
<b>Hematite</b>	0.5	Tr	Tr	-
<b>Ilmenite</b>	Tr	Tr	Tr	Tr
<b>Hidroilmenite</b>	Tr	Tr	Tr	Tr
<b>Zircon</b>	Tr	Tr	-	Tr
<b>Tourmaline</b>	-	Tr	-	-
<b>Monazite</b>	-	Tr	-	-
<b>TOTAL</b>	<b>100</b>	<b>100</b>	<b>100</b>	<b>100</b>

Note: Tr – Concentration less than 0.5%

Figure 4.5 shows the SWCC for the four types of soils employed in the study. The SWCC was determined by fitting the average values obtained from a series of pressure plate extractor tests. From the SWCC, the parameters include saturated volumetric water content ( $\theta_s$ ), air entry value ( $A_{ev}$ ) and residual volumetric water content ( $\theta_r$ ) were identified and tabulated in Table 4.6.

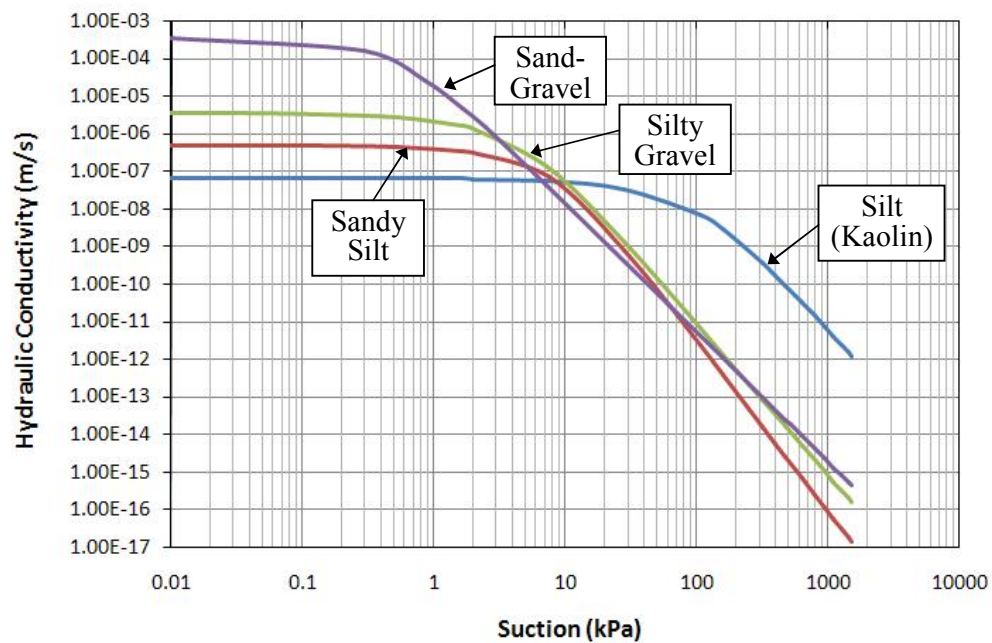
The hydraulic conductivity functions of the soils were predicted by using Van Genuchten's (1980) method, as illustrated in Figure 4.6. The Van Genuchten's method was preferred over the widely known Fredlund and Xing's method (1993) because the Fredlund and Xing's method (1993) could only give the best prediction provided the SWCC was in full curve (suction data up to residual water content). In this study, the full curve for silt (kaolin) was not obtained due to the suction corresponding to the residual water content is higher than the capacity of pressure plate apparatus (1500 kPa).



**Figure 4.5** SWCC of soils used in the study

**Table 4.6:** SWCC parameters of soils used in the study

Soil Type	Sand-Gravel	Silty Gravel	Sandy Silt	Silt (Kaolin)
Saturated Vol. Water Content, $\theta_s$	0.45	0.41	0.45	0.61
Air Entry Value, $A_{ev}$ (kPa)	0.3	3.5	7	70
Residual Water Content, $\theta_r$	0.08	0.28	0.34	-

**Figure 4.6** Hydraulic Conductivity function predicted by Van Genuchten's method (1980)

In general, the soil with larger grain size and inter-particle pores is less capable to maintain saturation. Furthermore, the large inter-particles pores could result in higher saturated permeability. Under such circumstances, the water can

easily drain out from the soil. As the result, the  $A_{ev}$  of coarse-grained soil was very low (i.e. 0.3 kPa for sand, and 3.5 kPa for silty gravel). Conversely, the soil that consisted of high fraction of fine particles has the ability to retain water under high suction, hence resulted in higher  $A_{ev}$ . Thus, it can be concluded that the PSD and the structure of the soils reflected their SWCC and hydraulic conductivity function.

#### **4.4 Concluding Remarks**

In conclusion, the preliminary input data for the experimental models are presented in this chapter. The statistical prediction of extreme rainfall distribution was used to characterize the rainfall pattern applied in the experiment, while the laboratory tests were conducted to determine the properties of the soil materials used in this study. In general, the chemical and physical properties of the soil reflected its hydraulic properties.

## **CHAPTER 5**

### **RESULTS AND DISCUSSIONS**

#### **5.1 Introduction**

This chapter presents the results of numerical simulations, laboratory tests and field monitoring. The purpose of conducting the laboratory tests and field studies are to verify the findings of numerical simulations.

#### **5.2 Numerical Simulations**

The results of numerical simulations are presented in the following sections: (a) parametric study, and (b) critical rainfall pattern analysis. A chart is developed to estimate the critical rainfall duration, critical rainfall intensity and minimum suction value for different types of soil at different locations considered in this study. The critical rainfall intensity and duration is the intensity and the duration of rainfall causing suction distribution which results in the lowest factor of safety. The minimum suction value is the lowest achievable suction induced by a certain rainfall pattern.

### **5.2.1 Parametric Study**

In this section, the responses of suction distribution to several variables including initial condition, rainfall intensity, rainfall duration, and slope inclination are discussed in detail.

#### **5.2.1.1 Influence of Initial Condition on Suction Distribution**

The initial condition refers to an initial suction distribution assigned to a soil model at the beginning of a transient analysis. As predicted, the computed suction distribution would be affected by its initial condition. In this section, the influence of initial condition on the suction distribution was analyzed for two patterns of rainfall, i.e.: a short and intense rainfall (major rainfall) and a long and less intense rainfall (antecedent rainfall), as illustrated in Figure 5.1 and Figure 5.2, respectively. The results showed that the initial condition has no influence on the resultant minimum suction value. Conversely, the propagations of wetting front were greatly affected by the initial condition, with the impact was particularly obvious for the case of prolonged antecedent rainfall. The results can be explained by the water balance theory. When the slopes of two different initial conditions were subjected to equal rainfall infiltration, the resultant minimum suction or volumetric water content value were the same, hence the soil with wetter initial condition would definitely induce greater wetting front depth compared to the soil with dryer initial condition.

Considering the importance of the initial condition in a transient state analysis; it is thus essential to assign an initial condition representative of the natural moisture condition of a soil slope. To determine the initial condition for each type of soil, a numerical simulation was performed by assigning an initial condition of 5kPa to

represent a very wet condition. The suction of 5kPa was preferred over 0kPa because it is unlikely for the highly permeable soil (i.e. sand-gravel) to achieve zero suction under typical rainfall condition in the Malaysian Peninsular. The soil model was then left dry for three months.

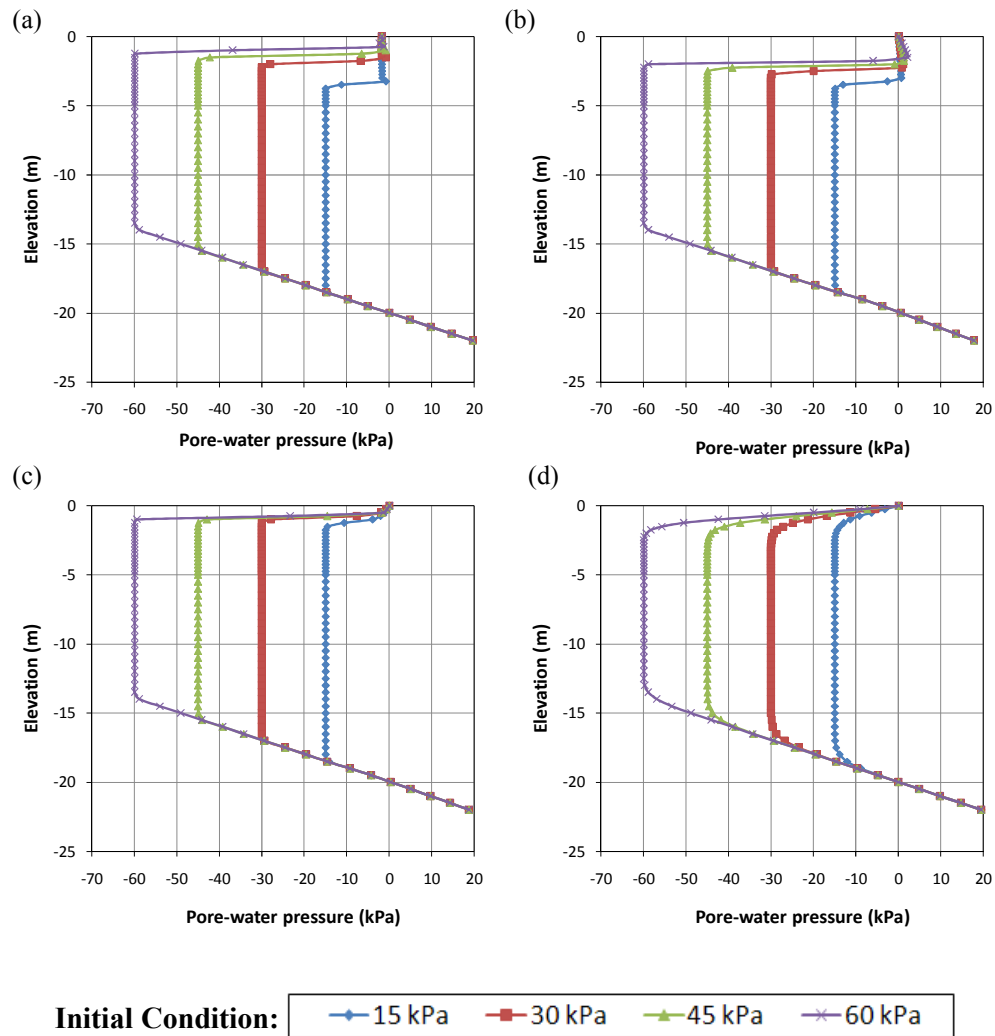


**Figure 5.1** Influence of initial condition on suction distribution as the result of short and intense rainfall for (a) sand-gravel, (b) silty gravel, (c) sandy silt, and (d) silt (kaolin)

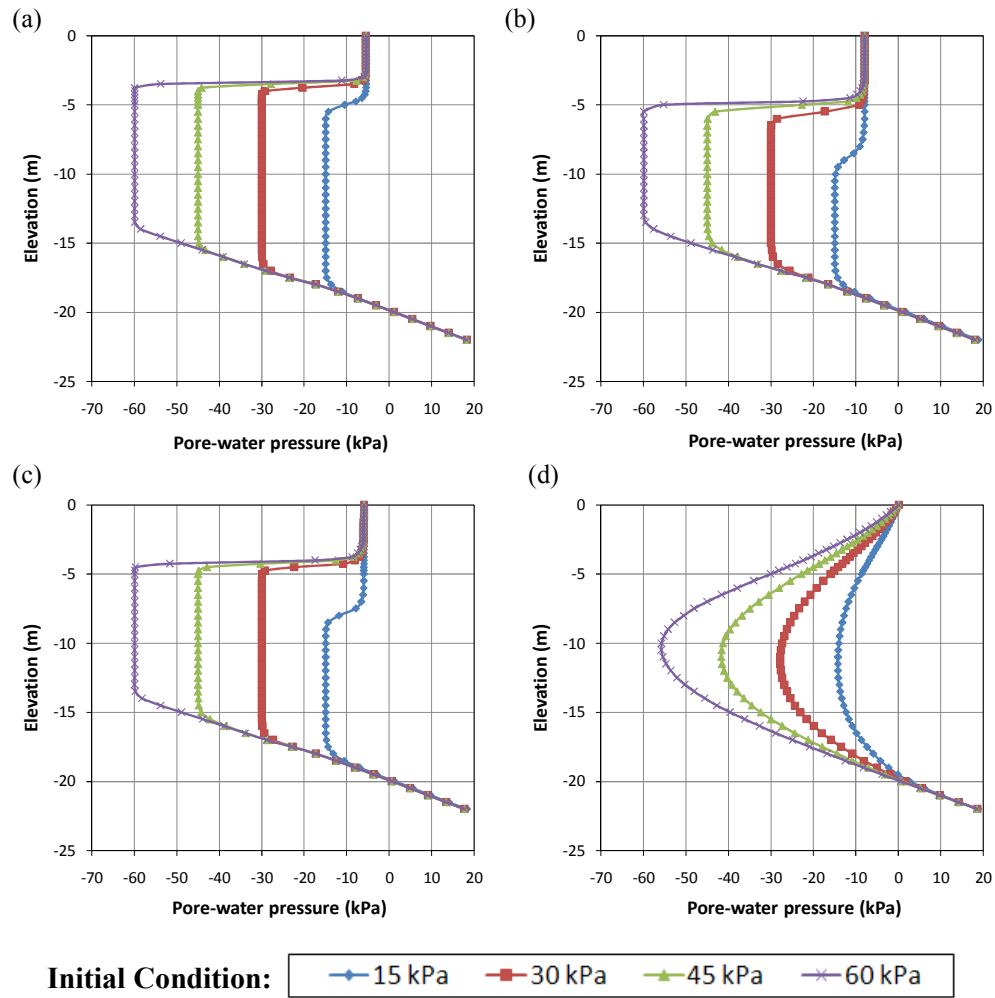


**Figure 5.2** Influence of initial condition on suction distribution as the result of prolonged rainfall for (a) sand-gravel, (b) silty gravel, (c) sandy silt, and (d) silt (kaolin)

Figure 5.3 shows the drying paths of the suction distributions for the four types of soil. It was found that the increment of suction retarded when the volumetric water content of soil was approaching its residual value ( $\theta_r$ ). For instance, the suction corresponding to the residual volumetric water content ( $\psi_r$ ) of sand-gravel was 10 kPa (refer to Figure 4.5). Obviously, the increment rate of suction became very slow when the suction approached 10 kPa. The suction increment rate for silt (kaolin) has no sign of retarding after 120 days of drying

because the suction corresponding to the residual volumetric water content of the soil was extremely high (greater than 1500kPa).

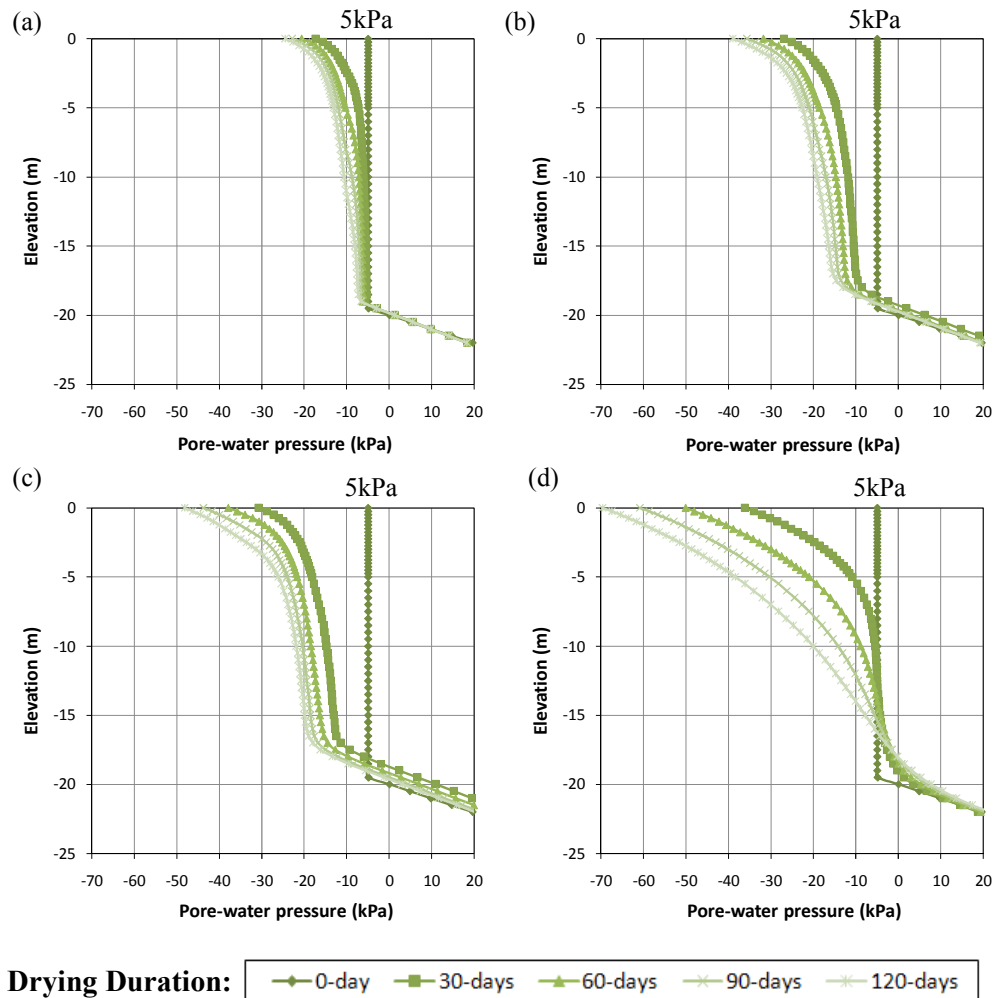


**Figure 5.3** Drying paths of suction for (a) sand-gravel, (b) silty gravel, (c) sandy silt, and (d) silt (kaolin)

In this study, the initial condition for a soil was determined based on two criteria: i) the initial condition should represent the dry condition of soil, and ii) it is realistic and achievable in actual site condition. Exception to the silt (kaolin) that has a very high  $\psi_r$ , the initial limiting suction predicted from the residual volumetric water content ( $\theta_r$ ) of SWCC met well with these criteria. Thus, 10kPa, 23kPa, and

30kPa were chosen as the limiting values of the initial condition for sand-gravel, silty gravel, and sandy silt, respectively (Figure 5.4). As for silt (kaolin), the initial condition could be as high as 1500kPa if predicted by using the same approach, which is quite unrealistic. Thus, considering the drying paths shown in Figure 5.3d and the suction monitored from the field study, a limiting value of 50 kPa was more appropriate for the initial condition of silt (kaolin). Since the suction of 50 kPa is still lower than the air-entry value ( $A_{ev}$ ) of silt (approximately 70 kPa), the unsaturated hydraulic conductivity of the soil could be assumed to be a constant (refer to Figure 4.5 and 4.6). Therefore, a sloping initial condition was predicted. The initial conditions for the four types of soil are illustrated in Figure 5.5.

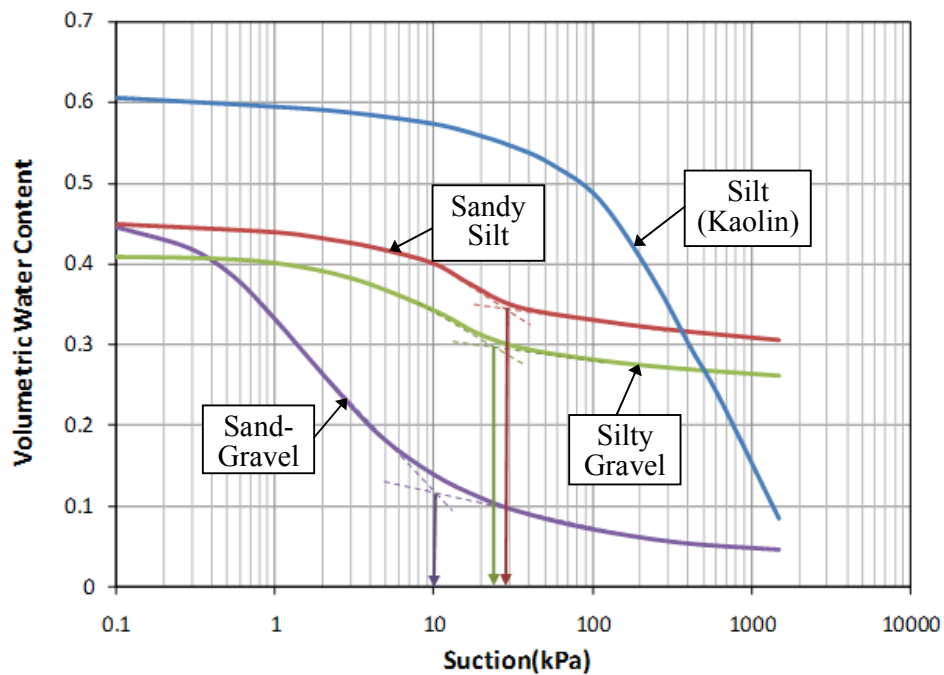


**Figure 5.4** Estimation of initial condition from SWCC

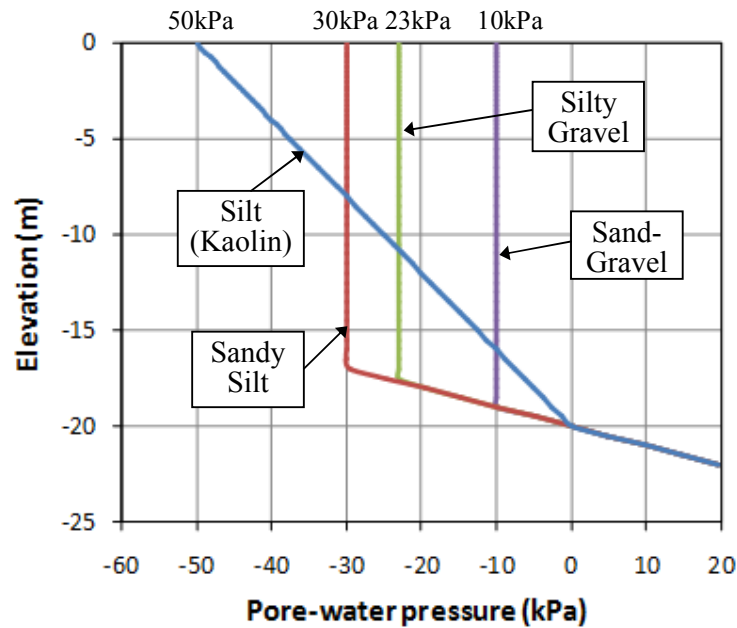


**Figure 5.5** Initial conditions for the four types of soil

### 5.2.1.2 Influence of Rainfall Intensity on Suction Distribution

Figure 5.6 (a-d) show the suction distributions generated in sand-gravel, silty gravel, sandy silt and silt (kaolin) as the result of 1-day rainfall of various intensities. For sand-gravel with high saturated permeability ( $k_{sat} = 3.4 \times 10^{-4}$  m/s), it was found that higher rainfall intensity resulted in deeper wetting front (Figure 5.6a). The minimum suction values were just slightly altered by the rainfall intensities as more water infiltrated into the soil. The result implies that the influence of rainfall intensity on the minimum suction at shallow depth was not significant for soil with high saturated permeability.

For silty gravel and sandy silt with moderate saturated permeability,  $k_{sat} = 3.7 \times 10^{-6}$  m/s and  $5.0 \times 10^{-7}$  m/s respectively, the responses of the suction distributions

to rainfall intensity were largely influenced by the relative value of  $q/k_{sat}$ . As illustrated in Figure 5.6b and 5.6c, the suction distribution and the minimum suction value for  $q/k_{sat} < 1$  were greatly affected by the rainfall intensities. Conversely, the rainfall with  $q/k_{sat} > 1$  had no influence on the suction distribution. Thus, the ratio of rainfall intensity to the saturated permeability of soil is the dominant factor that controls the rainfall infiltration.

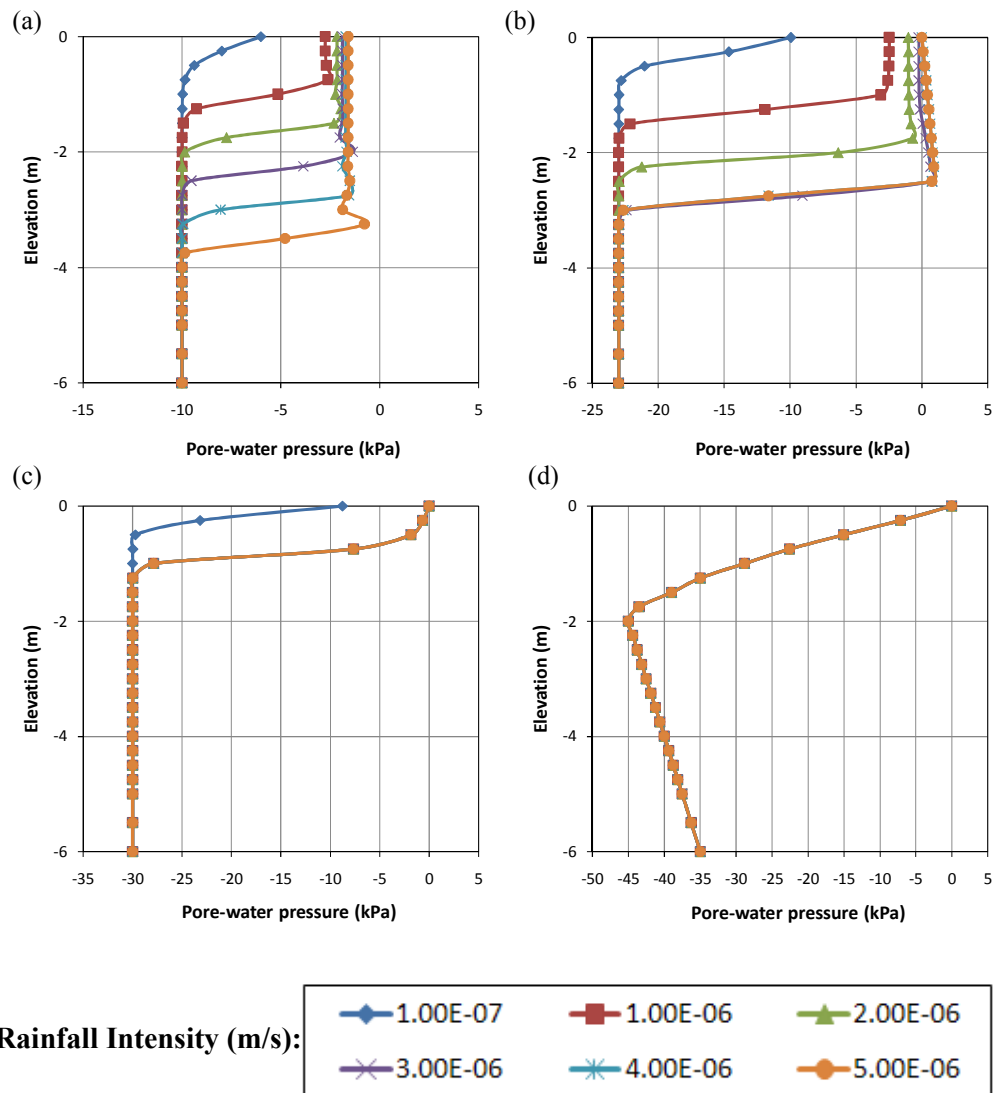


**Figure 5.6** Influence of rainfall intensity on the suction distribution for (a) sand-gravel, (b) silty gravel, (c) sandy silt, and (d) silt (kaolin)

Regarding the soil with very low saturated permeability (i.e. silt,  $k_{sat} = 6.8 \times 10^{-8}$  m/s), the rainfall intensity does not play any role in the resultant suction distribution because, as observed in the IDF curve of five selected locations in the Malaysian Peninsular,  $q/k_{sat}$  is always  $> 1$  (Figure 5.6d). Therefore, the influence of rainfall intensity on suction distribution for kaolin can be disregarded.

In conclusion, the study on the effect of rainfall intensity on the suction distribution should look into two areas, i.e. the minimum suction value and the wetting front depth. The minimum suction value can be predicted from the hydraulic conductivity function. By taking the unsaturated hydraulic conductivity equivalent to the applied rainfall intensity, the minimum suction value can be estimated directly from the function. The variation in minimum suction value of a soil was largely influenced by the applied rainfall intensity, and the slope of the hydraulic conductivity function of the soil concerned. As for the depth of wetting front, it can be explained by the water balance theory which will be discussed in detail in the following section.

### **5.2.1.3 Influence of Rainfall Duration on Suction Distribution**

Figures 5.7 (a-d) show the influence of rainfall duration on the suction distribution for sand-gravel, silty gravel, sandy silt and silt (kaolin), respectively with the constant rainfall intensity equal to  $1 \times 10^{-7}$  m/s. The study showed that the rainfall duration had no influence on the reduction of minimum suction values for all types of soil. However, the duration of rainfall had a significant influence on the advancement depth of wetting front in soil.

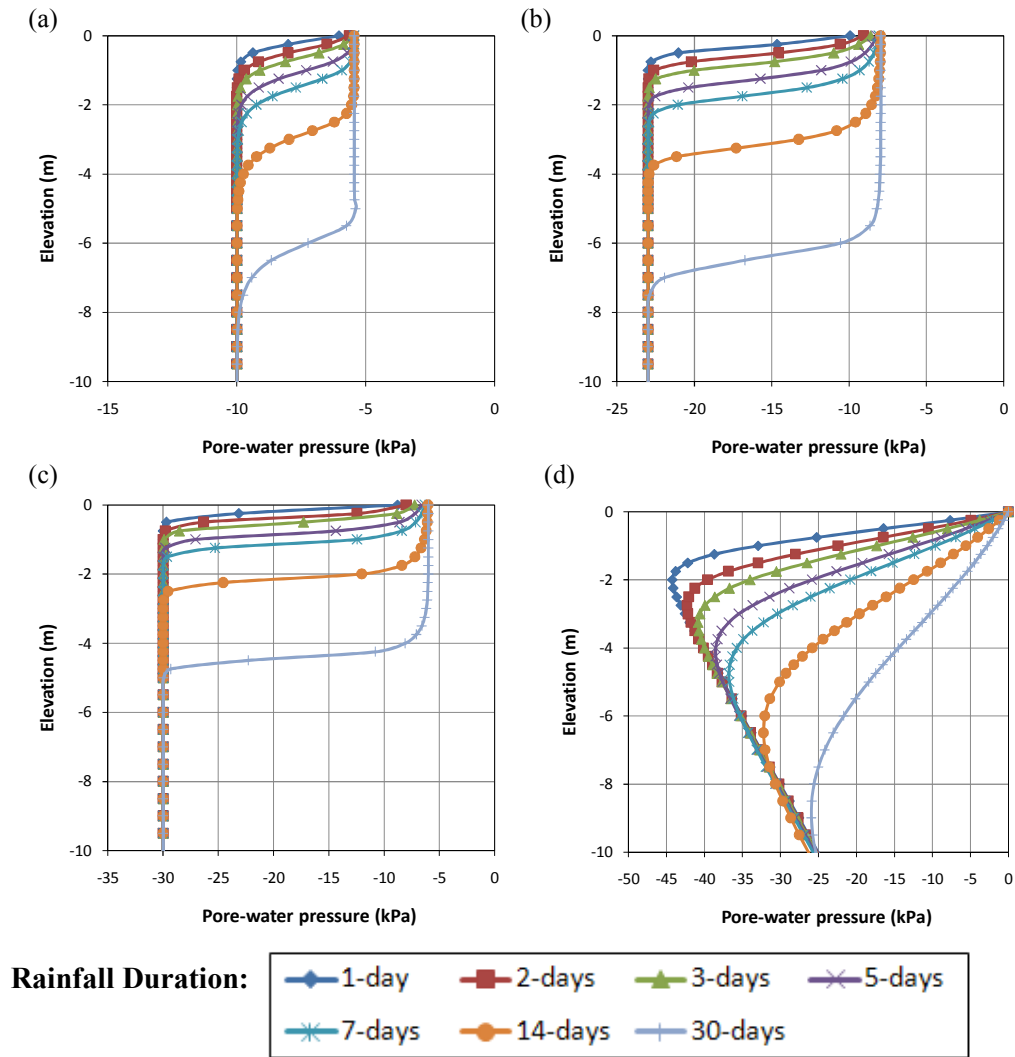


**Figure 5.7** Influence of rainfall duration on suction distribution for (a) sand-gravel, (b) silty gravel, (c) sandy silt, and (d) silt (kaolin)

An idealized infiltration model (Figure 5.8) is used to further explain the mechanism of rainfall infiltration due to various rainfall intensities and durations. Assuming that all rainfall infiltrates effectively into the soil mass, Equation 5.1 and Equation 5.2 are proposed:

$$I \times t = L_f \times (\theta_a - \theta_i) \quad \text{for } q/k_{sat} < 1 \quad (5.1)$$

$$k_{sat} \times t = L_f \times (\theta_{sat} - \theta_i) \quad \text{for } q/k_{sat} > 1 \quad (5.2)$$

Where  $L_f$  is the depth of wetting front,  $\theta_a$  is the average volumetric water content after rainfall, and  $\theta_i$  is the initial volumetric water content. Equation 5.1 and Equation 5.2 can be rewritten to estimate the depth of wetting front ( $L_f$ ) as follows:

$$L_f = \frac{I \times t}{(\theta_a - \theta_i)} \quad \text{for } q/k_{sat} < 1 \quad (5.3)$$

$$L_f = \frac{k_{sat} \times t}{(\theta_{sat} - \theta_i)} \quad \text{for } q/k_{sat} > 1 \quad (5.4)$$

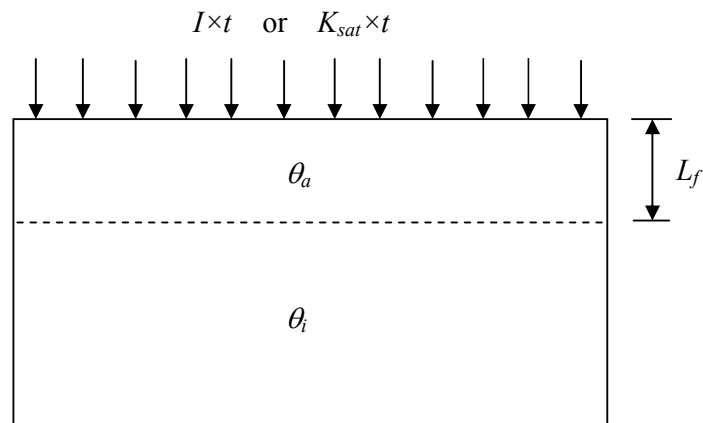


**Figure 5.8** An idealized infiltration model

In conclusion, the analytical approach can be used to estimate the depth of wetting front. Equation 5.3 and Equation 5.4 demonstrate the depth of wetting front as a function of rainfall intensity, saturated permeability and rainfall duration. However, only the rainfall intensity affected the minimum suction value. Previous studies suggested that the soil with low saturated permeability would permit less rainfall infiltration, hence resulted in very small suction variation. The results from this parametric study showed that the suction variation in less permeable soil could be greater than those of high permeable soils. Despite of the fact that the infiltration rate was controlled by the saturated permeability of the soil, the slopes of

SWCC and hydraulic conductivity function of less permeable soil were commonly gentler, hence little changes in volumetric water content would induce large suction variation.

#### **5.2.1.4 Influence of Slope Inclination on Suction Distribution**

The influence of slope inclination on the suction distribution was investigated for two patterns of rainfall, i.e.: short and intense rainfall (major rainfall) and long and less intense rainfall (antecedent rainfall). The results showed that the response of suction distribution to the slope inclination was governed by the total amount of infiltrated rainfall. The influence of slope inclination on the suction distribution under the infiltration of major rainfall (Figure 5.9) was relatively less significant compared to the antecedent rainfall that has a greater total rainfall amount (Figure 5.10). Both the reduction in minimum suction value and the propagation of wetting front were positively correlated with the slope inclination. The results implied that the stability of a steep slope was not only affected by higher mobilized force, but also lower soil suction than the gentle slope.

Figure 5.11 depicts the precipitation vector components involved in a process of infiltration on a sloping ground. Assuming that an amount of precipitation ( $P$ ) falls on a slope that inclined at  $\beta$  angle, the normal component can be deviated from the vertical precipitation vector. This is in conjunction with the model established by Fredlund and Rahardjo (1993) who found that the equipotential line and water table were parallel with the sloping ground surface. Similar pattern of equipotential lines were also observed from the results of this numerical simulation. Thus, the infiltrated precipitation amount on a sloping ground should be revised to  $P/\cos\beta$ , which would definitely result in a lower minimum suction value than that of the flat

surface. As for the wetting front depth ( $L_f$ ), the  $\cos\beta$  was introduced into the Equation 5.3, hence the equation can be rewritten as follows:

$$L_f = \frac{I \times t}{\cos \beta (\theta_a - \theta_i)} \quad \text{for } q/k_{sat} < 1 \quad (5.5)$$

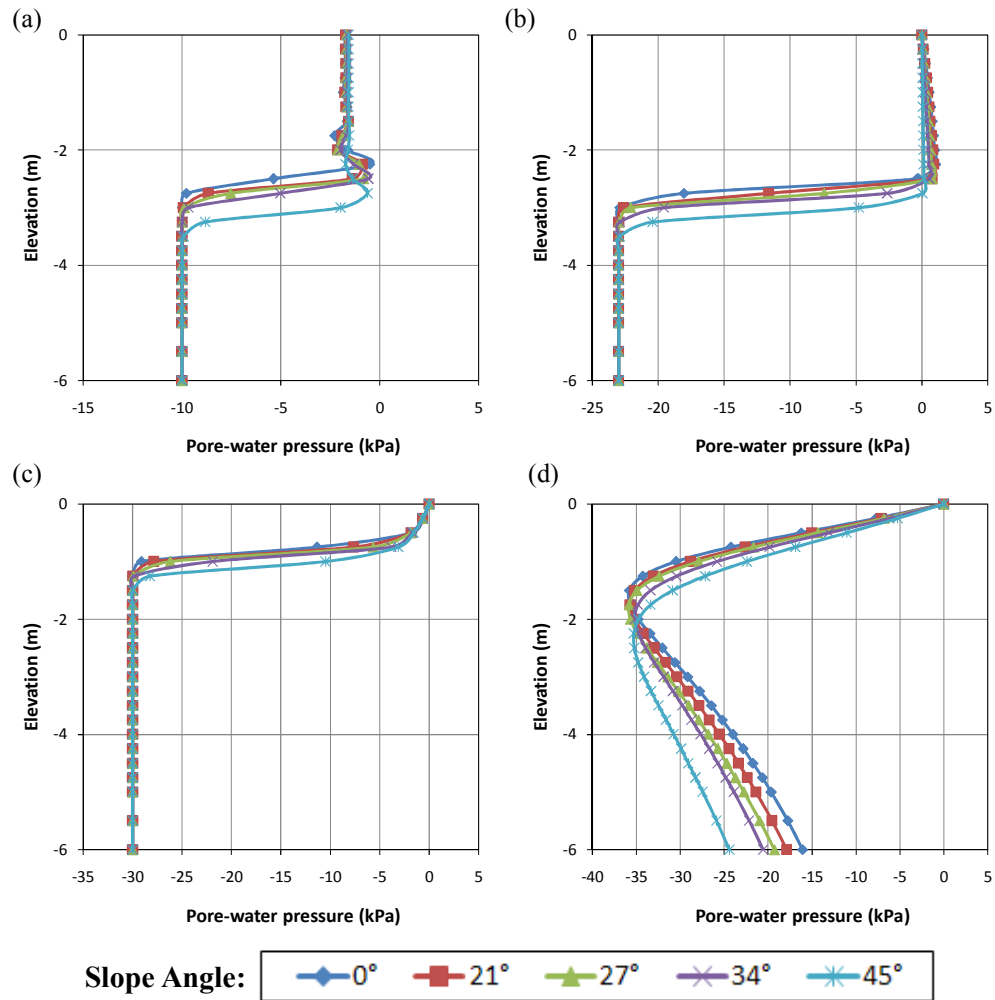


**Figure 5.9** Influence of slope inclination on suction distribution as the result of short and intense rainfall for (a) sand-gravel, (b) silty gravel, (c) sandy silt, and (d) silty (kaolin)

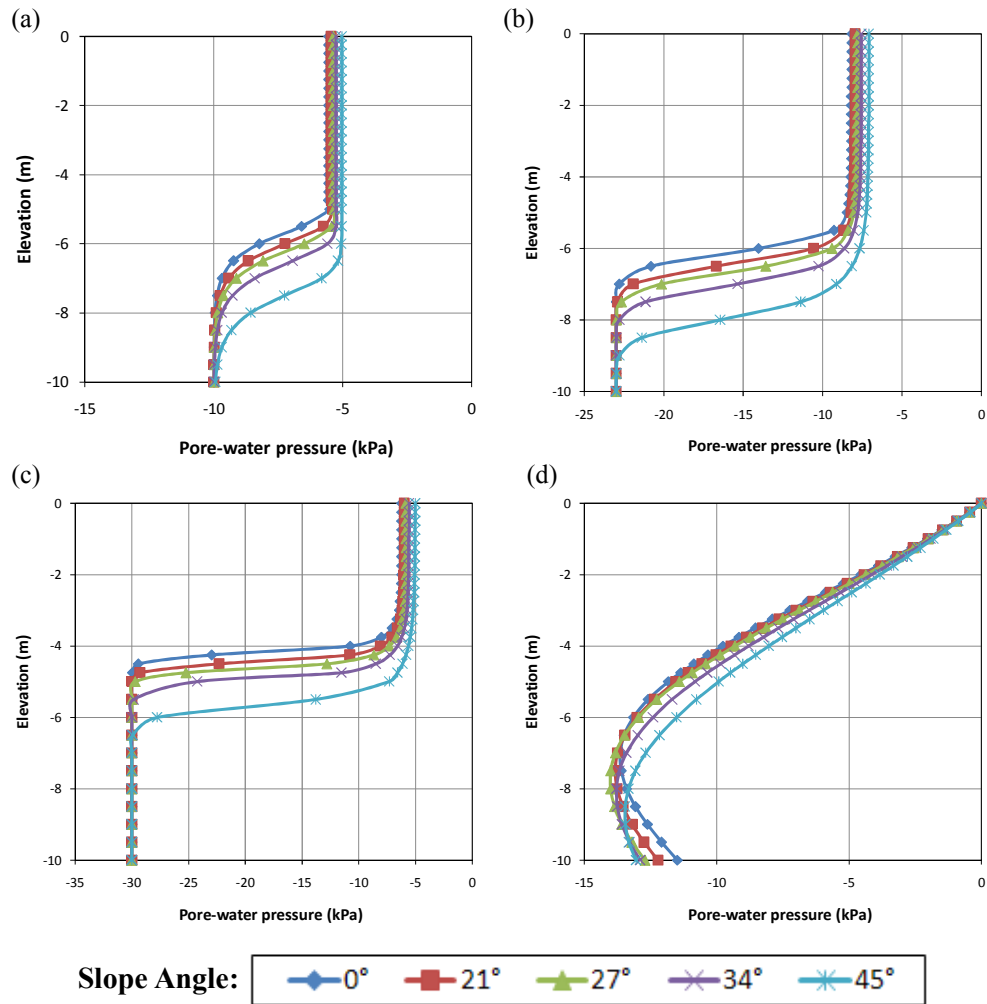


**Figure 5.10** Influence of slope inclination on suction distribution as the result of long and less intense rainfall for (a) sand-gravel, (b) silty gravel, (c) sandy silt, and (d) silt (kaolin)

From Equation 5.5, it is obvious that the steeper the slope, the deeper the wetting front will be generated, particularly when the soil slope is subjected to a great amount of rainfall. Generally, the estimated wetting front depth ( $L_f$ ) from Equation 5.5 showed good agreement with the results of numerical simulation.

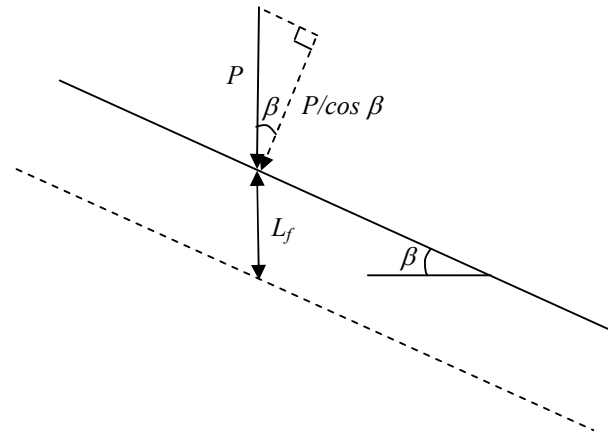


**Figure 5.11** Rainfall infiltration components on a sloping surface

### 5.2.2 Critical Rainfall Pattern Analysis

The critical rainfall duration and intensity for slope failures at each selected location were determined by performing slope stability analysis using the suction profiles resulting from various rainfall intensities and durations. The critical rainfall intensity is obtained from the statistical extreme rainfall analysis corresponding to the critical rainfall duration. The translational slip surface was imposed at the slope while pore-water pressure distributions computed by Seep/W during the transient analyses were used for the calculation.

Figure 5.12 shows the suction distributions as the result of extreme antecedent rainfalls at Johor Bahru (dry zone) and Kota Bharu (wet zone). Considering the slip plane at depths of 1 m, 3 m, and 5 m, Figure 5.13 shows the variation of factor of safety with the duration of the extreme antecedent rainfall.

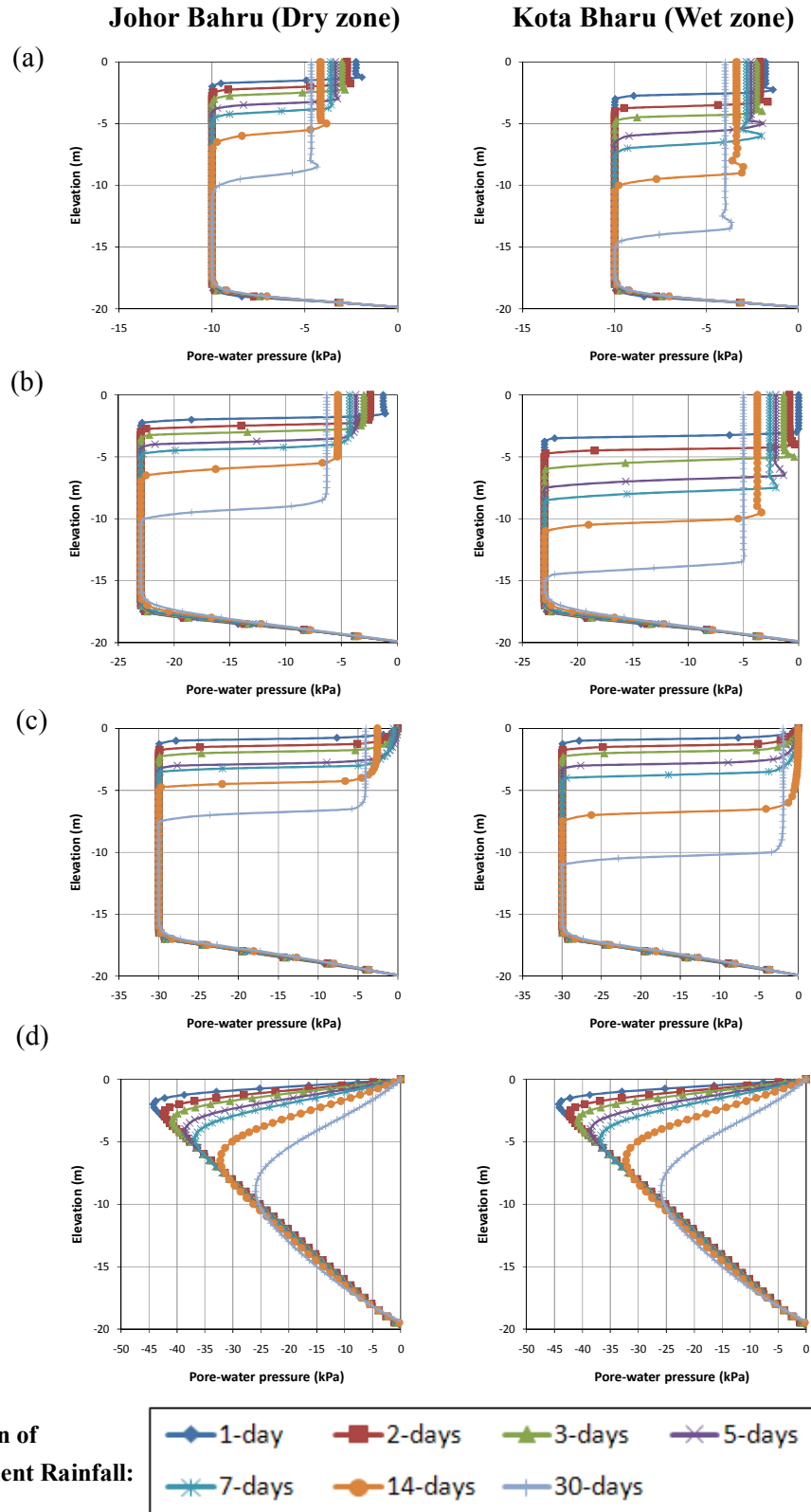


**Figure 5.12** Suction distributions as the result of various extreme antecedent rainfalls for (a) sand-gravel, (b) silty gravel, (c) sandy silt, and (d) silt (kaolin)

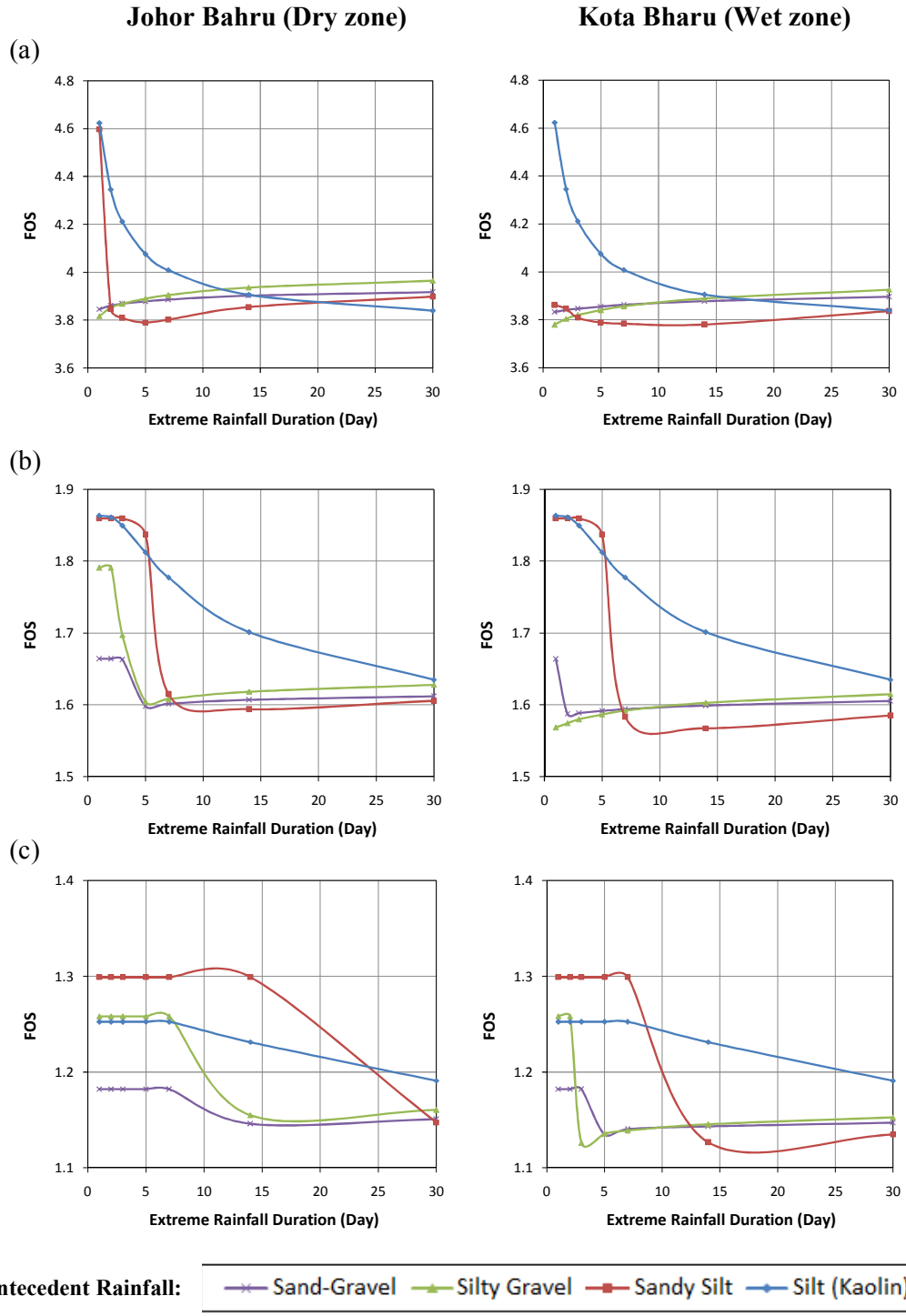


**Figure 5.13** Variation in factor of safety as the result of various extreme antecedent rainfalls at the slip planes of (a) 1m, (b) 3m, and (c) 5m depth

From the observation, it is clear that the critical duration of the antecedent rainfall is governed by three factors, i.e. the geographical location of the soil slope (wet vs. dry), the type of the soil (sand-gravel, silty gravel, sandy silt, silt), and the depth of the slip plane. For instance, by considering the slip plane at a depth of 3 m, the critical duration for a sand-gravel slope at Kota Bharu and Johor Bahru was 2 days and 5 days, respectively. As for silty gravel, the critical duration for Kota Bharu and Johor Bahru was 1 days and 5 days, respectively.

The rainfall characteristics of a geographical location were represented by the IDF curve. As illustrated in Figure 5.12 and Figure 5.13, the critical duration of antecedent rainfall at Kota Bharu (wet zone) was generally shorter than Johor Bahru (dry zone). The rainfall with shorter duration was associated with higher intensity, as revealed in the IDF curve, hence contribute to a worse suction distribution and lower factor of safety at the wet zone.

The effect of soil type on the suction distribution is dominated by the  $q/k_{sat}$  ratio, as mentioned in the previous section. For a soil with  $q/k_{sat} > 1$ , such as silt (kaolin), the suction distribution is unaffected by the intensity of rainfall. Under the circumstances, the duration of rainfall becomes the dominant factor in producing the critical suction distribution. The longer the duration of rainfall, the lower the suction distribution will be generated. Thus, the 30-day extreme rainfall should be applied on slope made of silt (kaolin) with the minimum intensity equal to its saturated permeability. For sand-gravel with  $q/k_{sat} < 1$ , the short and intense rainfall will be the critical rainfall if the infiltrated water is capable to advance to the slip plane concerned. A more subjective condition was encountered for sandy silt and silty gravel with the saturated permeability ranging from  $1 \times 10^{-5}$  m/s to  $1 \times 10^{-7}$  m/s, and the extreme rainfalls for a tropical climate fall within this range. The conditions mean that the critical duration for the slopes in a tropical region is hard to

predict as both of the rainfall duration and the rainfall intensity could be the governing factors simultaneously.

The depth of the slip plane is another important factor that should be considered in determining the critical duration of antecedent rainfall. As shown in Figure 5.12 and 5.13, the shallow failure is generally governed by the short and intense rainfall, while the deep-seated failure is dominated by the antecedent rainfall with longer duration. Figures 5.15b and 5.15c show that the short and intense 1-hour rainfall is not the critical antecedent rainfall for sand-gravel because the rainfall is not capable to infiltrate beyond the slip plane of 3m and 5m respectively.

Considering the above-mentioned factors, a chart was developed to estimate the critical duration ( $t_{acr}$ ) and critical intensity ( $I_{acr}$ ) of antecedent rainfall and the resultant minimum suction ( $\psi_{min}$ ) for slopes in the Malaysian Peninsular (Figure 5.14). In general, the critical suction distribution occurred when the extreme rainfall intensity is identical to the saturated permeability of the soil ( $q/k_{sat} = 1$ ). However, the depth of slip plane could be a constraint as the wetting front might not capable to advance beyond the slip plane concerned. Under such circumstance, the critical antecedent rainfall should be defined as the rainfall with the highest intensity within the envelope of the slip plane. The required input parameters include the specific hydraulic conductivity function of soil and the IDF curve. Furthermore, the envelope for the depth of wetting front can be computed from Equation 5.3.

The application of the proposed chart (Figure 5.14) is demonstrated for a silty gravel slope having a potential slip plane of 3m depth at Johor Bahru (dry zone). At the point of  $q/k_{sat} = 1$ , the wetting front is only within 1 m depth. Thus, the critical duration and critical intensity are identified as the point where the 3-m advancement envelope of silty gravel intersects with the IDF of Johor Bahru, i.e. critical duration ( $t_{acr}$ ) = 4.5 days, and critical intensity ( $I_{acr}$ ) =  $6 \times 10^{-7}$  m/s. By extending the

intersection point to the left side of the chart and intersecting the hydraulic conductivity function of silty gravel, the minimum suction is identified as 3.4 kPa.

The critical durations for the four soil types with respect to different depths of wetting front at the two distinctive climate zones are summarized in Table 5.1. For soil with high saturated permeability (i.e. sand-gravel), the shear strength of the soil is usually dominated by the friction angle, hence the slope is more susceptible to shallow failure. Thus, for the potential slip plane at depths of 1 to 2 m, the short and intense 1-day rainfall appears to most influence the slope instability. Water infiltrates into the soil rapidly and reduces the soil suction. However, the influence of rainfall intensity on the minimum suction of sand-gravel is not significant because the slope of the SWCC and hydraulic conductivity function of sand is considerably steep compared to other soil types. Nonetheless, 1-day extreme rainfall is still the most critical duration for very shallow failure on a sand slope even though the difference is not significant compared to the extreme rainfalls with longer duration but lower intensity.

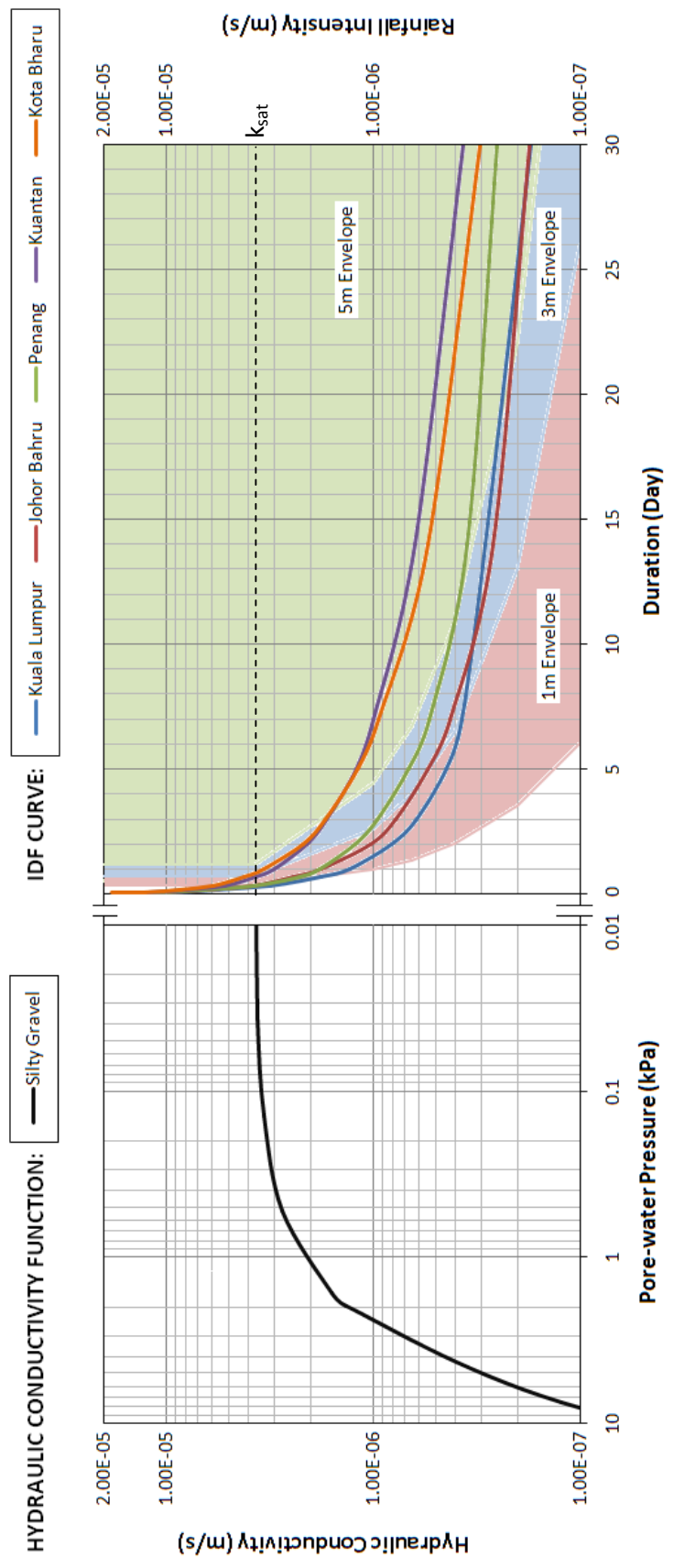


Figure 5.14 Proposed chart to predict critical antecedent rainfall and critical suction value of a soil slope

**Table 5.1:** Critical duration of antecedent rainfall for different locations and depths of slip plane

	1m Depth		3m Depth		5m Depth	
	Kota Bharu	Johor Bahru	Kota Bharu	Johor Bahru	Kota Bharu	Johor Bahru
Sand	1 day	1day	4day	7days	7days	20days
Silty Gravel	1day	1day	1day	4days	3days	20days
Sandy Silt	1day	1day	1day	7days	4days	18days
Silt (kaolin)	30 days	30 days	30 days	30 days	30 days	30 days

As for the soil with low permeability (i.e. silt), the duration of rainfall becomes the controlling factor to the slope instability. The infiltration rate is limited by the low saturated permeability instead of the rainfall intensity. The critical suction value of 0 kPa encountered at the ground surface indicated that the rainwater is retained at the surface. Therefore, a long duration of rainfall could eventually allow more water to infiltrate into the soil, which in turn reduces the soil suction and factor of safety.

For silty gravel and sandy silt with saturated permeability ranging from  $1 \times 10^{-5}$  m/s to  $1 \times 10^{-7}$  m/s, the critical duration of antecedent rainfall varies with geographical location. Moreover, the critical depth of the slip surface varies from one type of soil to another as both friction angle and cohesion play a role in the shear strength of silty soil. Thus, by adopting the proposed chart, the uncertainties in determining the critical duration of the silty soil can be effectively solved.

As the conclusion, the critical duration of antecedent rainfall is governed by three factors, i.e. the geographical location of the soil slope, the type of soil, and the depth of slip plane. The slip plane in turn is governed by several factors such as slope geometry, friction angle and cohesive strength etc. Therefore, a chart is developed to determine the critical duration ( $t_{acr}$ ) and critical intensity ( $I_{acr}$ ) of

antecedent rainfall as well as the resultant minimum suction value ( $\psi_{min}$ ) for slopes in the Malaysian Peninsular.

### **5.3 Laboratory Soil Column Tests**

The laboratory soil column tests were carried out to verify the findings of numerical simulations. A total of ten tests were carried out for different combinations of rainfall patterns and soil types (refer to Table 3.1).

#### **5.3.1 Initial Condition of Soil Column Tests**

Figure 5.15 (a-d) shows the setup of the soil column models for the four types of soil. From the laboratory measurements, the initial suction for sand-gravel (approximately 8 kPa) was slightly lower than that of estimated from the SWCC (10 kPa). The differences were probably caused by the inefficiency in the tensiometer to measure the suction in granular soil since the contact between ceramic sensor and soil particles were poor. For the silty gravel, sandy silt and silt (kaolin) which contained considerable amount of cohesive particles, the contact between ceramic sensor and soil particles were significantly improved, hence the suction measurements showed good agreement with the value predicted from SWCC. The measured initial suctions for silty gravel, sandy silt and silt (kaolin) were 17 to 23 kPa, 26 to 32 kPa, and 46 to 50 kPa, respectively.

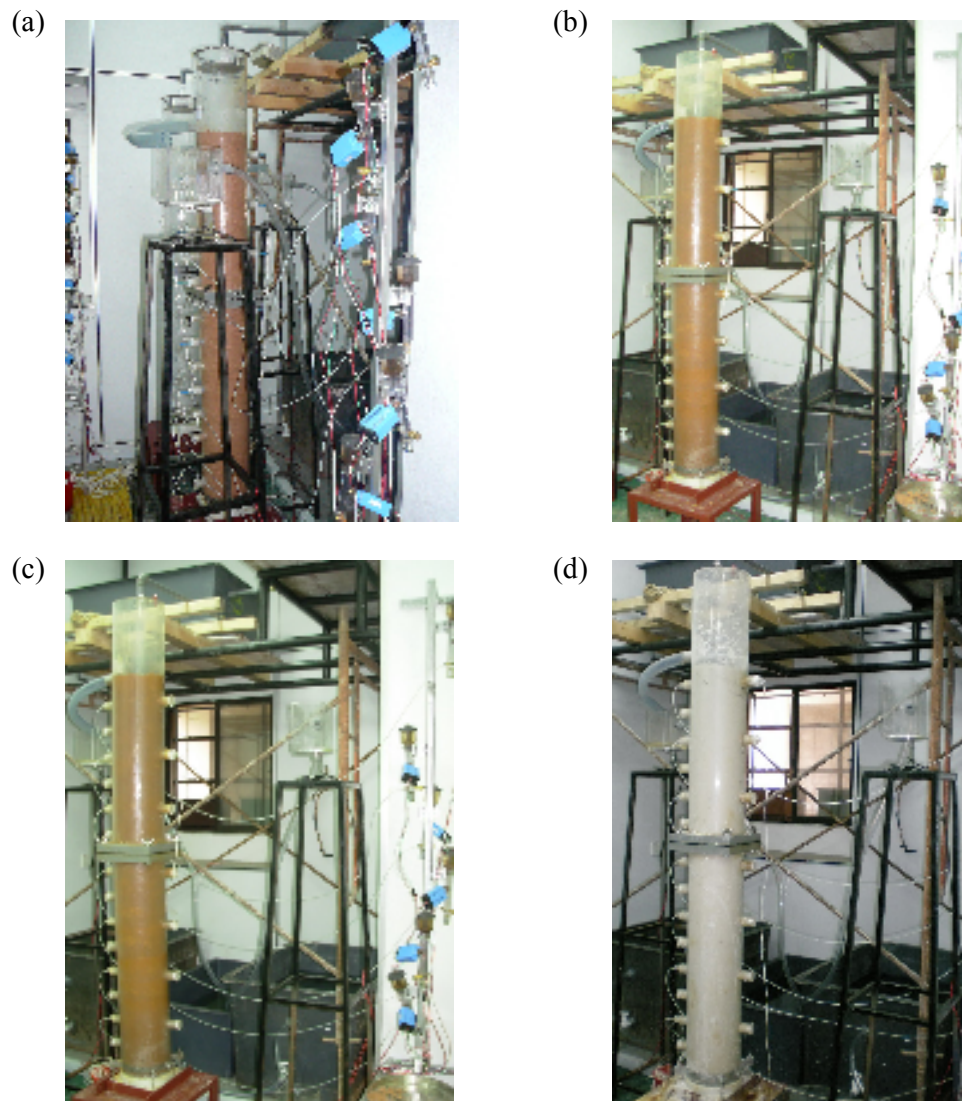


**Figure 5.15** The setup of soil column models for (a) sand-gravel, (b) silty gravel, (c) sandy silt, and (d) silt (kaolin)

### 5.3.2 Relationships between Infiltration and Runoff

Figure 5.16 (a-c) illustrates the relationships between infiltration and runoff for silty gravel, sandy silt and silt (kaolin). It should be noted that the runoff was not generated throughout the experiments of sand-gravel column. This was because the applied rainfall has an intensity lower than the saturated permeability of soil.

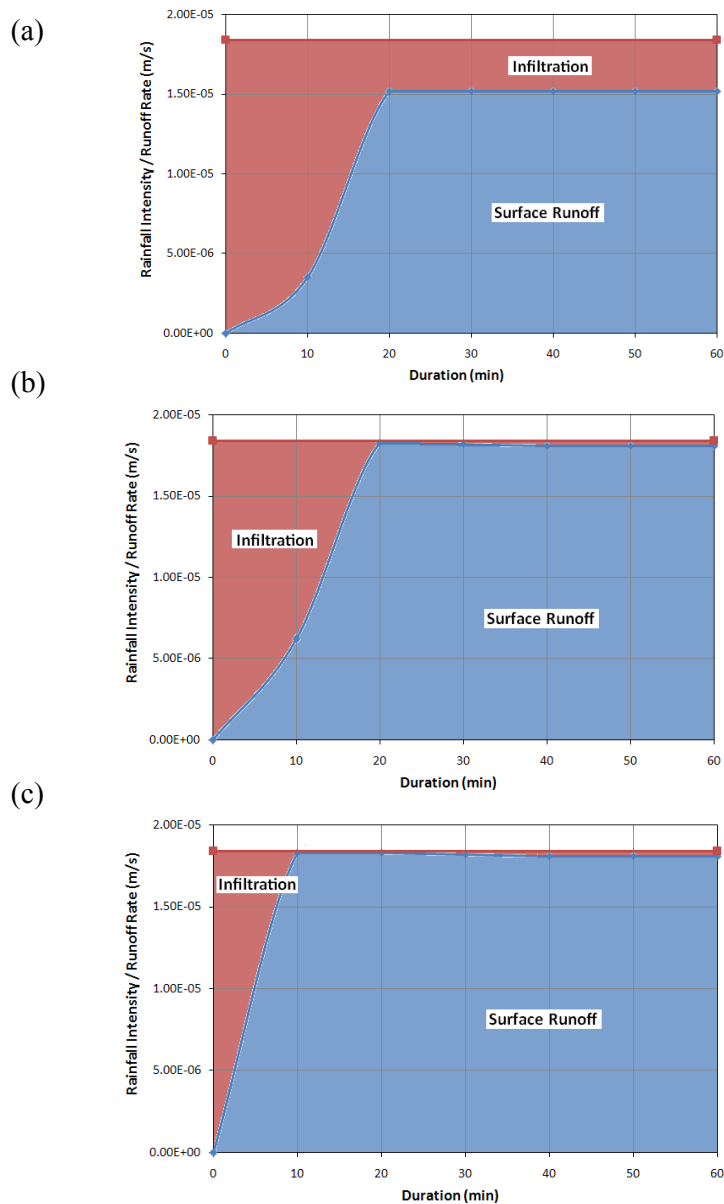


**Figure 5.16** Relationships between rainfall and surface runoff for (a) silty gravel, (b) sandy silt, and (c) silt (kaolin)

As shown in Figure 5.16a, the rainfall infiltrated effectively into the silty gravel for the first 10 minutes. Subsequently, the surface runoff was generated and the rate of infiltration and runoff became constant after 20 minutes. The measured runoff rate was  $1.52 \times 10^{-5}$  m/s indicating large portion of rainfall has contributed to the surface runoff (the applied rainfall =  $1.84 \times 10^{-5}$  m/s). Subtracting the surface

runoff from the applied rainfall, the effective infiltration rate was  $3.2 \times 10^{-6}$  m/s. This value was very close to the saturated permeability of silty gravel ( $k_{sat} = 3.68 \times 10^{-6}$  m/s).

The amount of surface runoff was greater for the soils with lower saturated permeability. For instances, the runoff rate of sandy silt ( $k_{sat} = 5.00 \times 10^{-7}$  m/s) constant at  $1.81 \times 10^{-5}$  m/s, indicating the infiltration rate was  $3.0 \times 10^{-7}$  m/s. As for the silt ( $k_{sat} = 6.78 \times 10^{-8}$  m/s), the runoff rate constant at  $1.83 \times 10^{-5}$  m/s with the infiltration rate approximated to  $1.0 \times 10^{-7}$  m/s. This infiltration rate, however, was almost twice the magnitude of saturated permeability of silt (kaolin) obtained from the falling head permeability test. It was thought that the tendencies of silt (kaolin) to shrink and crack have caused the infiltration capacities far in exceedance of the expected saturated permeability. This finding was supported by the observation of the desiccated surface and cracks at the silt (kaolin) column. (Figure 5.17).



**Figure 5.17** Cracks formed at the surface of silt (kaolin)

### 5.3.3 Saturation Profiles

The saturation profiles for the prescribed test combinations were measured and compared with the results of numerical simulation, as shown in Figure 5.18.

In the sand-gravel column (Figure 5.18a), the short and intense 1-hour major rainfall has resulted in the lowest minimum suction value, but limited to a very shallow depth of 0.3 m. Conversely, the wetting front resulted from the long and less intense 24-hour major rainfall has advanced beyond the entire length of the soil column (1.5m). This was revealed through the measurement of percolated flow at the bottom of the soil column after eight hours of rainfall. Whilst the wetting front was much deeper, the minimum suction value induced by the 24-hour major rainfall was just slightly higher than that of 1-hour major rainfall.

The silty gravel column exhibited similar trend as the sand-gravel (Figure 5.18b). It should be noted that the intensity of 1-hour rainfall ( $1.84 \times 10^{-5}$  m/s) was greater than the saturated permeability of silty gravel ( $k_{sat} = 3.68 \times 10^{-6}$  m/s). Under such circumstances, the effective infiltration of silty gravel was controlled by the saturated permeability, hence the minimum suction value induced by the 1-hour rainfall was almost identical to that of 24-hour rainfall ( $i = 3.35 \times 10^{-6}$  m/s). Nonetheless, the 24-hour rainfall still resulted in deeper wetting front than the 1-hour rainfall. The results implied that for  $q/k_{sat} < 1$ , the minimum suction value is governed by the rainfall intensity, while the wetting front depth was influenced by the total amount of rainfall infiltrated into the soil. As for  $q/k_{sat} > 1$ , the infiltration and minimum suction value was controlled by the saturated permeability, while the wetting front depth was only influenced by the rainfall duration.

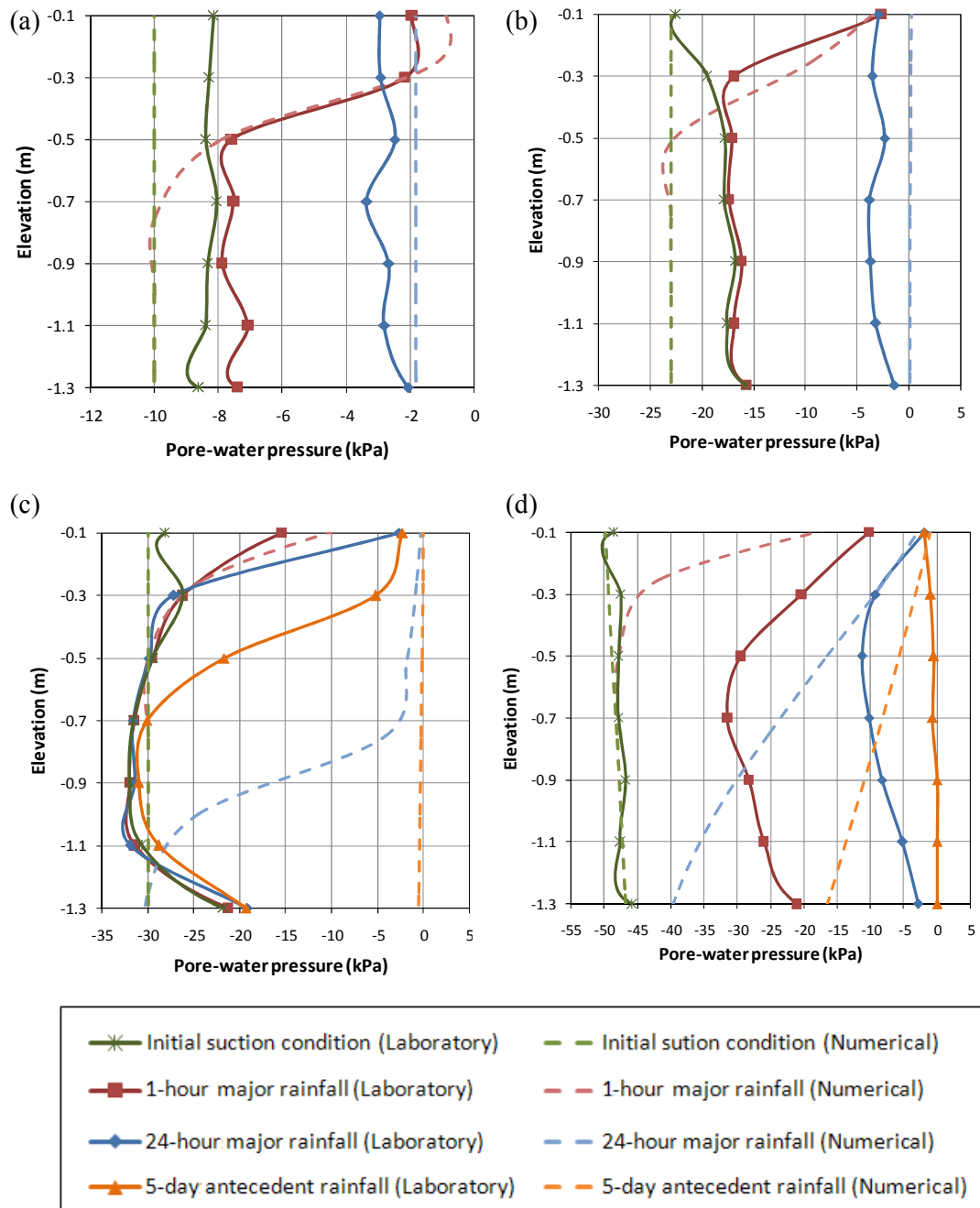


**Figure 5.18** Saturation profiles in (a) sand-gravel, (b) silty gravel, (c) sandy silt, and (d) silt (kaolin)

The wetting front measured in the sandy silt column was much shallower than that of numerical simulation (Figure 5.18c). For instance, numerical simulation result showed that the 24-hour rainfall should cause a propagation of

wetting front beyond 0.8 m depth. However, the wetting front depth measured from the laboratory was only 0.3 m. The inhomogeneity in the compacted soils, and the inconsistency between the measured and actual SWCC as well as the predicted hydraulic conductivity function could be the reason for these deviations.

In addition to the 1-hour and 24-hour major rainfalls, a ponding condition was created in the sandy silt column to study the response of suction distribution to the infiltration of longer duration (5 days). Whilst the minimum suction value was the same as the 24-hour major rainfall, the 5-day infiltration has resulted in a deeper wetting front.

The mechanism of suction loss in sandy silt under rainfall infiltration condition is as follows: (1) the low saturated permeability of sandy silt limits the infiltrated rainfall amount, hence large amount of rainfall contributes to runoff, (2) the infiltrated rainfall reduces the soil suction gradually until a minimum suction value is achieved, (3) beyond this point, the rainfall infiltration will cause deeper propagation of wetting front. Apparently, the long duration rainfall appears to be a more critical rainfall for sandy silt.

For the silt (kaolin) column, the suction distribution measured in the laboratory was generally lower than that of numerical prediction (Figure 5.18d). The results indicated that more water was actually infiltrating into the soil due to the cracks and desiccated surfaces. Besides, the capillary rise effect was found very significant in kaolin. The upward flow from the simulated water table has caused the suction loss at the bottom of the soil column.

In conclusion, the initial suction of coarse-grained soil is lower than fine-grained soil. In fact, the suctions of 2 to 4 kPa were very common for

sand-gravel soil under typical rainfall condition. While the initial suction of fine-grained soil was higher, the capillary rise effect from the water table was comparatively significant. It is thus essential to consider the effect of water table on the suction distribution of fine-grained soil slope if the water table is high. In general, the suction and seepage observed in physical laboratory model showed good agreement with the results of numerical simulations. Nonetheless, the accuracy of the numerical predictions is governed by the consistency of the soil properties input parameters e.g. SWCC and hydraulic conductivity between numerical simulation and actual soil behaviour.

#### **5.3.4 Suction Redistributions**

The redistribution pattern for each laboratory test was observed until the initial suction condition was obtained. Figure 5.19 (a-d) illustrates the redistribution pattern after the 24-hour rainfall for sand-gravel, silty gravel, sandy silt and silt (kaolin), respectively.

In general, the water content in coarse-grained soil redistributed quicker than that of fine-grained soil. Three days was required for the sand-gravel to regain its initial condition after the 24-hour rainfall event. However, 16 days and 32 days were required for silty gravel and sandy silt, respectively. As for silt (kaolin), the initial condition was not recovered after 32 days of drying. The phenomena can be explained by the low saturated permeability of fine-grained soil. However, as observed in the SWCC and hydraulic conductivity function (refer to Figure 4.5 and 4.6), the permeability of coarse-grained soil decreased in tandem with the increase of suction, until a stage where the permeability of coarse-grained soil could be lower than that of fine-grained soil. This behaviour of soil has caused the redistribution

rate of coarse-grained soil decrease in exponential fashion towards the higher suction. As for the fine-grained soil (i.e. silt), the redistribution rate was more consistent over the suction range concerned.

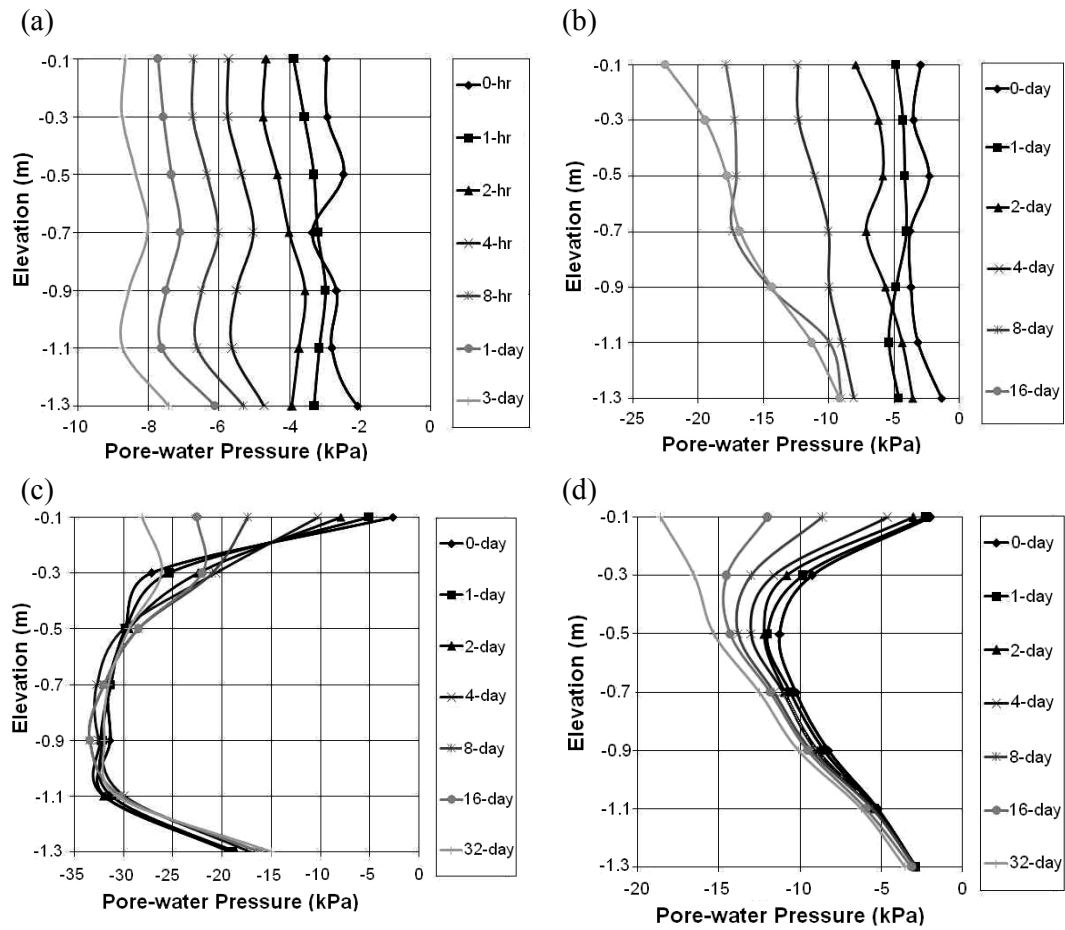


**Figure 5.19** Suction redistributions in (a) sand-gravel, (b) silty gravel, (c) sandy silt, and (d) silt (kaolin)

#### 5.4 Field Study

The effect of soil type on the suction distribution was revealed through numerical simulations and laboratory modelling. In this section, field monitoring

on a coarse-grained soil slope (Balai Cerapan) and a fine-grained soil slope (Kolej 12) was performed to give an insight to the mechanism of rainfall-induced slope failure within each type of soil. The transient suction and rainfall distribution were monitored for a period of one year.

#### **5.4.1 Overall Trend of Suction Distributions**

Figures 5.20 and Figure 5.21 illustrate the daily rainfall and the suction measured at 0.5m, 1m and 1.5m depths for Balai Cerapan site and Kolej 12 site respectively. The temporal distribution of the recorded rainfall is the typical of Johor Bahru area, with most of the annual precipitation fall during the monsoon seasons. Obviously, Johor Bahru experienced two monsoon seasons within a year, namely the Southwest Monsoon from May to September and the Northeast Monsoon from November to March.

From the overall trend of suction distributions, it was obvious that the suctions recorded at Balai Cerapan site were generally more consistent and lower than that of Kolej 12 site. During the driest condition in February 2007, the suction of Balai Cerapan soil could only increase to 26 kPa, while the suction recorded at Kolej 12 soil was 74 kPa. Apparently, with the same lowest limit of suction (0 kPa) for both sites, the Kolej 12 soil displayed a wider range of suction variation than Balai Cerapan soil.

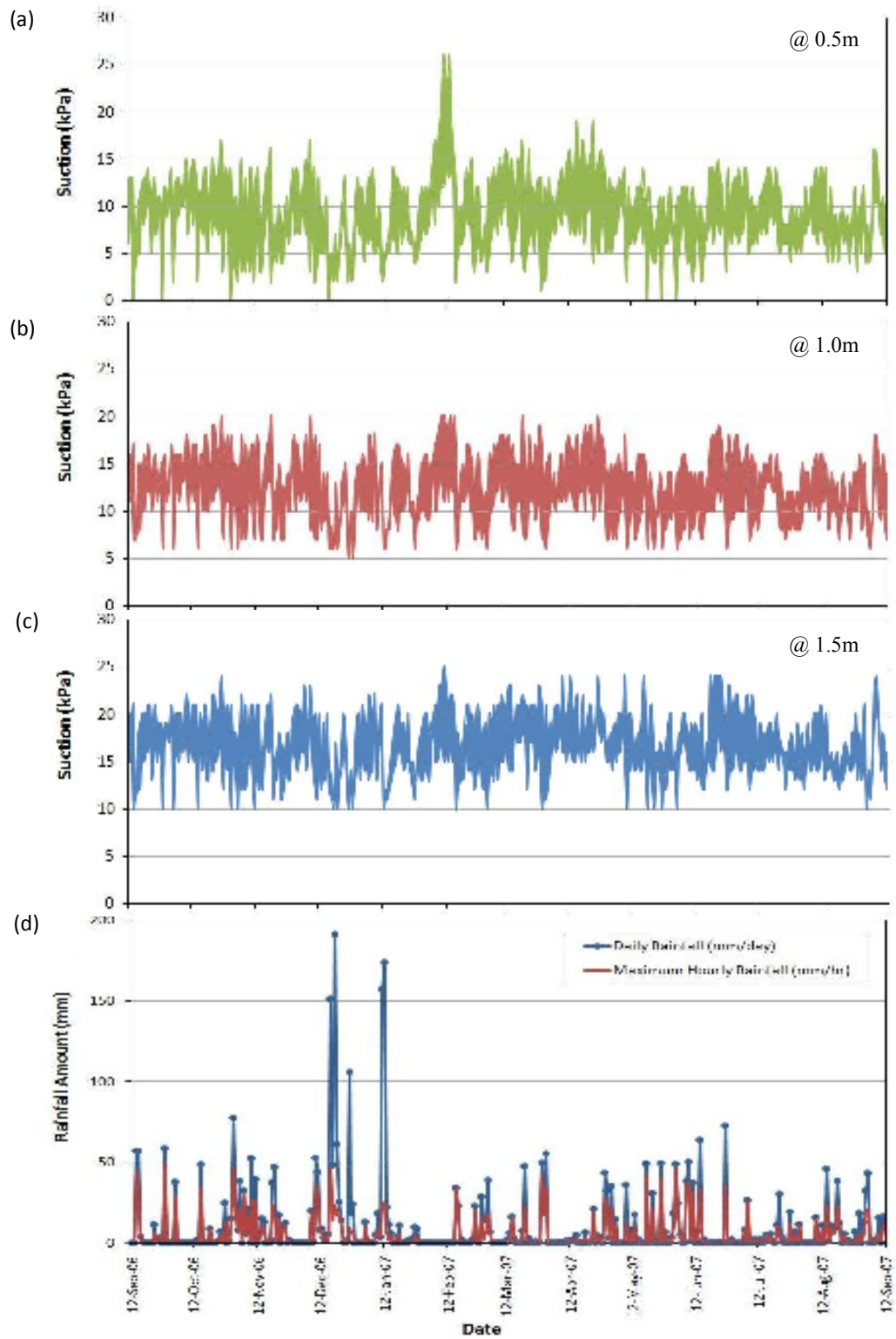


**Figure 5.20** Rainfall and suction distributions monitored for 12 months at Balai Cerapan site

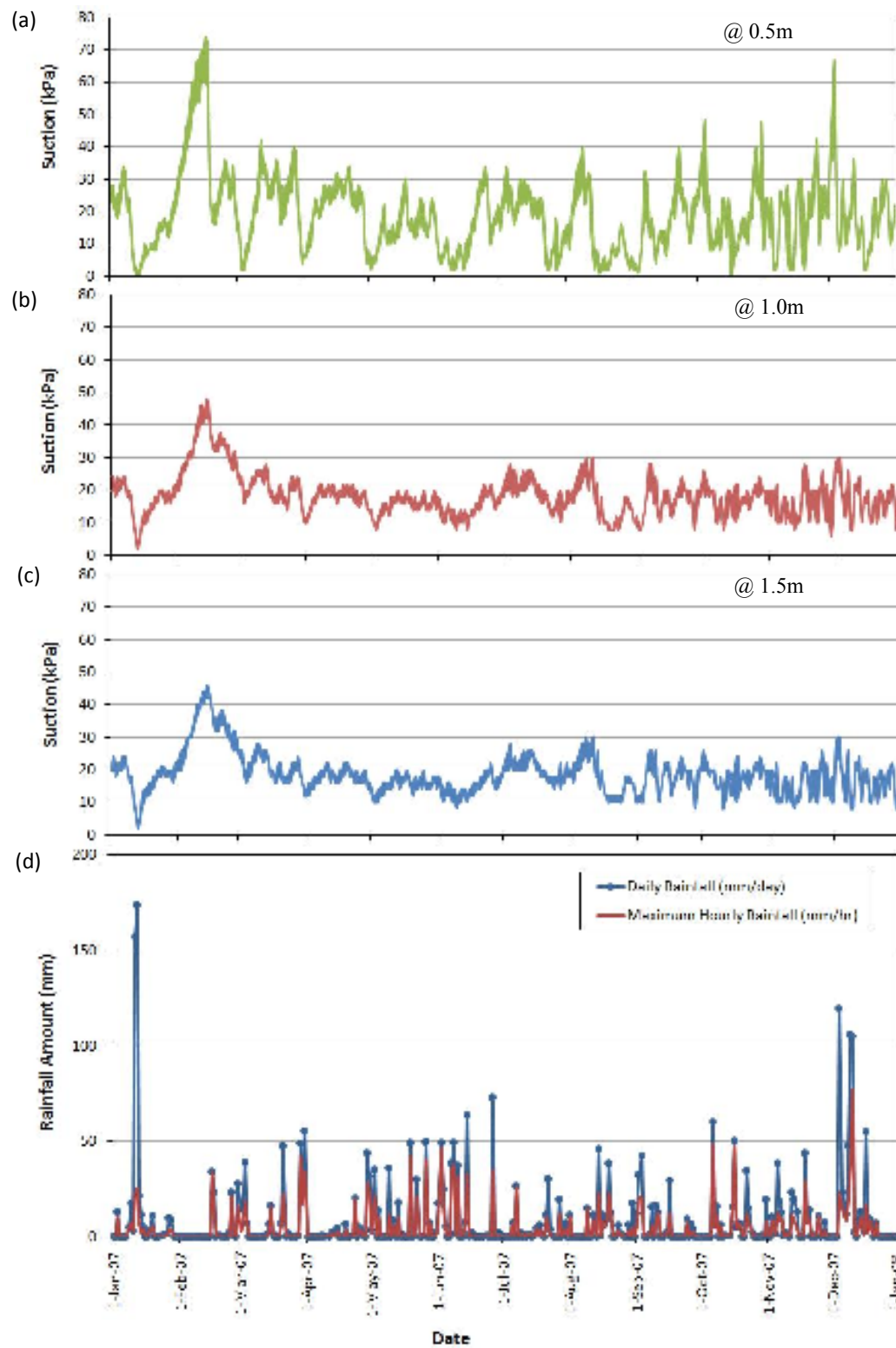


**Figure 5.21** Rainfall and suction distributions monitored for 12 months at Kolej 12 site

Another consistent observation emerged from the analysis was that the Balai Cerapan soil exhibits greater daily suction variation compared to the Kolej 12 soil. It was quite frequent to observe the suction of Balai Cerapan soil dropped dramatically from 20 kPa to 0 kPa after a typical short and intense tropical rainfall event, and yet the initial suction was recovered within one day. On the other hand, the seasonal fluctuation of the overall suction trend was more obvious at the Kolej 12 site. During raining season, the Kolej 12 soil loss its suction gradually. As observed in the suction variation at 0.5m depth (Figure 5.21a), the suctions of less than 5 kPa were achieved after a few continuous rainfall events, instead of single rainstorm. At depths of 1 m and 1.5 m, the loss of suction was only affected by the prolonged and greater amount of rainfall, as observed in January 2007. The results implied that the type of soil play an essential role on the response of suction distribution to rainfall infiltration.

#### **5.4.2 Response of Suction Distribution to Single Rainfall Pattern**

The response of suction distribution to single rainfall pattern was studied by further reducing the temporal interval of the observation. Three rainfall patterns were isolated during the herein reported monitoring period for Balai Cerapan site, denoted as rainfall pattern A, B, and C.

Rainfall pattern A (Figure 5.22a) consists of two rainfall events (14 and 15 September 2006) that have the same total rainfall amount but different in maximum hourly intensity. The first rainfall event that occurred on 14 September 2006 was short and intense, while the second one on 15 September 2006 has lower intensity but lasted for longer duration. Obviously, the effect of the first rainfall on the suction distribution was more significant than the latter. The result implied that the

suction distribution of Balai Cerapan soil is more influenced by the short and intense rainfall.

Rainfall pattern B (Figure 5.22b) describes a prolonged dry period (from 29 November 2006 to 7 December 2006) followed by a prolonged wet period (from 8 December 2006 to 20 December 2006). The suctions exhibited cyclic fluctuation during dry period mainly due to the cyclic variation in solar radiation (day and night). When the slope was subjected to a moderate rainfall amount (20mm/day) on 8 December 2006, the suctions at 0.5m and 1.0m dropped gradually, while the suction at 1.5m remained unchanged. The suction at 1.5m was only altered by the intense rainfall falling from 17 to 20 December 2006. The result showed that the rainfall amount plays a vital role in the propagation of wetting front.

Rainfall pattern C (Figure 5.22c) is an intense rainfall occurred after a prolonged dry season. In February 2007, the Balai Cerapan slope experienced the driest condition throughout the course of monitoring, i.e. continuous 18 days without rainfall. The highest suction recorded at 0.5m, 1.0m and 1.5m were 26, 20 and 25 respectively. The results showed that the highest suction reached by the soil is 26kPa, even during the driest condition. This limiting suction is approximately identical to the suction corresponding to residual water content of the soil (i.e. 23 kPa). Subsequently, a typical short and intense tropical rainfall occurred on 16 February 2007 has caused the suction dropped dramatically to a value that was identical to the suction distribution during prolonged wet season in December 2006 (i.e. below 2 kPa).

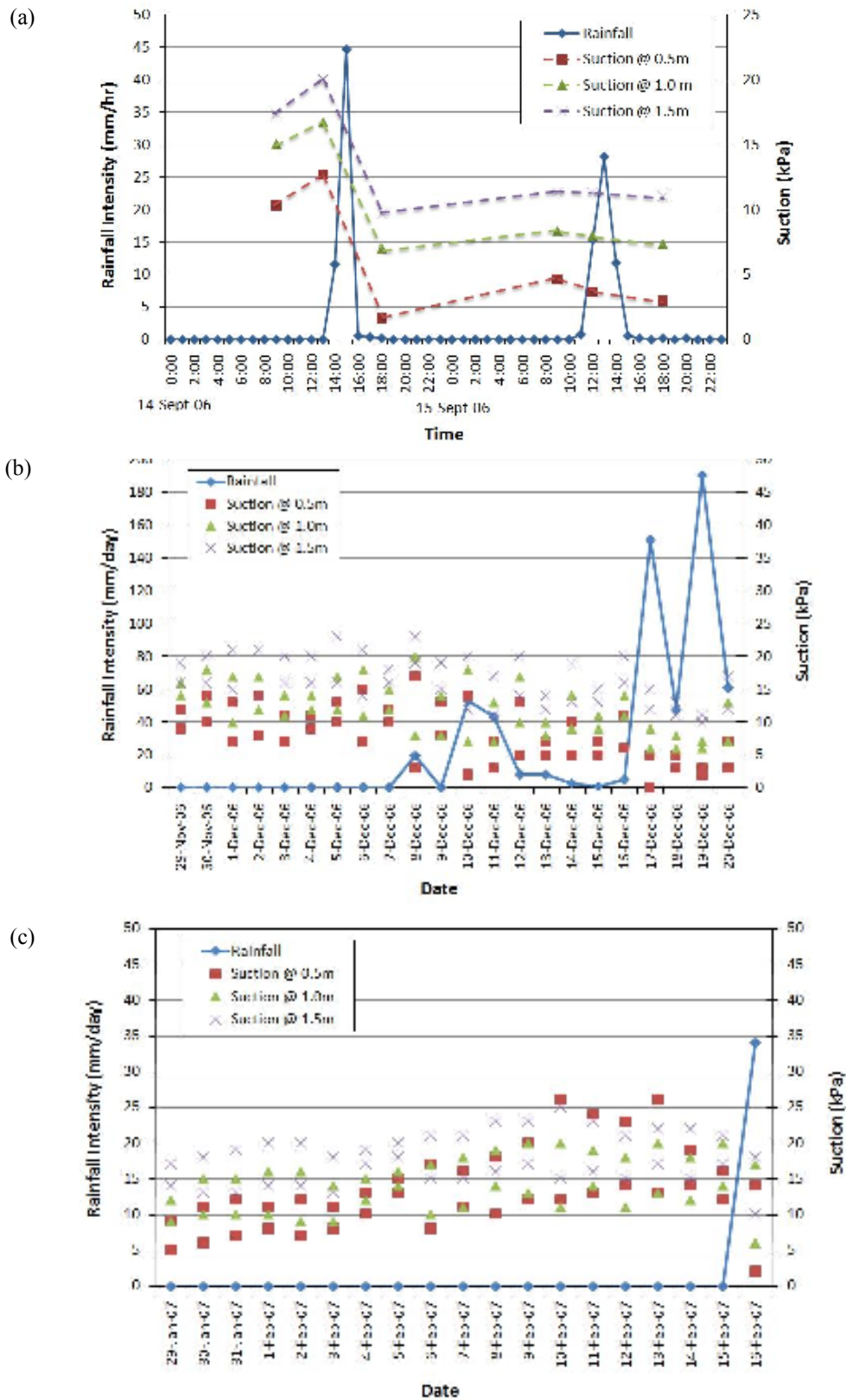


**Figure 5.22** Suction distributions as the result of (a) Rainfall pattern A, (b) Rainfall pattern B, and (c) Rainfall pattern C at Balai Cerapan site

Two rainfall patterns (rainfall pattern D and E) were isolated during the course of monitoring at Kolej 12 site (Figure 5.23). Rainfall pattern D (Figure 5.23a) is characterized by an extremely intense rainfall followed by a low intensity long duration rainfall occurred on 4 December 2007. The suction at shallow depth (0.5m) dropped dramatically as the result of the intense rainfall. Theoretically, the low saturated permeability of the fine-grained soil should only allow little infiltration from the intense rainfall. The desiccated surface observed at the site might cause the infiltration capacity exceeded the expected saturated permeability. Nonetheless, the suctions at 1.0m and 1.5m were just slightly altered by the intense rainfall. The results revealed that the fine grained soil has high water retention ability.

Rainfall pattern E (Figure 5.23b) depicts a prolonged dry period (from 2 to 8 August 2007) followed by a prolonged wet period (from 9 to 20 August 2007). It was found that the suctions at all depths increase gradually during the dry period, and drop gradually during the wet period. The suction variation was greater at shallower depth. Contrary to the Balai Cerapan site, few days of continuous daily rainfall were required to induce the minimum suction of 0 kPa at Kolej 12 slope. Thus, it can be concluded that the suction distribution of fine-grained soil is more influenced by the prolonged rainfall.

From the foregoing discussion, the contrasting responses of suction distribution to rainfall infiltration for a coarse-grained soil slope and a fine-grained soil slope are summarized in Table 5.2. The complete set of the field rainfall and suction data for both instrumented sites are presented in Appendix D.

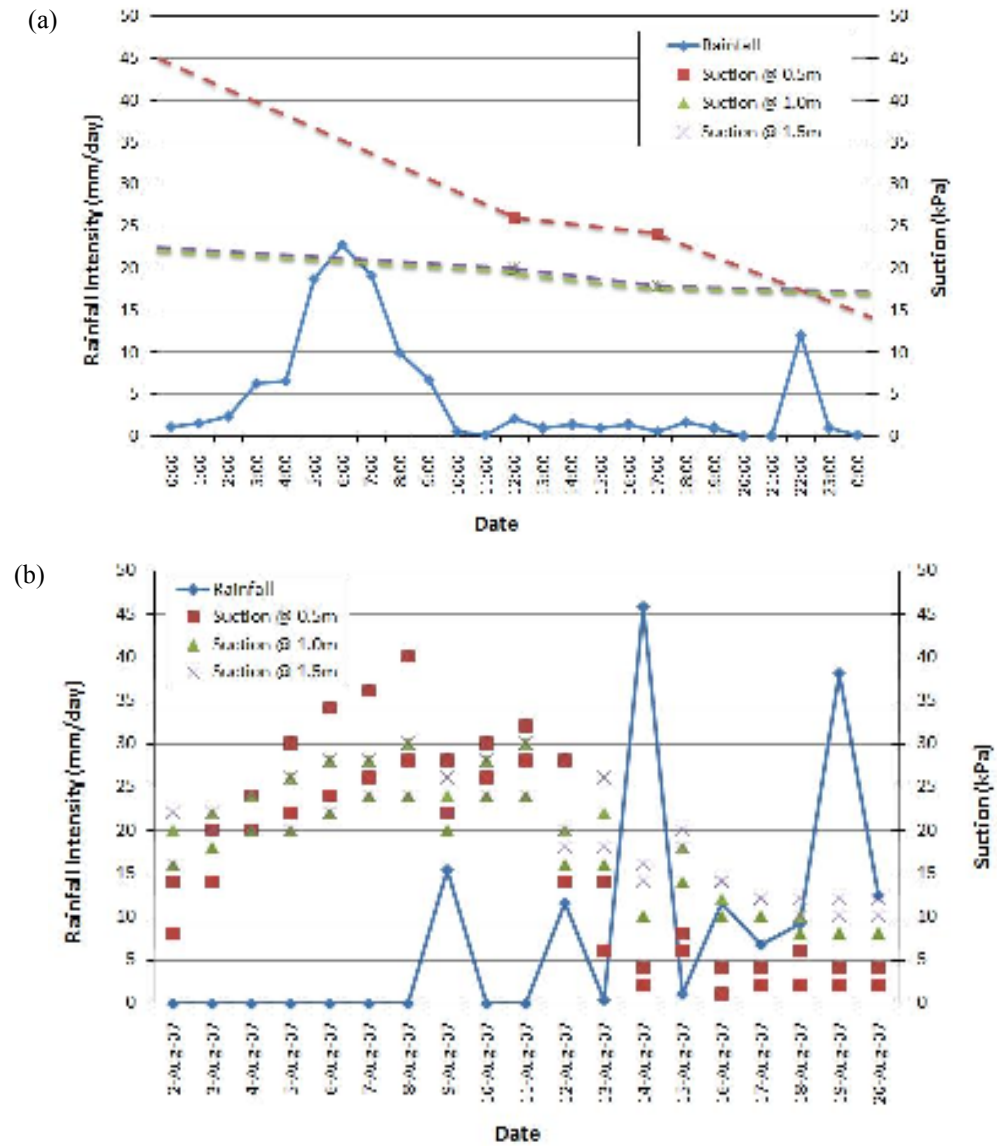


**Figure 5.23** Suction distributions as the result of (a) Rainfall pattern D, and (b) Rainfall pattern E at Kolej 12 site

**Table 5.2:** Contrasting responses of suction distribution to rainfall infiltration for a coarse-grained soil slope and a fine-grained soil slope

	Coarse-grained soil	Fine-grained soil
i. Response time:	Very fast	Very slow
ii. Suction variation:	Insignificant (0 kPa to 26 kPa)	Very significant (0 kPa to 74kPa)
iii. Wetting front:	Influenced by the amount of rainfall	Influenced by the duration and amount of rainfall
iv. Infiltration characteristics:	Allow great infiltration due to high permeability of soil	Allow great infiltration at the surficial soil (i.e. 0.5m) due to the existence of desiccated surface.
v. Potential threshold rainfall pattern:	Short and intense rainfall	Prolonged rainfall

## 5.5 Concluding Remarks

Tropical rainfall in Malaysia is highly influenced by two monsoon seasons, namely the Southwest Monsoon from May to September and the Northeast Monsoon from November to March. Prolonged and continuous low intensity rainfall is common during these periods. Under this circumstance, the antecedent rainfall plays a significant role in reducing the soil suction, hence slope stability. The application of extreme rainfall could provide the appropriate input parameters to represent the worst rainfall condition within the specified return period for slope stability analysis.

From the parametric study, it was found that the soil with low saturated permeability (i.e. silt) is unaffected by the rainfall intensity within the range of

extreme rainfalls in the Malaysian Peninsular. Thus, the critical rainfall pattern for silt (kaolin) is the rainfall with the longest duration (i.e. 30 days).

For soil with high saturated permeability (i.e. sand-gravel), the potential slip plane is generally shallow, hence very short and intense major rainfall appear to be the critical rainfall pattern.

In actual cases, most of the residual soils in tropical regions consist of gravelly or sandy silt with the saturated permeability ranging from  $1 \times 10^{-5}$  m/s to  $1 \times 10^{-7}$  m/s. The critical rainfall pattern for this type of soil is very subjective as both the rainfall duration and the rainfall intensity could be the governing factors simultaneously. Thus, a chart was proposed in this study to determine the critical duration and intensity of rainfall, as shown in Figure 5.14.

In the laboratory soil column tests, the behaviours of four types of soil (i.e. sand, silty gravel, sandy silt and kaolin) under various rainfall conditions were investigated. In general, the responses of suction distribution and redistribution to the rainfall infiltration were governed by the SWCC and hydraulic conductivity of soil.

The suction existed in the soil with high saturated permeability (i.e. sand) was very low (typically in between 2 to 4 kPa). The short and intense major rainfall (i.e. 1-hour rainfall) has resulted in the lowest minimum suction value, but limited to a very shallow depth (i.e. 0.3 m)

For soil with moderate saturated permeability (i.e. silty gravel and sandy silt), both major rainfall and antecedent rainfall could govern the suction distribution. The initial suctions existed in these types of soil were relatively high (18 to 33 kPa). However, the redistribution rate was significantly reduced by the existence of the fine particles.

For soil with low saturated permeability (i.e. silt), the suction distribution was more influenced by the duration of rainfall. The longer the duration of rainfall, the lower the suction generated. At the initial condition, the suction in silt (kaolin) can be as high as 50kPa. However, the suction decreased gradually when the soil column was subjected to rainfall infiltration. The lowest suction measured in the laboratory test was 0kPa, indicating  $q/k_{sat} > 1$ . Despite of the fact that the infiltration was limited by the soil's saturated permeability, the suction can be altered significantly with little changes in the water content. Besides, the shrink and crack behaviours of clayey soil permitted more water to infiltrate into the soil through the desiccated surface.

In general, the water content in the coarse-grained soil redistributed quicker than the fine-grained soil. The initial suctions were regained in sand-gravel, silty gravel and sandy silt after 3 day, 16 days, and 32 days, respectively. However, the initial condition of 50 kPa in silt (kaolin) was not recovered after 32 days of drying. The slow redistribution rate can be attributed to the high water retention ability and low saturated permeability of fine-grained soil.

From the comparison between the results of laboratory measurement and numerical simulation, it can be concluded that the numerical simulation could give a good prediction on the actual behaviour of soil, provided the SWCC and hydraulic conductivity of the soil are well defined.

In addition to the laboratory tests and numerical simulations, the suction variations in a coarse-grained soil slope and a fine-grained soil slope were monitored for a period of one year. The contrasting behaviours of the two types of soil slope were revealed and summarized in Table 5.2. In general, the effect of rainfall infiltration on the stability of a coarse-grained soil slope is less significant than the fine-grained soil slope.

## **CHAPTER 6**

### **CONCLUSIONS AND SUGGESTIONS**

#### **6.1 Introduction**

A study on the saturation profile for various combinations of rainfall pattern and soil type is reported in this report. The specific objectives of the study were stated in the Chapter 1, as the ultimate goal of the study is to investigate the mechanisms involved in the development of saturation profile. In this Chapter, the conclusions of the study are presented after which the recommendations for future research are presented.

#### **6.2 Conclusions**

The main outcomes and conclusions of the study are drawn in view of the objectives as formulated on page 3.

### **6.2.1 Extreme Rainfall Characteristics for the Malaysian Peninsular**

The statistical prediction of extreme rainfall was carried out to determine the IDF curves of ten-year return period for five selected locations in the Malaysian Peninsular. This statistical prediction of extreme rainfall represents the maximum rainfall intensity that may occur at the selected slope location for ten-year return period. Generally, the cities located on the east coast of the Peninsula (i.e. Kuantan and Kota Bharu) receive greater amounts of rainfall compared to cities on the west coast (i.e. Pulau Pinang, Johor Bahru and Kuala Lumpur) due to the geographical location and the direction of monsoon wind. Thus, it is adequate to categorize the rainfall distribution in the Malaysian Peninsular into two zones i.e. the wet zone on the east coast and the dry zone on the west coast.

### **6.2.2 Relationships between Rainfall, Runoff and Infiltration Rate**

The surface runoff generated from a rainfall event is a function of both rainfall intensity and rainfall total amount, as expressed by Equation 4.1. Under typical rainfall condition, most of the runoff amounts measured from the research site were within 30% of total rainfall. As for the case of intense rainfall (rainfall depth greater than 70mm), the runoff amount can be as high as 90% of total rainfall. Thus, the assumption of 30% of total rainfall contribute to the runoff should be deemed as a conservative assumption for the extreme rainfall assigned in the present study.

### **6.2.3 Effect of Soil Permeability on Suction Distribution and Redistribution**

Generally, the high permeable soil is characterized by high saturated permeability and low water retention ability. As such, the suction exists in this type of soil is generally low and the effect of rainfall infiltration on the suction variation is less significant. Nonetheless, the short and intense rainfall is still a more critical rainfall for this type of soil.

Conversely, the less permeable soil is characterized by low saturated permeability and high water retention ability. Whilst the response of suction variation to the rainfall infiltration is considerably slow, the variation of suction can be very significant due to the wide differences of suction between dry condition and wet condition. The prolonged rainfall appears to be the threshold rainfall pattern for this type of soil. The shrink and crack nature of the fine-grained soil has not helped the problem but allow more water to infiltrate into the surficial soil through the desiccated surface. The presence of water in soil reduced the strength and increases the driving force and therefore induced slope instability.

In terms of suction redistribution, the suction in high permeable soil can be redistributed quicker than less permeable soil. However, the permeability of high permeable soil decrease gradually as the suction became higher, until a stage where the permeability could be lower than that of less permeable soil. This behaviour of soil has caused the suction redistribution rate of high permeable soil decrease in exponential fashion towards the higher suction. As for the less permeable soil (i.e. silt), the redistribution rate was more consistent over time.

#### **6.2.4 A Chart for Preliminary Evaluation of Rainfall-Induced Slope Instability**

A chart is proposed in the present study to determine the critical duration, critical intensity and critical suction for each type of soil, as shown in Figure 5.14. The application of the chart was demonstrated and verified with the laboratory and field monitoring.

#### **6.3 Suggestions for Future Researches**

In light of the limitations of the present study, a few areas were identified where further research were required:

- i. **The study on a full scale model constructed under natural environment.** From the field measurement, it was found that the changes in ambient environment (i.e. solar radiation, humidity, temperature etc.) could also alter the soil suction. It would enhance the findings from the present study by accounting more surface boundary conditions.
- ii. **The numerical simulation and laboratory modeling by using two dimensional slope model.** The two dimensional analysis is required to consider for the horizontal flow in the soil slope.
- iii. **The study on the behaviour of layered soil.** The behaviour of homogeneous soil has been investigated in the present study. It is believed that the findings from the present study could provide the fundamental knowledge for the study in the behaviour of layered soil which sustained much more complexity.

- iv. **The improvement on the laboratory modeling technique, particularly for the rainfall simulator.** An advanced rainfall simulator should be used to enable the simulation of low rainfall intensity for longer duration of antecedent rainfall. Besides, the installation of Time-Domain Reflectometry (TDR) probe that provides the measurement of volumetric water content would allow the inferences of the suction measurements from tensiometer.
  
- v. **The study on the mitigation measures of rainfall-induced slope failure.** The mechanisms of the rainfall-induced slope failure for different types of soil have been identified in this study. The further study may look into the possible mitigation measures.

**APPENDIX A**

## APPENDIX A

### Example of Statistical Extreme Rainfall Analysis for Johor Bahru

1. Determine the IDF curve for duration shorter than 24 hours (MASMA, 2000)

$$\ln(^R I_t) = a + b \ln(t) + c(\ln(t))^2 + d(\ln(t))^3$$

Where

a = 4.4896

b = 0.9971

c = -0.3279

d = 0.0205

<i>t (min)</i>	<i>ln(<sup>R</sup>I<sub>t</sub>)</i>	<i>I (mm/hr)</i>
60	4.48231	88.44
120	3.997173	54.44
240	3.479876	32.46
480	2.97138	19.52
960	2.512647	12.34

2. Determine the IDF curve for duration longer than 24 hours (Gumbel, 1954)
  - i. The annual maximum 1-day, 2-days, 3-days, 5-days, 7-days, 14-days, and 30-days rainfall amounts extracted from the 30 years historical daily rainfall data.

<b>Year</b>	<b>1-day</b>	<b>2-days</b>	<b>3-days</b>	<b>5-days</b>	<b>7-days</b>	<b>14-days</b>	<b>30-days</b>
<b>1957</b>	289.0	388.2	461.8	533.3	535.7	629.7	775.2
<b>1958</b>	271.7	305.0	305.0	318.5	428.1	498.3	630.5
<b>1959</b>	157.7	234.1	256.9	313.7	361.0	426.5	625.6
<b>1960</b>	149.6	215.0	243.5	306.3	334.0	421.5	591.7
<b>1961</b>	139.0	193.0	229.7	280.5	324.2	388.0	580.0
<b>1962</b>	133.0	191.9	213.5	266.5	280.5	361.5	559.0
<b>1963</b>	125.0	190.4	208.5	261.5	263.0	353.0	558.1
<b>1964</b>	120.6	180.5	206.6	235.9	249.0	350.7	553.0
<b>1965</b>	117.8	168.3	204.0	235.5	243.5	347.0	550.3
<b>1966</b>	117.5	154.1	184.8	225.0	240.4	337.9	532.5
<b>1967</b>	116.5	146.5	177.5	214.7	238.5	315.5	531.5
<b>1968</b>	114.5	145.5	175.5	213.2	236.2	308.7	502.5
<b>1969</b>	108.0	141.4	169.3	196.7	235.0	297.7	482.0
<b>1970</b>	104.9	140.0	168.8	187.7	225.0	294.8	476.3
<b>1971</b>	103.1	139.0	163.7	184.7	213.2	288.0	472.2
<b>1972</b>	102.6	139.0	153.5	181.0	209.0	276.4	465.8
<b>1973</b>	102.1	137.0	152.0	180.0	205.5	274.4	461.0
<b>1974</b>	99.3	132.5	148.7	178.8	196.0	270.0	458.0
<b>1975</b>	99.3	132.0	146.5	177.0	193.0	270.0	452.6
<b>1976</b>	98.0	130.2	146.0	176.0	192.5	269.3	444.0
<b>1977</b>	94.4	130.2	145.9	171.2	189.1	264.5	429.3
<b>1978</b>	90.0	127.2	141.0	161.5	188.2	262.5	427.5
<b>1979</b>	88.3	123.1	141.0	158.5	186.8	258.7	422.0
<b>1998</b>	83.0	121.0	138.8	157.5	185.0	255.5	399.0
<b>1999</b>	80.0	116.0	133.4	156.5	175.7	245.7	388.8
<b>2000</b>	74.9	114.0	132.0	154.1	174.2	237.0	344.2
<b>2001</b>	73.5	112.5	131.7	141.7	166.0	226.7	324.7
<b>2002</b>	72.5	99.3	121.0	137.3	157.1	207.9	310.4
<b>2003</b>	70.5	98.5	112.9	122.9	153.3	198.5	294.5
<b>2004</b>	66.5	83.7	99.7	121.0	125.0	156.8	251.5

- ii. Calculate the  $X$  value ( $=P$ , extreme rainfall amount) for 1-day, 2-days, 3-days, 5-days, 7-days, 14-days, and 30-days rainfalls.

Max. 1-day	$m$	$m/(N+1)$	$Y_n$
289.00	1	0.032258	3.417637
271.70	2	0.064516	2.70768
270.00	3	0.096774	2.284915
222.00	4	0.129032	1.979413
189.00	5	0.16129	1.737893
160.00	6	0.193548	1.536599
145.00	7	0.225806	1.362838
120.60	8	0.258065	1.209009
117.80	9	0.290323	1.070186
117.50	10	0.322581	0.942982
116.50	11	0.354839	0.824955
114.50	12	0.387097	0.714272
108.00	13	0.419355	0.609513
104.90	14	0.451613	0.509537
103.10	15	0.483871	0.413399
102.60	16	0.516129	0.320292
102.10	17	0.548387	0.229501
99.30	18	0.580645	0.140369
99.30	19	0.612903	0.052262
98.00	20	0.645161	-0.03546
94.40	21	0.677419	-0.12346
90.00	22	0.709677	-0.2125
88.30	23	0.741935	-0.30347
83.00	24	0.774194	-0.39748
80.00	25	0.806452	-0.49605
74.90	26	0.83871	-0.60133
73.50	27	0.870968	-0.71671
72.50	28	0.903226	-0.84817
70.50	29	0.935484	-1.00826
66.50	30	0.967742	-1.23372
Total	3744.50		16.09

$$\bar{X} = 124.82 \qquad \bar{Y} = 0.536221$$

$$S_x = 61.79439 \qquad \sigma_y = 1.13139$$

$$1/\alpha = 54.61812$$

$$\mu = 95.52929$$

$$R = 10$$

$$Y = 2.2503$$

$$X = \mathbf{218.44}$$

Max. 2-days	$m$	$m/(N+1)$	$Y_n$
388.20	1	0.032258	3.417637
305.00	2	0.064516	2.70768
234.10	3	0.096774	2.284915
215.00	4	0.129032	1.979413
193.00	5	0.16129	1.737893
191.90	6	0.193548	1.536599
190.40	7	0.225806	1.362838
180.50	8	0.258065	1.209009
168.30	9	0.290323	1.070186
154.10	10	0.322581	0.942982
146.50	11	0.354839	0.824955
145.50	12	0.387097	0.714272
141.40	13	0.419355	0.609513
140.00	14	0.451613	0.509537
139.00	15	0.483871	0.413399
139.00	16	0.516129	0.320292
137.00	17	0.548387	0.229501
132.50	18	0.580645	0.140369
132.00	19	0.612903	0.052262
130.20	20	0.645161	-0.03546
130.20	21	0.677419	-0.12346
127.20	22	0.709677	-0.2125
123.10	23	0.741935	-0.30347
121.00	24	0.774194	-0.39748
116.00	25	0.806452	-0.49605
114.00	26	0.83871	-0.60133
112.50	27	0.870968	-0.71671
99.30	28	0.903226	-0.84817
98.50	29	0.935484	-1.00826
83.70	30	0.967742	-1.23372
Total	4729.10		16.09

$$\bar{X} = 157.64 \qquad \bar{Y} = 0.536221$$

$$S_x = 62.81449 \qquad \sigma_y = 1.13139$$

$$1/\alpha = 55.51974$$

$$\mu = 127.8658$$

$$R = 10$$

$$Y = 2.2503$$

$$X = \mathbf{252.81}$$

Max. 3-days	$m$	$m/(N+1)$	$Y_n$
461.80	1	0.032258	3.417637
305.00	2	0.064516	2.70768
256.90	3	0.096774	2.284915
243.50	4	0.129032	1.979413
229.70	5	0.16129	1.737893
213.50	6	0.193548	1.536599
208.50	7	0.225806	1.362838
206.60	8	0.258065	1.209009
204.00	9	0.290323	1.070186
184.80	10	0.322581	0.942982
177.50	11	0.354839	0.824955
175.50	12	0.387097	0.714272
169.30	13	0.419355	0.609513
168.80	14	0.451613	0.509537
163.70	15	0.483871	0.413399
153.50	16	0.516129	0.320292
152.00	17	0.548387	0.229501
148.70	18	0.580645	0.140369
146.50	19	0.612903	0.052262
146.00	20	0.645161	-0.03546
145.90	21	0.677419	-0.12346
141.00	22	0.709677	-0.2125
141.00	23	0.741935	-0.30347
138.80	24	0.774194	-0.39748
133.40	25	0.806452	-0.49605
132.00	26	0.83871	-0.60133
131.70	27	0.870968	-0.71671
121.00	28	0.903226	-0.84817
112.90	29	0.935484	-1.00826
99.70	30	0.967742	-1.23372
Total	5413.20		16.09

$$\bar{X} = 180.44 \qquad \bar{Y} = 0.536221$$

$$S_x = 70.24734 \qquad \sigma_y = 1.13139$$

$$1/\alpha = 62.08941$$

$$\mu = 147.1464$$

$$R = 10$$

$$Y = 2.2503$$

$$X = \mathbf{286.87}$$

Max. 5-days	$m$	$m/(N+1)$	$Y_n$
533.30	1	0.032258	3.417637
318.50	2	0.064516	2.70768
313.70	3	0.096774	2.284915
306.30	4	0.129032	1.979413
280.50	5	0.16129	1.737893
266.50	6	0.193548	1.536599
261.50	7	0.225806	1.362838
235.90	8	0.258065	1.209009
235.50	9	0.290323	1.070186
225.00	10	0.322581	0.942982
214.70	11	0.354839	0.824955
213.20	12	0.387097	0.714272
196.70	13	0.419355	0.609513
187.70	14	0.451613	0.509537
184.70	15	0.483871	0.413399
181.00	16	0.516129	0.320292
180.00	17	0.548387	0.229501
178.80	18	0.580645	0.140369
177.00	19	0.612903	0.052262
176.00	20	0.645161	-0.03546
171.20	21	0.677419	-0.12346
161.50	22	0.709677	-0.2125
158.50	23	0.741935	-0.30347
157.50	24	0.774194	-0.39748
156.50	25	0.806452	-0.49605
154.10	26	0.83871	-0.60133
141.70	27	0.870968	-0.71671
137.30	28	0.903226	-0.84817
122.90	29	0.935484	-1.00826
121.00	30	0.967742	-1.23372
Total	6348.70		16.09

$$\bar{X} = 211.62 \qquad \bar{Y} = 0.536221$$

$$S_x = 82.13134 \qquad \sigma_y = 1.13139$$

$$1/\alpha = 72.5933$$

$$\mu = 172.6973$$

$$R = 10$$

$$Y = 2.2503$$

$$X = \mathbf{336.06}$$

Max. 7-days	$m$	$m/(N+1)$	$Y_n$
535.70	1	0.032258	3.417637
428.10	2	0.064516	2.70768
361.00	3	0.096774	2.284915
334.00	4	0.129032	1.979413
324.20	5	0.16129	1.737893
280.50	6	0.193548	1.536599
263.00	7	0.225806	1.362838
249.00	8	0.258065	1.209009
243.50	9	0.290323	1.070186
240.40	10	0.322581	0.942982
238.50	11	0.354839	0.824955
236.20	12	0.387097	0.714272
235.00	13	0.419355	0.609513
225.00	14	0.451613	0.509537
213.20	15	0.483871	0.413399
209.00	16	0.516129	0.320292
205.50	17	0.548387	0.229501
196.00	18	0.580645	0.140369
193.00	19	0.612903	0.052262
192.50	20	0.645161	-0.03546
189.10	21	0.677419	-0.12346
188.20	22	0.709677	-0.2125
186.80	23	0.741935	-0.30347
185.00	24	0.774194	-0.39748
175.70	25	0.806452	-0.49605
174.20	26	0.83871	-0.60133
166.00	27	0.870968	-0.71671
157.10	28	0.903226	-0.84817
153.30	29	0.935484	-1.00826
125.00	30	0.967742	-1.23372
Total	7103.70		16.09

$$\bar{X} = 236.79 \qquad \bar{Y} = 0.536221$$

$$S_x = 86.61477 \qquad \sigma_y = 1.13139$$

$$1/\alpha = 76.55606$$

$$\mu = 195.739$$

$$R = 10$$

$$Y = 2.2503$$

$$X = 368.02$$

Max. 14-days	$m$	$m/(N+1)$	$Y_n$
629.70	1	0.032258	3.417637
498.30	2	0.064516	2.70768
426.50	3	0.096774	2.284915
421.50	4	0.129032	1.979413
388.00	5	0.16129	1.737893
361.50	6	0.193548	1.536599
353.00	7	0.225806	1.362838
350.70	8	0.258065	1.209009
347.00	9	0.290323	1.070186
337.90	10	0.322581	0.942982
315.50	11	0.354839	0.824955
308.70	12	0.387097	0.714272
297.70	13	0.419355	0.609513
294.80	14	0.451613	0.509537
288.00	15	0.483871	0.413399
276.40	16	0.516129	0.320292
274.40	17	0.548387	0.229501
270.00	18	0.580645	0.140369
270.00	19	0.612903	0.052262
269.30	20	0.645161	-0.03546
264.50	21	0.677419	-0.12346
262.50	22	0.709677	-0.2125
258.70	23	0.741935	-0.30347
255.50	24	0.774194	-0.39748
245.70	25	0.806452	-0.49605
237.00	26	0.83871	-0.60133
226.70	27	0.870968	-0.71671
207.90	28	0.903226	-0.84817
198.50	29	0.935484	-1.00826
156.80	30	0.967742	-1.23372
Total	9292.70		16.09

$$\bar{X} = 309.76 \qquad \bar{Y} = 0.536221$$

$$S_x = 94.47964 \qquad \sigma_y = 1.13139$$

$$1/\alpha = 83.50757$$

$$\mu = 264.9782$$

$$R = 10$$

$$Y = 2.2503$$

$$X = 452.90$$

Max. 30-days	$m$	$m/(N+1)$	$Y_n$
775.20	1	0.032258	3.417637
630.50	2	0.064516	2.70768
625.60	3	0.096774	2.284915
591.70	4	0.129032	1.979413
580.00	5	0.16129	1.737893
559.00	6	0.193548	1.536599
558.10	7	0.225806	1.362838
553.00	8	0.258065	1.209009
550.30	9	0.290323	1.070186
532.50	10	0.322581	0.942982
531.50	11	0.354839	0.824955
502.50	12	0.387097	0.714272
482.00	13	0.419355	0.609513
476.30	14	0.451613	0.509537
472.20	15	0.483871	0.413399
465.80	16	0.516129	0.320292
461.00	17	0.548387	0.229501
458.00	18	0.580645	0.140369
452.60	19	0.612903	0.052262
444.00	20	0.645161	-0.03546
429.30	21	0.677419	-0.12346
427.50	22	0.709677	-0.2125
422.00	23	0.741935	-0.30347
399.00	24	0.774194	-0.39748
388.80	25	0.806452	-0.49605
344.20	26	0.83871	-0.60133
324.70	27	0.870968	-0.71671
310.40	28	0.903226	-0.84817
294.50	29	0.935484	-1.00826
251.50	30	0.967742	-1.23372
Total	14293.70		16.09

$$\bar{X} = 476.46 \qquad \bar{Y} = 0.536221$$

$$S_x = 112.3889 \qquad \sigma_y = 1.13139$$

$$1/\alpha = 99.33703$$

$$\mu = 423.1901$$

$$R = 10$$

$$Y = 2.2503$$

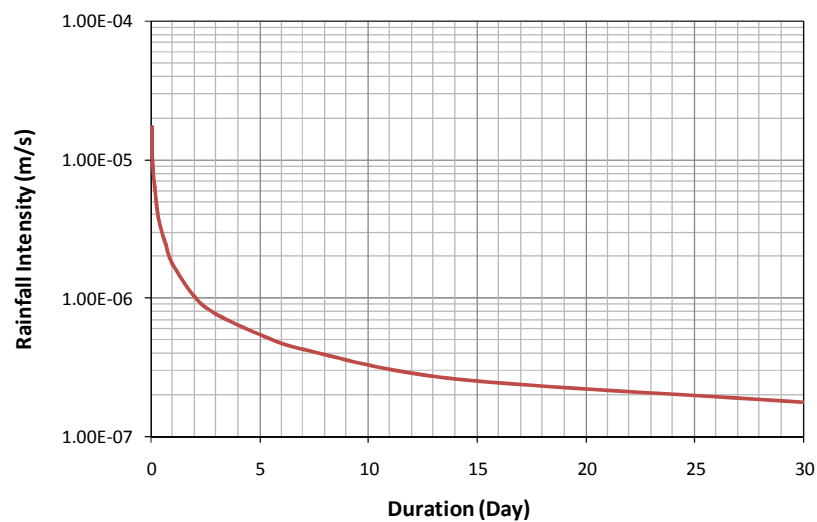
$$X = \mathbf{616.73}$$

- iii. Calculate the rainfall intensity for each duration

Duration (day)	<i>P</i> (mm)	<i>I</i> (mm/hr)
1	218.44	9.10
2	252.81	5.27
3	286.87	3.98
5	336.06	2.80
7	368.02	2.19
14	452.90	1.35
30	646.73	0.90

3. Plot the IDF curve for Johor Bahru

Duration (day)	Intensity (mm/hr)	Intensity (m/s)
0.042	88.44	$2.46 \times 10^{-5}$
0.083	54.44	$1.51 \times 10^{-5}$
0.167	32.46	$9.02 \times 10^{-6}$
0.333	19.52	$5.42 \times 10^{-6}$
0.667	12.34	$3.43 \times 10^{-6}$
1.000	9.10	$2.53 \times 10^{-6}$
2.000	5.27	$1.46 \times 10^{-6}$
3.000	3.98	$1.11 \times 10^{-6}$
5.000	2.80	$7.78 \times 10^{-7}$
7.000	2.19	$6.08 \times 10^{-7}$
14.000	1.35	$3.75 \times 10^{-7}$
30.000	0.90	$2.50 \times 10^{-7}$



**APPENDIX B**

## APPENDIX B

### Program for CR10X Data Logger

```

;{CR10X}
;Program Name: cr10x_program
;Date: 29th January 2007
;
;This program will monitor
;32 x 5301 Pressure Transducers (connected to Jetfill Tensiometer) 4-20mA output.
0-100kPa (0-1 bar) range
;32 x 5201f1L06 Gypsum Moisture Block
;-----
;Wiring for 5301 Pressure Transducers (qty 32)
; CR10X - AM416#1
;-----
; C1    - RES
; C2    - CLK
; 12V   - 12V
; G     - G

; SE1   - COM H1
; SE2   - COM L1
; SE3   - COM H2
; SE4   - COM L2

;SE2 loop to G
;SE4 loop to G
;100 Ohm precision resistor needs to be wired between SE1 and SE2
;100 Ohm precision resistor needs to be wired between SE3 and SE4

;Channel 1 on AM416
;-----
;Sensor#1 - AM416#1
; White   - H1
; Green   - L1
;Sensor#2 - AM416#1
; White   - H2
; Green   - L2
;Repeat the above for each of the 16 channels on the AM416.
; Relay
; C8
; G

```

;Note: The Pressure Transducers require a independent 24V power supply. The power supply is to be connected to the sensors via a relay (see wiring above)  
 ; The ground for the sensor power supply and the CR10X power supply need to be linked.

-----  
 ;Wiring for the 5201f1L106 Gypsum Blocks (qty 32)  
 ; CR10X - AM416#2

-----  
 ; C3 - RES  
 ; C4 - CLK  
 ; 12V - 12V  
 ; G - G

; SE5 - COM H1  
 ; AG - COM L1  
 ; SE6 - COM H2  
 ; AG - COM L2

;Channel 1 on AM416

-----  
 ;Sensor#1 - AM416#1  
 ; Wire1 - H1  
 ; Wire2 - L1  
 ;Sensor#2 - AM416#1  
 ; Wire1 - H2  
 ; Wire2 - L2

;Repeat the above for each of the 16 channels on the AM416

; 1k Ohm resistor needs to be wired between E1 and SE5  
 ; 1k Ohm resistor needs to be wired between E1 and SE6

-----  
 \*Table 1 Program  
 01: 10 Execution Interval (seconds) ;

-----

; Every minute, set Flag 1 to measure the sensors. Flag 1 can be set manually at any time to make measurements.

32: If time is (P92)  
 1: 0 Minutes (Seconds --) into a  
 2: 1 Interval (same units as above)  
 3: 11 Set Flag 1 High

-----

; If Flag 1 is high, make measurements.

4: If Flag/Port (P91)

1: 11 Do if Flag 1 is High

2: 30 Then Do

; Switch relay ON to power the pressure transducers

5: Do (P86)

1: 48 Set Port 8 High

; Turn the multiplexer#1 ON.

6: Do (P86)

1: 41 Set Port 1 High

; Loop of 16 (w/2 reps) for 32 pressure transducer sensors.

7: Beginning of Loop (P87)

1: 0 Delay

2: 16 Loop Count

; Switch the multiplexer to the next channel.

8: Do (P86)

1: 72 Pulse Port 2

; Allow a delay for switch bounce and for the sensor output to stabilize.

9: Excitation with Delay (P22)

1: 3 Ex Channel

2: 0 Delay W/Ex (0.01 sec units)

3: 5 Delay After Ex (0.01 sec units)

4: 0 mV Excitation

10: Step Loop Index (P90)

1: 2 Step

; Take measurement

11: Volt (Diff) (P2)

1: 2 Reps

2: 5 2500 mV Slow Range

3: 1 DIFF Channel

4: 1 -- Loc [ PresKPa\_1 ]

5: 0.0625 Multiplier

6: -25 Offset

12: End (P95) ; End of Loop.

; Turn the multiplexer#1 OFF.

```

13: Do (P86)
    1: 51      Set Port 1 Low

```

```

;Switch relay OFF.

```

```

14: Do (P86)
    1: 58      Set Port 8 Low

```

```

;Convert KPa to bar

```

```

15: Beginning of Loop (P87)
    1: 0        Delay
    2: 32       Loop Count

```

```

    16: Z=X/Y (P38)
        1: 1      -- X Loc [ PresKPa_1 ]
        2: 488    Y Loc [ BarConver ]
        3: 33     -- Z Loc [ PresBar_1 ]

```

```

17: End (P95)

```

```

; Turn the multiplexer#2 ON.

```

```

18: Do (P86)
    1: 43      Set Port 3 High

```

```

; Loop of 16 (w/2 reps) for 32 pressure transducer sensors.

```

```

19: Beginning of Loop (P87)
    1: 0        Delay
    2: 16       Loop Count

```

```

    20: Step Loop Index (P90)
        1: 2      Step

```

```

; Switch the multiplexer to the next channel.

```

```

21: Do (P86)
    1: 74      Pulse Port 4

```

```

; Allow a delay for switch bounce and for the sensor output to stabilize.

```

```

22: Excitation with Delay (P22)
    1: 1      Ex Channel
    2: 0      Delay W/Ex (0.01 sec units)
    3: 5      Delay After Ex (0.01 sec units)
    4: 0      mV Excitation

```

```

;Take measurement

```

23: AC Half Bridge (P5)  
 1: 2 Reps  
 2: 14 250 mV Fast Range  
 3: 5 SE Channel  
 4: 1 Excite all reps w/Exchan 1  
 5: 250 mV Excitation  
 6: 65 -- Loc [ Ohm\_1 ]  
 7: 1.0 Multiplier  
 8: 0.0 Offset

24: BR Transform  $R_f[X/(1-X)]$  (P59)  
 1: 2 Reps  
 2: 65 -- Loc [ Ohm\_1 ]  
 3: 1 Multiplier (Rf)

25: End (P95) ; End of Loop.

; Turn the multiplexer#2 OFF.

26: Do (P86)  
 1: 53 Set Port 3 Low

; Turn Switch 12V on for AVW1

27: Do (P86)  
 1: 47 Set Port 7 High

-----  
 ;Set Output flag high and store data

28: If time is (P92)  
 1: 0 Minutes (Seconds --) into a  
 2: 5 Interval (same units as above)  
 3: 10 Set Output Flag High (Flag 0)

29: Set Active Storage Area (P80)^21267  
 1: 1 Final Storage Area 1  
 2: 100 Array ID

30: Sample (P70)^13475  
 1: 20 Reps  
 2: 1 Loc [ PresKPa\_1 ]

31: Sample (P70)^4633  
 1: 20 Reps

2: 65            Loc [ Ohm\_1        ]

32: Sample (P70)^27719

1: 20            Reps

2: 456           Loc [ SucKPA\_1    ]

\*Table 2 Program

02: 0.0000      Execution Interval (seconds)

\*Table 3 Subroutines

End Program

-Input Locations-

1 PresKPa\_1 7 2 1

2 PresKPa\_2 27 1 1

3 PresKPa\_3 11 1 0

4 PresKPa\_4 3 1 0

5 PresKPa\_5 3 1 0

6 PresKPa\_6 3 1 0

7 PresKPa\_7 3 1 0

8 PresKPa\_8 3 1 0

9 PresKPa\_9 3 1 0

10 PresKP\_10 3 1 0

11 PresKP\_11 3 1 0

12 PresKP\_12 3 1 0

13 PresKP\_13 3 1 0

14 PresKP\_14 3 1 0

15 PresKP\_15 3 1 0

16 PresKP\_16 3 1 0

17 PresKP\_17 3 1 0

18 PresKP\_18 3 1 0

19 PresKP\_19 3 1 0

20 PresKP\_20 3 1 0

21 PresKP\_21 3 0 0

22 PresKP\_22 3 0 0

23 PresKP\_23 3 0 0

24 PresKP\_24 3 0 0

25 PresKP\_25 3 0 0

26 PresKP\_26 3 0 0

27 PresKP\_27 3 0 0

28 PresKP\_28 3 0 0

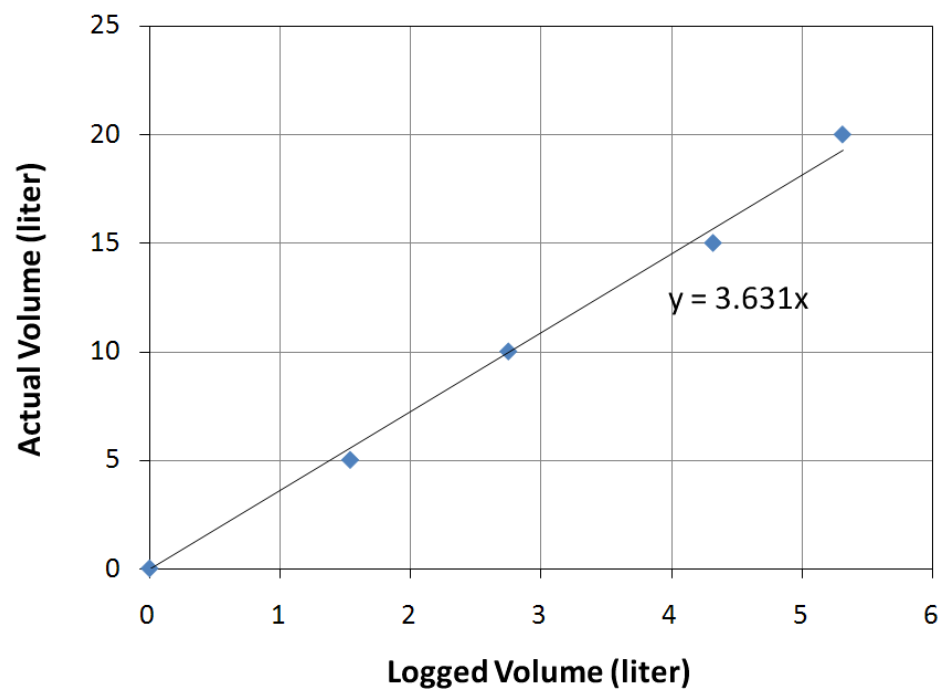
29 PresKP\_29 3 0 0

30 PresKP\_30 3 0 0

31 PresKP\_31 3 0 0  
32 PresKP\_32 19 0 0  
33 Ohm\_1 7 3 2  
34 Ohm\_2 27 2 2  
35 Ohm\_3 11 1 0  
36 Ohm\_4 11 1 0  
37 Ohm\_5 11 1 0  
38 Ohm\_6 11 1 0  
39 Ohm\_7 11 1 0  
40 Ohm\_8 11 1 0  
41 Ohm\_9 11 1 0  
42 Ohm\_10 11 1 0  
43 Ohm\_11 11 1 0  
44 Ohm\_12 11 1 0  
45 Ohm\_13 11 1 0  
46 Ohm\_14 11 1 0  
47 Ohm\_15 11 1 0  
48 Ohm\_16 11 1 0  
49 Ohm\_17 11 1 0  
50 Ohm\_18 11 1 0  
51 Ohm\_19 11 1 0  
52 Ohm\_20 11 1 0  
53 Ohm\_21 11 0 0  
54 Ohm\_22 11 0 0  
55 Ohm\_23 11 0 0  
56 Ohm\_24 11 0 0  
57 Ohm\_25 11 0 0  
58 Ohm\_26 11 0 0  
59 Ohm\_27 11 0 0  
60 Ohm\_28 11 0 0  
61 Ohm\_29 11 0 0  
62 Ohm\_30 11 0 0  
63 Ohm\_31 11 0 0  
64 Ohm\_32 19 0 0  
-Program Security-  
0000  
0000  
0000  
-Mode 4-  
-Final Storage Area 2-0  
-CR10X ID-0  
-CR10X Power Up-3

**APPENDIX C**

**APPENDIX C**  
**Calibration Result of Runoff Collector**



**APPENDIX D**

## APPENDIX D

### Field Monitoring Data

#### 1. Monitoring Data of Balai Cerapan Site

Date	Daily Rainfall Intensity (mm/day)	Max. Hourly Rainfall (mm/hr)	Suction Measurements (kPa)					
			0.5m		1.0m		1.5m	
			Max	Min	Max	Min	Max	Min
12-Sep-06	0	0	13	6	16	11	20	15
13-Sep-06	0	0	13	10	14	12	18	17
14-Sep-06	57.4	44.6	13	0	17	7	21	10
15-Sep-06	57.4	28	4	3	8	7	12	11
16-Sep-06	3.6	2.4	10	5	15	8	18	12
17-Sep-06	1.2	0.2	11	5	14	8	19	12
18-Sep-06	0	0	12	9	15	12	20	17
19-Sep-06	0	0	13	8	16	10	20	15
20-Sep-06	0	0	12	9	15	12	20	16
21-Sep-06	0	0	14	10	17	12	21	16
22-Sep-06	0	0	12	10	15	12	21	17
23-Sep-06	11.4	6.4	11	5	14	10	18	13
24-Sep-06	1.4	1.2	13	9	16	13	21	17
25-Sep-06	3.4	3.2	10	7	14	11	19	15
26-Sep-06	4	3.2	11	9	13	12	19	16
27-Sep-06	0	0	11	9	15	13	19	17
28-Sep-06	59	49	10	0	15	6	18	10
29-Sep-06	0	0	12	8	16	12	19	17
30-Sep-06	0	0	12	10	13	11	19	18
1-Oct-06	0	0	11	9	13	12	18	17
2-Oct-06	0	0	14	12	17	15	21	18
3-Oct-06	37.6	29	11	2	14	6	18	10
4-Oct-06	0	0	12	6	16	12	20	15
5-Oct-06	0	0	13	9	16	12	20	16
6-Oct-06	0	0	13	9	16	11	20	15
7-Oct-06	0	0	12	10	16	13	20	18
8-Oct-06	0	0	11	10	14	13	18	16
9-Oct-06	0	0	15	11	18	14	22	18
10-Oct-06	0	0	14	7	17	10	21	15
11-Oct-06	0	0	11	9	14	12	18	16
12-Oct-06	0	0	14	10	17	13	21	16

13-Oct-06	1.4	1.2	15	8	17	11	21	15
14-Oct-06	0	0	14	11	17	12	21	17
15-Oct-06	48.4	34.6	12	2	14	6	17	10
16-Oct-06	0	0	11	9	16	14	20	16
17-Oct-06	0	0	12	7	16	10	19	14
18-Oct-06	0	0	14	8	18	11	21	16
19-Oct-06	0	0	14	6	18	10	20	13
20-Oct-06	9.4	9.2	11	5	15	10	17	13
21-Oct-06	0	0	11	10	15	13	19	18
22-Oct-06	0.8	0.4	15	7	19	11	22	14
23-Oct-06	0.8	0.6	14	8	19	12	22	15
24-Oct-06	1	0.8	13	8	17	12	20	15
25-Oct-06	7	4.4	14	7	16	14	21	17
26-Oct-06	1.6	1.2	17	8	20	10	24	15
27-Oct-06	24.8	12.8	15	3	17	7	21	12
28-Oct-06	0	0	12	7	16	11	20	15
29-Oct-06	1.8	0.8	14	8	18	11	21	14
30-Oct-06	15.2	14.8	12	5	16	11	19	14
31-Oct-06	77.8	47	14	0	18	6	21	10
1-Nov-06	24.4	19.2	10	3	15	11	18	15
2-Nov-06	8.2	8	11	4	15	10	18	13
3-Nov-06	38.2	21.2	8	2	14	6	17	10
4-Nov-06	0	0	12	6	15	12	19	16
5-Nov-06	32.2	31	15	3	18	7	22	12
6-Nov-06	6	5.8	9	4	13	9	16	13
7-Nov-06	20.8	16.4	13	3	17	7	21	12
8-Nov-06	0	0	9	5	13	10	16	14
9-Nov-06	52.4	27.2	14	3	17	12	21	16
10-Nov-06	0.8	0.8	13	5	17	9	21	13
11-Nov-06	39.2	26	10	2	15	7	18	10
12-Nov-06	0	0	13	8	18	12	21	14
13-Nov-06	6	3.4	14	6	17	10	21	12
14-Nov-06	15.8	11.4	7	3	12	7	16	13
15-Nov-06	13	6.2	9	3	12	7	15	12
16-Nov-06	0	0	11	6	15	11	18	15
17-Nov-06	0	0	14	9	17	13	21	17
18-Nov-06	0	0	14	10	18	13	21	16
19-Nov-06	37.2	24	16	2	20	13	22	17
20-Nov-06	46.8	15.4	7	4	12	7	16	11
21-Nov-06	1.4	1.2	8	5	12	8	15	13
22-Nov-06	17.2	15.2	7	4	13	8	16	13
23-Nov-06	0	0	10	6	15	12	18	16
24-Nov-06	10.8	8.4	9	4	13	7	17	11

25-Nov-06	12.2	10.2	8	4	12	7	16	12
26-Nov-06	0	0	10	8	13	12	17	14
27-Nov-06	2.4	0.6	11	7	14	10	18	13
28-Nov-06	1.2	0.6	8	6	12	10	15	13
29-Nov-06	0	0	12	9	16	14	19	16
30-Nov-06	0	0	14	10	18	13	20	16
1-Dec-06	0	0	13	7	17	10	21	15
2-Dec-06	0	0	14	8	17	12	21	14
3-Dec-06	0	0	11	7	14	11	20	16
4-Dec-06	0	0	11	9	14	12	20	16
5-Dec-06	0	0	13	10	17	12	23	16
6-Dec-06	0	0	15	7	18	11	21	14
7-Dec-06	0	0	12	10	15	12	18	16
8-Dec-06	20	19.6	17	3	20	8	23	19
9-Dec-06	0.6	0.4	13	8	14	8	19	15
10-Dec-06	53	36.4	14	2	18	7	20	12
11-Dec-06	43.6	27	7	3	13	7	17	11
12-Dec-06	8	7.8	13	5	17	10	20	14
13-Dec-06	8.4	4.6	7	5	10	8	14	12
14-Dec-06	3	1.2	10	5	14	9	19	13
15-Dec-06	1	0.8	7	5	11	9	15	13
16-Dec-06	5.4	5.4	11	6	14	11	20	16
17-Dec-06	150.8	46.4	5	0	9	6	15	12
18-Dec-06	48	14.6	5	3	8	6	13	11
19-Dec-06	190.8	23.6	3	2	7	6	11	10
20-Dec-06	60.8	17.4	7	3	13	7	17	12
21-Dec-06	25.2	16.6	5	2	7	6	12	10
22-Dec-06	13.8	12.4	5	4	9	8	14	13
23-Dec-06	0.8	0.4	9	6	13	10	17	14
24-Dec-06	0	0	11	8	14	11	20	16
25-Dec-06	1.6	0.8	13	8	15	11	18	15
26-Dec-06	105.8	9.8	3	2	7	5	12	10
27-Dec-06	19	6.6	6	5	10	9	14	13
28-Dec-06	24.4	6.8	4	2	7	5	12	10
29-Dec-06	0	0	7	3	12	7	15	12
30-Dec-06	0	0	11	8	14	11	19	14
31-Dec-06	0	0	13	8	15	13	20	16
1-Jan-07	0	0	10	7	14	10	17	13
2-Jan-07	0	0	12	7	16	10	21	15
3-Jan-07	13	10.2	10	4	15	10	19	14
4-Jan-07	0	0	10	7	14	10	19	14
5-Jan-07	0	0	13	6	18	9	22	13
6-Jan-07	0	0	12	7	17	11	21	15

7-Jan-07	0	0	14	6	16	9	20	14
8-Jan-07	4.8	4.8	12	5	18	16	22	20
9-Jan-07	18.2	7	8	5	10	8	15	13
10-Jan-07	3.6	3.4	10	6	14	12	20	17
11-Jan-07	157	23	7	3	15	14	21	18
12-Jan-07	173.8	25.6	3	2	7	6	11	10
13-Jan-07	22	6.4	5	4	8	6	12	11
14-Jan-07	11.4	2.2	6	5	8	8	12	11
15-Jan-07	5.8	4.2	7	5	10	8	14	12
16-Jan-07	0	0	10	6	14	12	16	13
17-Jan-07	0	0	14	7	16	10	18	14
18-Jan-07	3.6	3.4	13	6	17	9	20	15
19-Jan-07	10.8	5.6	13	5	17	8	21	17
20-Jan-07	0	0	12	9	16	12	19	16
21-Jan-07	0	0	11	6	15	10	19	15
22-Jan-07	0	0	12	7	15	10	19	14
23-Jan-07	1	0.8	10	8	14	12	17	15
24-Jan-07	0.6	0.2	12	7	16	12	20	15
25-Jan-07	2	0.8	8	6	11	10	15	14
26-Jan-07	2	0.6	7	6	11	9	15	12
27-Jan-07	9.8	4	5	4	9	6	13	11
28-Jan-07	8.6	4	6	4	11	9	15	14
29-Jan-07	0	0	9	5	12	9	17	14
30-Jan-07	0	0	11	6	15	10	18	13
31-Jan-07	0	0	12	7	15	10	19	13
1-Feb-07	0	0	11	8	16	10	20	14
2-Feb-07	0	0	12	7	16	9	20	14
3-Feb-07	0	0	11	8	14	9	18	13
4-Feb-07	0	0	13	10	15	12	19	17
5-Feb-07	0	0	15	13	16	14	20	18
6-Feb-07	0	0	17	8	17	10	21	15
7-Feb-07	0	0	16	11	18	11	21	15
8-Feb-07	0	0	18	10	19	14	23	16
9-Feb-07	0	0	20	12	20	13	23	17
10-Feb-07	0	0	26	12	20	11	25	15
11-Feb-07	0	0	24	13	19	14	23	16
12-Feb-07	0	0	23	14	18	11	21	15
13-Feb-07	0	0	26	13	20	13	22	17
14-Feb-07	0	0	19	14	18	12	22	15
15-Feb-07	0	0	16	12	20	14	21	17
16-Feb-07	34	33.8	14	2	17	6	18	10
17-Feb-07	23.4	13.8	9	4	11	7	18	12
18-Feb-07	0.4	0.2	10	6	14	12	16	13

19-Feb-07	1.4	0.8	9	6	15	11	17	13
20-Feb-07	0	0	11	7	14	11	19	14
21-Feb-07	0	0	14	9	17	13	21	17
22-Feb-07	0	0	13	8	17	12	21	14
23-Feb-07	0	0	14	9	16	10	19	14
24-Feb-07	2.2	1.4	15	6	15	10	20	14
25-Feb-07	23.4	21.2	10	3	11	7	18	12
26-Feb-07	2.8	1.2	12	5	16	8	21	14
27-Feb-07	0	0	12	6	15	9	20	15
28-Feb-07	28.4	16.4	7	4	12	7	18	13
1-Mar-07	14.8	2.8	6	5	11	8	18	12
2-Mar-07	14	6.4	8	5	12	7	19	13
3-Mar-07	38.8	18.6	8	3	11	6	17	10
4-Mar-07	7.2	6.4	13	4	16	9	20	13
5-Mar-07	0	0	11	6	15	10	19	14
6-Mar-07	0	0	14	8	17	11	21	13
7-Mar-07	0	0	13	9	16	13	19	17
8-Mar-07	0	0	12	7	17	12	21	13
9-Mar-07	0	0	15	10	18	14	21	17
10-Mar-07	0	0	14	8	18	11	22	15
11-Mar-07	0	0	13	10	18	11	20	15
12-Mar-07	0	0	16	11	17	14	21	17
13-Mar-07	2	0.8	15	8	18	11	23	14
14-Mar-07	6.6	2.2	13	7	16	10	23	14
15-Mar-07	16.2	15.8	15	4	17	8	19	14
16-Mar-07	2.6	2.2	10	6	15	8	19	18
17-Mar-07	0	0	12	7	15	11	21	17
18-Mar-07	0	0	15	9	15	11	21	17
19-Mar-07	0	0	14	10	15	11	21	17
20-Mar-07	7.4	7.2	17	5	20	8	22	18
21-Mar-07	47.4	22.8	12	3	15	7	21	17
22-Mar-07	0	0	9	5	14	8	21	12
23-Mar-07	2.6	0.8	16	6	18	12	20	17
24-Mar-07	0	0	12	7	15	11	21	17
25-Mar-07	0	0	12	7	15	11	21	17
26-Mar-07	1	1	11	5	17	9	21	14
27-Mar-07	0	0	12	8	16	10	20	15
28-Mar-07	0.6	0.2	13	7	19	11	23	16
29-Mar-07	49.4	42.4	13	1	17	7	21	10
30-Mar-07	26.8	17.2	7	4	13	7	17	11
31-Mar-07	55.8	34	12	2	15	6	21	11
1-Apr-07	0.4	0.2	10	5	15	8	18	12
2-Apr-07	0	0	13	6	16	10	19	14

3-Apr-07	0	0	8	7	12	11	18	16
4-Apr-07	0	0	11	8	14	11	20	17
5-Apr-07	0	0	9	7	12	10	21	16
6-Apr-07	0	0	12	9	14	12	21	17
7-Apr-07	0.4	0.4	13	9	16	11	19	18
8-Apr-07	0.8	0.4	14	8	16	11	24	16
9-Apr-07	0	0	12	10	13	12	18	16
10-Apr-07	1	0.6	14	9	17	11	20	15
11-Apr-07	0	0	15	11	18	13	21	17
12-Apr-07	2.4	1.8	16	7	17	12	24	16
13-Apr-07	1.6	1.4	13	8	16	11	20	15
14-Apr-07	1.8	1.4	14	7	17	10	21	15
15-Apr-07	4.6	2.8	19	7	18	10	22	16
16-Apr-07	0	0	15	9	13	12	17	17
17-Apr-07	0.4	0.2	15	7	17	12	19	15
18-Apr-07	0	0	17	11	17	14	22	17
19-Apr-07	6.4	3.8	16	6	19	10	18	15
20-Apr-07	0	0	13	9	18	13	19	16
21-Apr-07	0	0	15	10	19	12	21	16
22-Apr-07	1	0.8	16	9	19	11	20	17
23-Apr-07	20.8	19.6	19	4	14	9	17	16
24-Apr-07	0	0	13	7	17	12	19	18
25-Apr-07	5	3.8	14	5	20	12	24	20
26-Apr-07	3.4	3	15	5	18	10	21	18
27-Apr-07	1.8	1	16	8	18	13	20	17
28-Apr-07	0	0	15	9	17	13	20	18
29-Apr-07	43.8	28.2	13	5	14	7	17	15
30-Apr-07	32.2	23	10	5	13	7	17	15
1-May-07	3.4	2	13	6	15	9	18	16
2-May-07	35	21.2	10	5	14	7	18	14
3-May-07	0	0	12	7	15	8	19	16
4-May-07	14.4	10.6	11	7	14	7	18	15
5-May-07	0	0	12	8	16	9	20	16
6-May-07	0	0	13	10	15	10	20	16
7-May-07	0	0	12	10	14	12	20	18
8-May-07	0	0	14	8	18	10	24	14
9-May-07	36.4	12.2	8	2	10	6	14	10
10-May-07	0	0	12	6	14	8	20	14
11-May-07	8.8	6	10	6	14	10	20	14
12-May-07	0	0	10	7	14	10	18	16
13-May-07	18	10.4	10	6	12	7	16	14
14-May-07	0	0	12	7	16	8	18	15
15-May-07	2	1.2	12	8	16	9	18	14

16-May-07	0	0	12	8	16	10	20	14
17-May-07	0	0	14	6	16	12	24	16
18-May-07	0	0	12	8	15	11	21	14
19-May-07	49	42.2	10	0	12	6	16	10
20-May-07	0	0	12	7	14	10	20	15
21-May-07	0.6	0.6	10	5	13	8	21	13
22-May-07	30.6	21.4	7	4	10	6	16	10
23-May-07	0.4	0.4	8	4	10	9	16	14
24-May-07	0	0	9	6	12	10	16	14
25-May-07	1	0.6	11	7	14	10	17	13
26-May-07	49.8	40.4	10	0	12	6	16	10
27-May-07	0	0	11	6	12	8	16	14
28-May-07	7.2	7.2	8	6	12	8	17	12
29-May-07	0	0	10	6	14	10	19	14
30-May-07	0	0	12	8	14	9	20	14
31-May-07	3	1.4	8	7	11	10	15	14
1-Jun-07	18.2	10.6	8	4	12	10	16	14
2-Jun-07	49.2	46.6	10	0	14	6	16	10
3-Jun-07	25	15.8	11	4	14	7	18	15
4-Jun-07	5.6	4	11	6	15	7	18	16
5-Jun-07	0	0	12	8	16	8	20	17
6-Jun-07	0	0	12	8	16	8	20	17
7-Jun-07	38.4	34.8	12	4	14	10	18	15
8-Jun-07	50	38	10	4	14	7	18	14
9-Jun-07	1.8	1.4	11	4	14	10	19	14
10-Jun-07	37.2	31.2	12	2	13	8	18	14
11-Jun-07	0	0	10	4	14	10	19	14
12-Jun-07	0	0	8	7	12	10	18	13
13-Jun-07	7.8	7.6	10	6	14	8	18	14
14-Jun-07	63.6	33.2	10	2	14	7	20	12
15-Jun-07	0	0	6	4	12	9	14	12
16-Jun-07	2.2	1	8	6	13	10	17	14
17-Jun-07	1.2	1	10	7	14	10	17	15
18-Jun-07	0	0	14	8	17	10	24	15
19-Jun-07	0.4	0.4	14	8	18	10	22	14
20-Jun-07	0	0	14	6	18	10	24	14
21-Jun-07	0	0	13	8	18	12	24	16
22-Jun-07	0	0	15	8	19	12	24	18
23-Jun-07	0.6	0.6	13	7	18	11	24	16
24-Jun-07	0	0	12	8	16	13	22	17
25-Jun-07	0.4	0.2	9	8	12	10	18	16
26-Jun-07	73	35	10	3	14	6	20	12
27-Jun-07	0	0	14	7	18	8	23	13

28-Jun-07	0	0	10	7	16	10	22	15
29-Jun-07	2.2	1.4	12	6	16	9	20	14
30-Jun-07	0	0	13	8	18	10	22	16
1-Jul-07	0	0	13	7	18	10	22	16
2-Jul-07	0	0	14	6	16	10	20	14
3-Jul-07	0	0	12	7	15	10	20	14
4-Jul-07	0	0	12	7	15	10	19	15
5-Jul-07	8	6.8	14	9	16	12	21	15
6-Jul-07	0	0	14	10	17	14	22	16
7-Jul-07	26.4	26	10	5	15	7	20	12
8-Jul-07	0	0	11	6	16	8	22	14
9-Jul-07	2.2	1.2	10	6	14	9	20	14
10-Jul-07	0	0	10	7	15	9	19	15
11-Jul-07	2	2	8	6	10	8	15	14
12-Jul-07	0	0	11	8	14	10	19	14
13-Jul-07	2	2	11	7	13	10	18	14
14-Jul-07	0	0	12	8	15	12	18	14
15-Jul-07	0.6	0.4	13	7	15	13	18	16
16-Jul-07	4.6	4.6	14	8	15	13	19	15
17-Jul-07	1.8	1	14	10	16	13	19	16
18-Jul-07	6.2	3.8	12	9	13	12	18	15
19-Jul-07	1.2	0.8	12	8	14	12	18	16
20-Jul-07	0	0	14	9	16	12	20	16
21-Jul-07	11.6	10.6	12	6	14	9	18	14
22-Jul-07	30.2	5.2	12	5	14	8	17	16
23-Jul-07	3.8	0.4	8	6	11	8	16	15
24-Jul-07	0	0	8	6	11	7	16	12
25-Jul-07	0	0	8	6	12	8	16	14
26-Jul-07	0	0	8	6	12	8	17	14
27-Jul-07	19.6	12.2	10	4	12	8	18	14
28-Jul-07	0	0	10	6	12	9	17	14
29-Jul-07	6	3.2	8	6	10	8	15	13
30-Jul-07	7	3.8	10	5	12	8	19	14
31-Jul-07	0	0	8	6	12	8	17	13
1-Aug-07	11.4	11	10	5	15	9	18	14
2-Aug-07	0	0	8	8	14	11	16	12
3-Aug-07	0	0	12	7	14	11	17	14
4-Aug-07	0	0	10	8	14	11	19	16
5-Aug-07	0	0	10	8	12	10	16	14
6-Aug-07	0	0	12	10	14	12	18	14
7-Aug-07	0	0	12	7	15	10	20	15
8-Aug-07	0	0	14	7	16	11	20	14
9-Aug-07	15.4	15	12	6	14	9	20	14

10-Aug-07	0	0	14	8	16	10	21	15
11-Aug-07	0	0	14	9	16	12	20	16
12-Aug-07	11.6	8.8	12	6	14	11	18	13
13-Aug-07	0.4	0.4	14	8	15	12	20	14
14-Aug-07	45.8	23	8	4	11	8	15	14
15-Aug-07	1	0.6	12	7	14	10	16	15
16-Aug-07	11.6	8.4	8	4	13	10	15	13
17-Aug-07	6.8	6	9	6	12	10	15	13
18-Aug-07	9.2	9	9	6	13	9	16	13
19-Aug-07	38.2	22.8	7	4	10	7	14	12
20-Aug-07	12.4	12.2	9	6	12	9	15	13
21-Aug-07	0	0	10	8	14	10	16	13
22-Aug-07	0	0	8	6	12	11	17	14
23-Aug-07	6.2	3.6	9	8	10	9	16	15
24-Aug-07	1.8	1.2	8	4	13	7	15	14
25-Aug-07	1.4	1	8	6	12	10	18	14
26-Aug-07	0	0	10	7	14	10	18	15
27-Aug-07	0	0	12	8	14	10	20	15
28-Aug-07	6.8	3.2	8	3	14	10	16	13
29-Aug-07	0.4	0.2	10	8	16	14	18	16
30-Aug-07	18.2	5.2	10	5	14	8	16	13
31-Aug-07	0	0	12	9	15	11	21	16
1-Sep-07	12.8	6.2	5	4	10	8	12	10
2-Sep-07	32.4	20.8	8	5	10	7	14	12
3-Sep-07	43	20.6	6	4	8	6	12	11
4-Sep-07	0	0	8	6	10	9	16	14
5-Sep-07	0	0	16	10	18	13	23	19
6-Sep-07	0	0	16	10	18	16	24	20
7-Sep-07	2	2	14	10	16	10	21	19
8-Sep-07	15.6	5.6	9	7	14	9	16	14
9-Sep-07	0	0	11	8	16	11	18	16
10-Sep-07	17	8.6	10	5	14	8	16	13
11-Sep-07	13.4	12.4	10	5	14	7	16	12

## 2. Monitoring Data of Kolej 12 site

Date	Daily Rainfall Intensity (mm/day)	Max. Hourly Rainfall (mm/hr)	Suction Measurements (kPa)					
			0.5m		1.0m		1.5m	
			Max	Min	Max	Min	Max	Min
1-Jan-07	0	0	28	24	24	20	22	20
2-Jan-07	0	0	28	22	24	20	24	20
3-Jan-07	13	10.2	24	20	20	18	20	18
4-Jan-07	0	0	24	18	24	20	22	20
5-Jan-07	0	0	26	20	22	20	22	20
6-Jan-07	0	0	30	24	24	22	24	20
7-Jan-07	0	0	34	28	24	22	24	22
8-Jan-07	4.8	4.8	32	28	20	18	20	20
9-Jan-07	18.2	7	24	20	20	18	18	16
10-Jan-07	3.6	3.4	24	20	18	16	18	16
11-Jan-07	157	23	10	6	12	10	12	10
12-Jan-07	173.8	25.6	4	2	8	6	10	8
13-Jan-07	22	6.4	2	0	8	6	10	6
14-Jan-07	11.4	2.2	2	0	8	6	12	8
15-Jan-07	5.8	4.2	4	2	10	8	12	8
16-Jan-07	0	0	6	4	14	10	14	10
17-Jan-07	0	0	10	6	12	10	14	12
18-Jan-07	3.6	3.4	8	6	14	12	16	12
19-Jan-07	10.8	5.6	8	8	16	14	16	14
20-Jan-07	0	0	10	8	16	14	18	14
21-Jan-07	0	0	10	8	18	16	18	16
22-Jan-07	0	0	12	8	18	16	20	18
23-Jan-07	1	0.8	16	12	20	18	20	18
24-Jan-07	0.6	0.2	16	14	20	20	21	18
25-Jan-07	2	0.8	16	14	20	18	21	20
26-Jan-07	2	0.6	18	16	18	16	20	18
27-Jan-07	9.8	4	16	14	20	18	20	18
28-Jan-07	8.6	4	16	12	18	16	20	18
29-Jan-07	0	0	18	14	20	18	20	16
30-Jan-07	0	0	22	18	22	18	22	18
31-Jan-07	0	0	24	20	22	20	22	20
1-Feb-07	0	0	30	24	24	20	24	20
2-Feb-07	0	0	34	30	26	22	26	20
3-Feb-07	0	0	36	32	28	26	26	22
4-Feb-07	0	0	40	34	28	26	28	24
5-Feb-07	0	0	46	38	30	28	30	28

6-Feb-07	0	0	48	42	32	30	30	30
7-Feb-07	0	0	54	44	32	30	32	30
8-Feb-07	0	0	60	50	36	34	36	34
9-Feb-07	0	0	60	52	40	36	40	36
10-Feb-07	0	0	66	54	42	38	40	38
11-Feb-07	0	0	67	54	46	42	42	40
12-Feb-07	0	0	70	60	46	40	44	40
13-Feb-07	0	0	70	60	44	42	44	42
14-Feb-07	0	0	74	60	48	42	46	42
15-Feb-07	0	0	72	58	46	42	44	42
16-Feb-07	34	33.8	34	30	38	36	40	40
17-Feb-07	23.4	13.8	20	18	34	32	36	34
18-Feb-07	0.4	0.2	22	16	34	32	36	32
19-Feb-07	1.4	0.8	22	16	36	32	36	32
20-Feb-07	0	0	24	20	38	34	38	34
21-Feb-07	0	0	30	24	36	34	38	34
22-Feb-07	0	0	32	28	36	34	36	34
23-Feb-07	0	0	36	30	34	32	34	30
24-Feb-07	2.2	1.4	34	30	34	30	34	30
25-Feb-07	23.4	21.2	28	24	30	28	30	28
26-Feb-07	2.8	1.2	30	24	30	26	32	26
27-Feb-07	0	0	34	28	32	28	32	26
28-Feb-07	28.4	16.4	24	20	26	24	28	26
1-Mar-07	14.8	2.8	18	14	24	22	26	24
2-Mar-07	14	6.4	14	12	24	22	26	22
3-Mar-07	38.8	18.6	4	2	18	16	20	18
4-Mar-07	7.2	6.4	6	2	20	18	20	16
5-Mar-07	0	0	10	6	20	18	22	18
6-Mar-07	0	0	10	8	22	20	22	18
7-Mar-07	0	0	16	12	24	22	24	22
8-Mar-07	0	0	18	14	24	22	26	22
9-Mar-07	0	0	24	20	26	24	28	24
10-Mar-07	0	0	26	20	26	24	28	26
11-Mar-07	0	0	34	26	26	24	26	24
12-Mar-07	0	0	42	32	26	22	26	22
13-Mar-07	2	0.8	36	32	28	24	26	24
14-Mar-07	6.6	2.2	34	30	26	22	24	22
15-Mar-07	16.2	15.8	28	24	20	18	20	18
16-Mar-07	2.6	2.2	28	24	20	18	20	20
17-Mar-07	0	0	30	24	18	16	18	16
18-Mar-07	0	0	32	28	18	16	20	16
19-Mar-07	0	0	36	30	20	16	22	18
20-Mar-07	7.4	7.2	34	26	22	18	22	18

21-Mar-07	47.4	22.8	22	16	18	16	18	16
22-Mar-07	0	0	28	18	18	16	18	16
23-Mar-07	2.6	0.8	26	18	16	14	18	16
24-Mar-07	0	0	28	22	22	20	20	16
25-Mar-07	0	0	32	26	24	20	22	18
26-Mar-07	1	1	36	26	24	20	22	20
27-Mar-07	0	0	40	32	22	20	22	20
28-Mar-07	0.6	0.2	38	30	24	22	24	20
29-Mar-07	49.4	42.4	24	20	22	18	20	18
30-Mar-07	26.8	17.2	16	12	16	14	16	16
31-Mar-07	55.8	34	6	4	12	10	14	12
1-Apr-07	0.4	0.2	6	6	12	10	14	12
2-Apr-07	0	0	8	6	14	12	16	12
3-Apr-07	0	0	12	8	16	14	16	14
4-Apr-07	0	0	16	10	18	16	18	14
5-Apr-07	0	0	20	18	18	16	18	16
6-Apr-07	0	0	24	20	20	18	18	16
7-Apr-07	0.4	0.4	22	20	22	20	20	16
8-Apr-07	0.8	0.4	20	18	22	18	20	18
9-Apr-07	0	0	24	20	20	18	20	18
10-Apr-07	1	0.6	28	22	20	18	22	20
11-Apr-07	0	0	28	24	22	20	22	20
12-Apr-07	2.4	1.8	26	24	20	18	20	16
13-Apr-07	1.6	1.4	28	22	22	20	20	18
14-Apr-07	1.8	1.4	26	24	20	18	18	16
15-Apr-07	4.6	2.8	30	24	18	16	18	16
16-Apr-07	0	0	32	26	20	18	20	16
17-Apr-07	0.4	0.2	30	28	20	18	20	18
18-Apr-07	0	0	30	26	22	18	22	18
19-Apr-07	6.4	3.8	28	24	20	18	22	20
20-Apr-07	0	0	28	26	22	20	22	20
21-Apr-07	0	0	32	30	20	18	20	18
22-Apr-07	1	0.8	34	30	22	18	20	18
23-Apr-07	20.8	19.6	28	22	20	16	18	16
24-Apr-07	0	0	26	22	20	16	20	16
25-Apr-07	5	3.8	26	20	18	15	18	16
26-Apr-07	3.4	3	28	22	18	16	18	16
27-Apr-07	1.8	1	26	22	20	18	20	16
28-Apr-07	0	0	26	24	20	18	20	18
29-Apr-07	43.8	28.2	12	10	16	14	16	14
30-Apr-07	32.2	23	6	4	14	14	16	14
1-May-07	3.4	2	8	4	14	12	14	12
2-May-07	35	21.2	4	2	10	10	12	10

3-May-07	0	0	6	4	10	8	12	10
4-May-07	14.4	10.6	6	4	12	10	14	10
5-May-07	0	0	10	8	14	12	14	12
6-May-07	0	0	14	10	16	12	16	12
7-May-07	0	0	18	14	16	14	16	14
8-May-07	0	0	22	18	16	14	16	14
9-May-07	36.4	12.2	12	10	14	12	16	14
10-May-07	0	0	14	10	18	14	18	14
11-May-07	8.8	6	12	10	18	16	18	16
12-May-07	0	0	16	12	18	16	20	18
13-May-07	18	10.4	12	10	20	18	20	16
14-May-07	0	0	16	12	18	16	18	14
15-May-07	2	1.2	18	12	18	16	18	16
16-May-07	0	0	24	18	18	16	18	16
17-May-07	0	0	28	22	20	18	20	18
18-May-07	0	0	30	24	18	16	18	16
19-May-07	49	42.2	18	16	18	16	16	14
20-May-07	0	0	16	14	16	14	16	12
21-May-07	0.6	0.6	18	14	18	14	18	14
22-May-07	30.6	21.4	14	12	16	14	16	14
23-May-07	0.4	0.4	18	12	16	14	18	16
24-May-07	0	0	20	14	18	16	18	14
25-May-07	1	0.6	24	18	20	16	20	16
26-May-07	49.8	40.4	22	14	16	14	16	14
27-May-07	0	0	16	14	16	14	16	14
28-May-07	7.2	7.2	14	12	16	14	16	14
29-May-07	0	0	18	16	18	16	18	16
30-May-07	0	0	24	20	20	16	18	16
31-May-07	3	1.4	22	20	18	14	18	14
1-Jun-07	18.2	10.6	18	14	18	16	18	16
2-Jun-07	49.2	46.6	10	8	16	12	16	12
3-Jun-07	25	15.8	6	4	14	10	14	10
4-Jun-07	5.6	4	6	4	12	10	14	12
5-Jun-07	0	0	8	6	16	14	16	12
6-Jun-07	0	0	12	8	14	12	16	12
7-Jun-07	38.4	34.8	6	4	14	10	14	10
8-Jun-07	50	38	4	2	14	10	14	10
9-Jun-07	1.8	1.4	6	2	12	8	12	8
10-Jun-07	37.2	31.2	4	2	12	10	12	10
11-Jun-07	0	0	8	4	14	10	14	10
12-Jun-07	0	0	10	8	12	10	14	12
13-Jun-07	7.8	7.6	8	6	14	12	14	12
14-Jun-07	63.6	33.2	4	2	12	8	12	10

15-Jun-07	0	0	10	4	12	12	14	12
16-Jun-07	2.2	1	12	6	14	12	14	12
17-Jun-07	1.2	1	14	10	14	12	16	12
18-Jun-07	0	0	18	14	16	14	16	14
19-Jun-07	0.4	0.4	18	14	16	14	16	14
20-Jun-07	0	0	24	20	18	14	18	14
21-Jun-07	0	0	28	22	20	16	18	16
22-Jun-07	0	0	30	26	22	18	20	16
23-Jun-07	0.6	0.6	30	26	20	18	20	18
24-Jun-07	0	0	34	28	20	18	20	18
25-Jun-07	0.4	0.2	30	28	22	20	22	20
26-Jun-07	73	35	12	10	18	16	18	16
27-Jun-07	0	0	16	12	16	14	16	14
28-Jun-07	0	0	18	16	18	16	18	14
29-Jun-07	2.2	1.4	20	16	18	16	18	16
30-Jun-07	0	0	22	18	20	18	20	18
1-Jul-07	0	0	20	14	22	18	22	20
2-Jul-07	0	0	24	20	24	20	24	20
3-Jul-07	0	0	30	22	26	20	26	20
4-Jul-07	0	0	34	24	28	22	28	22
5-Jul-07	8	6.8	28	20	26	18	22	20
6-Jul-07	0	0	28	26	26	20	24	20
7-Jul-07	26.4	26	20	16	22	18	22	20
8-Jul-07	0	0	22	18	22	20	22	20
9-Jul-07	2.2	1.2	24	20	24	20	24	20
10-Jul-07	0	0	30	22	26	20	26	20
11-Jul-07	2	2	28	22	24	20	24	20
12-Jul-07	0	0	30	24	26	22	26	22
13-Jul-07	2	2	28	22	26	22	26	24
14-Jul-07	0	0	28	24	26	24	26	24
15-Jul-07	0.6	0.4	26	22	24	22	24	22
16-Jul-07	4.6	4.6	24	18	22	18	22	20
17-Jul-07	1.8	1	24	20	22	18	22	20
18-Jul-07	6.2	3.8	22	18	20	16	20	18
19-Jul-07	1.2	0.8	24	18	20	16	20	18
20-Jul-07	0	0	24	20	20	18	20	18
21-Jul-07	11.6	10.6	20	14	18	16	18	16
22-Jul-07	30.2	5.2	10	4	16	14	18	16
23-Jul-07	3.8	0.4	4	2	14	12	18	16
24-Jul-07	0	0	5	2	14	12	18	14
25-Jul-07	0	0	8	6	16	14	18	16
26-Jul-07	0	0	10	8	18	14	18	18
27-Jul-07	19.6	12.2	18	2	20	10	22	14

28-Jul-07	0	0	6	4	16	14	18	16
29-Jul-07	6	3.2	8	6	16	14	18	16
30-Jul-07	7	3.8	14	10	20	16	22	18
31-Jul-07	0	0	14	10	20	16	20	18
1-Aug-07	11.4	11	16	14	18	18	20	18
2-Aug-07	0	0	14	8	20	16	22	16
3-Aug-07	0	0	20	14	22	18	22	20
4-Aug-07	0	0	24	20	24	20	24	20
5-Aug-07	0	0	30	22	26	20	26	20
6-Aug-07	0	0	34	24	28	22	28	22
7-Aug-07	0	0	36	26	28	24	28	24
8-Aug-07	0	0	40	28	30	24	30	24
9-Aug-07	15.4	15	28	22	24	20	26	22
10-Aug-07	0	0	30	26	28	24	28	24
11-Aug-07	0	0	32	28	30	24	30	24
12-Aug-07	11.6	8.8	28	14	20	16	20	18
13-Aug-07	0.4	0.4	14	6	22	16	26	18
14-Aug-07	45.8	23	4	2	10	10	16	14
15-Aug-07	1	0.6	8	6	18	14	20	18
16-Aug-07	11.6	8.4	4	1	12	10	14	14
17-Aug-07	6.8	6	4	2	10	10	12	12
18-Aug-07	9.2	9	6	2	10	8	12	10
19-Aug-07	38.2	22.8	4	2	8	8	12	10
20-Aug-07	12.4	12.2	4	2	8	8	12	10
21-Aug-07	0	0	6	4	10	8	12	10
22-Aug-07	0	0	10	8	12	10	12	10
23-Aug-07	6.2	3.6	8	6	10	8	12	10
24-Aug-07	1.8	1.2	8	6	12	10	12	10
25-Aug-07	1.4	1	10	8	14	12	14	12
26-Aug-07	0	0	16	14	18	16	18	16
27-Aug-07	0	0	14	12	18	16	18	16
28-Aug-07	6.8	3.2	8	6	16	14	18	16
29-Aug-07	0.4	0.2	6	4	14	14	16	16
30-Aug-07	18.2	5.2	4	2	10	10	16	14
31-Aug-07	0	0	6	4	12	10	12	10
1-Sep-07	12.8	6.2	2	2	10	8	12	10
2-Sep-07	32.4	20.8	4	2	8	8	12	10
3-Sep-07	43	20.6	1	1	10	10	14	10
4-Sep-07	0	0	6	4	14	14	16	16
5-Sep-07	0	0	14	12	20	18	23	20
6-Sep-07	0	0	32	16	28	20	26	20
7-Sep-07	2	2	28	18	28	20	26	20
8-Sep-07	15.6	5.6	16	12	20	16	22	18

9-Sep-07	0	0	18	14	24	16	26	20
10-Sep-07	17	8.6	14	10	16	12	16	12
11-Sep-07	13.4	12.4	8	4	12	10	12	10
12-Sep-07	0	0	10	8	16	14	16	16
13-Sep-07	0	0	14	12	20	18	22	20
14-Sep-07	1.6	1.4	14	10	20	16	22	20
15-Sep-07	2.4	2	14	10	20	16	22	18
16-Sep-07	30	12.4	12	6	14	12	14	12
17-Sep-07	0	0	16	10	16	12	16	14
18-Sep-07	0	0	20	18	18	16	18	16
19-Sep-07	0	0	24	20	20	18	20	18
20-Sep-07	0	0	28	18	22	18	22	20
21-Sep-07	0	0	36	30	24	18	24	17
22-Sep-07	0	0	40	26	22	20	22	20
23-Sep-07	0	0	28	24	20	20	20	20
24-Sep-07	9.2	7.6	24	20	20	16	20	14
25-Sep-07	0	0	24	22	20	18	20	18
26-Sep-07	7.4	2.6	18	16	16	14	16	14
27-Sep-07	3.8	2.8	14	10	12	8	12	8
28-Sep-07	0	0	24	14	20	12	20	12
29-Sep-07	0	0	24	20	20	18	20	18
30-Sep-07	0	0	26	22	22	18	22	20
1-Oct-07	0	0	28	24	26	22	26	20
2-Oct-07	0	0	36	30	24	18	24	20
3-Oct-07	0	0	40	26	22	20	22	20
4-Oct-07	0	0	48	20	20	18	20	18
5-Oct-07	0	0	28	24	20	20	20	20
6-Oct-07	60.8	48.8	24	8	20	16	20	16
7-Oct-07	10.8	5	12	8	16	10	16	14
8-Oct-07	16.6	10.8	10	8	14	10	14	14
9-Oct-07	0	0	14	10	18	16	18	16
10-Oct-07	6.8	5.8	18	10	12	8	12	8
11-Oct-07	0	0	12	8	16	10	16	10
12-Oct-07	0.6	0.6	24	14	20	12	20	12
13-Oct-07	1	0.8	24	20	20	18	20	18
14-Oct-07	0.6	0.6	18	12	18	12	18	12
15-Oct-07	15.6	14	24	14	20	12	20	12
16-Oct-07	50.4	47.6	18	0	22	10	24	10
17-Oct-07	5	4.6	16	2	22	12	24	12
18-Oct-07	8	7.4	6	6	16	14	16	14
19-Oct-07	6.4	6.2	12	8	18	16	20	18
20-Oct-07	0	0	14	12	18	16	18	16
21-Oct-07	0.4	0.2	18	14	20	16	20	16

22-Oct-07	34.6	12.2	18	12	18	14	20	14
23-Oct-07	15.4	7.4	14	12	18	16	18	16
24-Oct-07	3	3	20	10	20	18	20	18
25-Oct-07	0	0	20	18	22	20	22	20
26-Oct-07	0	0	28	18	22	18	22	20
27-Oct-07	0	0	36	30	24	18	24	17
28-Oct-07	0	0	40	26	22	20	22	20
29-Oct-07	0.6	0.2	28	24	20	20	20	20
30-Oct-07	0	0	48	20	20	16	20	14
31-Oct-07	19.6	8.4	24	8	20	16	20	16
1-Nov-07	2.8	1.4	24	14	20	12	20	12
2-Nov-07	0	0	24	22	20	18	20	18
3-Nov-07	10.2	8.8	18	12	18	12	18	12
4-Nov-07	2	2	24	12	22	10	22	10
5-Nov-07	38.2	12.6	2	2	12	10	12	10
6-Nov-07	18.6	8.4	4	2	12	10	12	10
7-Nov-07	13.4	9.8	8	6	18	16	18	16
8-Nov-07	0.6	0.2	26	24	18	10	18	10
9-Nov-07	2.2	1.6	22	20	16	12	16	12
10-Nov-07	2	2	24	18	12	10	12	10
11-Nov-07	0	0	28	6	18	10	18	10
12-Nov-07	23.2	11.6	20	2	14	8	10	8
13-Nov-07	19.4	9	4	2	12	10	12	10
14-Nov-07	13.2	4.4	4	2	12	10	12	10
15-Nov-07	0	0	16	10	16	12	16	12
16-Nov-07	0	0	28	26	26	20	22	18
17-Nov-07	0	0	30	26	28	20	22	20
18-Nov-07	43.8	29.4	30	6	26	16	20	16
19-Nov-07	8.2	7	18	2	16	10	16	10
20-Nov-07	14	9.4	16	10	20	14	20	14
21-Nov-07	0	0	26	18	20	14	20	12
22-Nov-07	1.4	1	24	18	20	10	20	10
23-Nov-07	0	0	30	20	20	10	20	10
24-Nov-07	11	10.8	36	30	22	20	22	20
25-Nov-07	0	0	42	32	26	20	26	20
26-Nov-07	1.4	1.2	22	10	20	12	20	12
27-Nov-07	7.6	3.4	28	18	22	10	22	12
28-Nov-07	0	0	26	18	16	12	16	12
29-Nov-07	0	0	28	22	20	6	18	10
30-Nov-07	0	0	22	18	18	10	16	10
1-Dec-07	0	0	40	38	28	24	28	20
2-Dec-07	0	0	54	36	30	26	30	24
3-Dec-07	0	0	66	50	30	22	30	22

4-Dec-07	120	22.8	26	24	20	18	20	18
5-Dec-07	23.4	14.6	10	8	18	12	18	12
6-Dec-07	16.8	10.8	14	10	20	12	20	10
7-Dec-07	12	8.6	30	24	26	18	26	18
8-Dec-07	47.6	19.4	18	10	12	8	12	8
9-Dec-07	105.8	38.2	18	10	12	8	12	8
10-Dec-07	105.4	77	20	18	22	20	22	20
11-Dec-07	2.4	1.2	28	18	22	20	22	20
12-Dec-07	0	0	36	30	24	18	24	17
13-Dec-07	10	5.6	18	16	12	10	12	10
14-Dec-07	13.2	10.4	12	8	18	16	20	18
15-Dec-07	3	1.4	14	12	18	16	18	16
16-Dec-07	55	17	18	14	20	16	20	16
17-Dec-07	4.8	2.2	2	2	12	10	12	10
18-Dec-07	9.2	8.8	4	2	12	10	12	10
19-Dec-07	5.6	3.4	8	6	18	16	18	16
20-Dec-07	0	0	12	8	16	10	16	10
21-Dec-07	8	7.6	24	14	20	12	20	12
22-Dec-07	1.4	1	24	22	20	18	20	18
23-Dec-07	0	0	18	12	18	12	18	12
24-Dec-07	0	0	20	18	16	12	16	12
25-Dec-07	0	0	30	20	20	18	20	18
26-Dec-07	0	0	26	22	20	16	20	14
27-Dec-07	0	0	30	28	22	20	22	20
28-Dec-07	0	0	24	22	20	18	20	18
29-Dec-07	0	0	16	10	12	8	12	8
30-Dec-07	0	0	14	12	12	10	12	10
31-Dec-07	0	0	22	20	20	14	22	14

## REFERENCES

- Agus, S.S., Leong, E.C. and Rahardjo, H. (2001). Soil-Water Characteristic Curves of Singapore Residual Soils. *Journal of Geotechnical and Geological Engineering*. 19: 285-309.
- Aitchison, G.D. (1961). Relationships of Moisture Stress and Effective Stress Functions in Unsaturated Soils. *Pore Pressure and Suction in Soils Conference*. London, England: 47-52.
- Ayalew, L. (1999). The Effect of Seasonal Rainfall on Landslides in the Highlands of Ethiopia. *Bulletin of Eng. Geology and the Environment*: 58: 9 - 19.
- Babu, G.L.S. and Murthy, D.S.N. (2005). Reliability Analysis of Unsaturated Soil Slopes. *Journal of Geotechnical and Geoenvironmental Engineering, ASCE*. 131(11): 1423-1428.
- Bao, C.G., Gong, B. and Zhan, L. (1998). Properties of Unsaturated Soils and Slope Stability of Expansive Soil. Keynote Lecture, *2nd Int. Conf. on Unsaturated Soils*. Beijing, China.
- Bishop, A.W. (1955). The Use of the Slip Circle in the Stability Analyses of slopes. *Geotechnique*. 5: 7-17.
- Bishop, A.W. (1959). *The Principle of Effective Stress*. Norwegian Geotechnical Institute. Oslo, Norway.
- Bouwer, H. (1966). Rapid Field Measurement of Air Entry Value and Hydraulic Conductivity of Soil as Significant Parameters in Flow System Analysis. *Water Resources Research*. 2(4): 729-738.
- Brand, E. W. (1984). Landslides in South Asia: A State-of-Art Report. *Proceedings, 4th Int. Symp. on Landslides*. 1: 17-59.
- Brisson, P., Garga, V.K. and Vanapalli, S.K. (2002) Determination of Unsaturated Flow Characteristics of Nickel Mine Tailings. *55th Canadian Geotechnical Conference*, Niagara, Canada, October 2002.

- Cai, F. and Ugai, K. (2004). Numerical Analysis of Rainfall Effects on Slope Stability. *International Journal of Geomechanics, ASCE*. 4(2): 69-78.
- Chapuis, R.P., Chenaf, D., Bussiere, B, Aubertin, M. and Crespo, R. (2001). A User's Approach to Assess Numerical Codes for Saturated and Unsaturated Seepage Conditions. *Canadian Geotechnical Journal*. 38: 1113-1126.
- Chen, H., Lee, C.F. and Law, K.T. (2004). Causative Mechanism of Rainfall-Induced Fill Slope Failures. *Journal of Geotechnical and Geoenvironmental Engineering, ASCE*. 130(6): 593-602.
- Chow, V.T., Maidment, D.R. and Mays, L.W. (1988). *Applied Hydrology*. New York: McGraw-Hill.
- Collins, B.D. and Znidarcic, D. (2004). Stability Analyses of Rainfall Induced Landslides. *Journal of Geotechnical and Geoenvironmental Engineering, ASCE*. 130 (4): 362\_372.
- Department of Drainage and Irrigation. (2001). *Urban Stormwater Management Manual for Malaysia (MASMA)*. Percetakan Nasional Berhad, Malaysia.
- Döll, P. (1997). Desiccation of Mineral Liners Below Landfills with Heat Generation. *Journal of Geotechnical and Geoenvironmental Engineering, ASCE*. 123(11): 1001–1009.
- Fourie, A.B. (1996). Predicting Rainfall-Induced Slope Instability. *Proc. Inst. Civil Eng. Geotech. Eng.* 119 (4): 211-218
- Fredlund, D. G., Morgenstern, N. R., and Widger, R. A. (1978). The Shear Strength of Unsaturated Soil. *Canadian Geotechnical Journal*. 15: 313–321.
- Fredlund, D. G., Ng, C. W. W., Rahardjo, H. and Leong, E. C. (2001). Unsaturated Soil Mechanics: Who Needs It? *Geotech. News, December*. GeoSpec., Bi-Tech Publishing. Vancouver, B.C., Canada: 43–45.
- Fredlund, D.G. and Rahardjo, H. (1993). *Soil Mechanics for Unsaturated Soils*. New York: John Wiley & Sons, Inc.
- Fredlund, D. G. and Xing, A. (1994). Equations for the Soil-Water Characteristic Curve. *Canadian Geotechnical Journal*. 31: 521–532.

- Fredlund, D.G., Xing, A. and Huang, S. (1994). Predicting the Permeability Function for Unsaturated Soils Using the Soil-Water Character Curve. *Canadian Geotechnical Journal*. 31(3): 533-546
- Freeze, R. A. and Cherry, J. A. (1979). *Groundwater*. New York: Prentice-Hall, Inc.
- Gasmo, J. M., Rahardjo, H., and Leong, E. C. (2000). Infiltration Effects on Stability of a Residual Soil Slope. *Computer Geotechnique*. 26: 145–165.
- GCO (1984). *Geotechnical Manual for Slopes. (2nd Ed.)*. Geotechnical Control Office, Hong Kong.
- Geiger, S.L., and Durnford, D.S. (2000). Infiltration in Homogeneous Sands and a Mechanistic Model of Unstable Flow. *Soil Science Society of America Journal*. 64: 460-469.
- GEO-SLOPE International Ltd. (2004a). *Stability Modeling with SLOPE/W*. Calgary, Alta., Canada.
- GEO-SLOPE International Ltd. (2004b). *Seepage Modeling with SEEP/W*. Calgary, Alta., Canada.
- Gitirana, G.Jr. and Fredlund, D.G. (2004). Soil-Water Characteristic Curve Equation with Independent Properties. *Journal of Geotechnical and Geoenvironmental Engineering, ASCE*. 130(2): 209-212.
- Gitirana, G. Jr., Fredlund, M.D. and Fredlund, D.G. (2005). Infiltration-Runoff Boundary Conditions in Seepage Analysis. *58th Canadian Geotechnical Conference and 6th Joint IAH-CGS Conference*, 19-21 September, 2005, Saskatoon, SK, Canada
- Glass, R.J., Steenhuis, T.S., and Parlange, J.Y. (1989). Wetting Front Instability, Experimental Determination of Relationships between System Parameters and Two Dimensional Unstable Flow Field Behavior in Initially Dry Porous Media. *Water Resource Research*. 25: 1195-1207.
- Gofar, N., Lee, M.L. and Kassim, A. (2007) Stability of Unsaturated Slopes Subjected to Rainfall Infiltration. *Proceedings of the Fourth International Conference on Disaster Prevention and Rehabilitation*, Semarang 10-11 September 2007: 158-167.

- Gofar, N., Lee, M.L. and Kassim, A. (2006a). Effect of Surface Boundary Condition on Rainfall Infiltration. *Journal Teknologi*. 44.
- Gofar, N., Lee, M.L. and Marwan, A. (2006b). Transient Seepage and Slope Stability Analysis for Rainfall-Induced Landslide: A Case Study. *Malaysian Journal of Civil Engineering*. 18(1): 1-13.
- Green, W.H. and Ampt, G.A.. (1911). Studies on Soil Physics I. The Flow of Air and Water through Soils. *Journal of Agricultural Research*. 4: 1-24.
- Gribb, M.M., Kodesova, R. and Ordway, S.E. (2004). Comparison of Soil Hydraulic Property Measurement Methods. *Journal of Geotechnical and Geoenvironmental Engineering, ASCE*. 130(10): 1084-1095.
- Gue, S.S. and Tan, Y.C. (2002). Mitigating the Risk of Landslide on Hill-Site Development in Malaysia. *2nd World Engineering Congress*. 22-25 July. Sarawak, Malaysia: 1-10.
- Gumbel, E. J. (1958). *Statistics of Extremes*. New York: Columbia University Press.
- Han, K.K., Rahardjo, H. and Broms, B.B. (1995). Effect of Hysteresis on the Shear-Strength of a Residual Soil, Unsaturated Soils. *Proc. 1st Int. Conf. on Unsaturated Soils (UNSAT 95)*. Paris, France: 499-504.
- Hazen, A. (1914). Storage to be Provided in Impounding Reservoirs for Municipal Water Supply. *Trans. ASCE*. 77: 1539–1640.
- Hincapié, I., Fässler, J., Vogt, P. and Germann, P. (2007). Rivulet Approach to Preferential Infiltration in a Soil Column. *Geophysical Research*. 9: 1539-1547.
- Horton, R.E. (1933). The role of infiltration in the hydrological cycle. *Trans. American Geophys. Union*. 14: 446-460.
- Janbu, N. (1954). Application of Composite Slip Surface for Stability Analysis. *European Conference on Stability Analysis*, Stockholm, Sweden.
- Jason, B.B. and Joel, C.R. (2004). Effect of Grasses on Herbicide Fate in the Soil Column: Infiltration of Runoff, Movement, and Degradation. *Environmental toxicology and chemistry*. 23(9): 2251-2258.

- Jenkinson, A. F. (1955). The Frequency Distribution of the Annual Maximum (or Minimum) Value of Meteorological Elements. *Q. J. Royal Meteorol. Soc.* 81: 158-171.
- Jennings, J.E. (1961). A Revised Effective Stress Law for Use in the Prediction of the Behavior of Unsaturated soils. *Pore Pressure and Suction in Soils Conference*. London, England: 26-30.
- Jennings, J.E. and Burland, J.B. (1962). Limitations to the Use of Effective Stresses in Partly Saturated Soils. *Géotechnique*. 12(2): 125-144.
- Joel, A., Messing, I., Seguel, O., and Casanova, M. (2002). Measurement of surface water runoff from plots of two different sizes. *Hydrological Processes*. 16(7): 1467-1478.
- Jury, W.A., Wang, Z. and Tuli, A. (2003). A Conceptual Model of Unstable Flow in Unsaturated Soil during Redistribution. *Vadose Zone Journal*. 2: 61-67.
- Kasim, F., Fredlund, D. G., and Gan, J. K. M. (1998). Effect of Steady State Rainfall on Long Term Matric Suction Conditions in Slopes. *Proceedings, 2nd Int. Conf. on Unsaturated Soils*. Beijing, China: 78-83.
- Kasim, F. (1998) Soil-Water Characteristic Curve and Seepage Flow in Unsaturated Soils. *Jurnal Teknologi*, 30(B): 69-86.
- Kim, J., Park, S. and Jeong, S. (2006). Effect of Wetting Front Suction Loss on Stability of Unsaturated Soil Slopes. *Unsaturated Soils, Seepage, and Environmental Geotechnics, ASCE*. 148: 70-77.
- Klemeš, V. (2000). Tall Tales about Tails of Hydrological Distributions. *J. Hydrol. Engineering*. 5(3): 227--239.
- Kwok, S.Y.F. and Tung, Y.K. (2003). Uncertainty and Sensitivity Analysis of Coupled Surface and Subsurface Flows. *Groundwater Quality Modeling and Management, ASCE*: 58-71.
- Lam, C.C. and Leung, Y.K. (1995) Extreme Rainfall Statistics and Design Rainstorm Profiles at Selected Locations in Hong Kong. *Technical Note No. 86. Royal Observatory*. Hong Kong.

- Lam, L., Fredlund D.G. and Barbour S.L. (1987). Transient Seepage Model for Saturated-Unsaturated Soil Systems: A Geotechnical Engineering Approach, *Canadian Geotechnical Journal*. 24: 565-580.
- Lee, M.L., Gofar, N., Kassim, A. and Noraieni, M. (2006). Effect of Vegetation Cover on Suction Variation and Slope Stability. *National Seminar on Civil Engineering Research (SEPKA)*. 19-20 December. Skudai, Malaysia.
- Leong, E.C. and Rahardjo, H. (1997). Permeability Functions for Unsaturated Soils. *Journal of Geotechnical and Geoenvironmental Engineering, ASCE*. 123(12): 1118-1126.
- Li, A.G., Tham, L.G., Yue, G.Q., Lee, C.F. and Law, K.T. (2005). Comparison of Field and Laboratory Soil-Water Characteristic Curves. *Journal of Geotechnical and Geoenvironmental Engineering, ASCE*. 131(9): 1176-1180.
- Li, C. and Young, M.H. (2006). Green-Ampt Infiltration Model for Sloping Surfaces. *Water Resources Research*. 42(7): W07420.
- Liew, S.S. (2005). Soil Nailing for Slope Strengthening. *Seminar on Geotechnical Engineering*. The Institution of Engineers, Malaysia. Penang, Malaysia.
- Lim, T.T., Rahardjo, H., Chang, M.F. and Fredlund, D.G. (1996) Effect of Rainfall on Matric Suctions in a Residual Soil Slope. *Canadian Geotechnical Journal*. 33(4): 618 – 628.
- Liu, Y., Bierck, B.R., Selker, J.S., Steenhuis, T.S. and Parlange, J.Y. (1993). High Density X-Ray and Tensiometer Measurements in Rapidly Changing Preferential Flow Fields. *Soil Science Society of America Journal*. 57: 1188-1192.
- Loáiciga, H.A. and Huang, A. (2007). Ponding Analysis with Green-and-Ampt Infiltration. *Journal of Hydrologic Engineering, ASCE*. 12(1): 109-112.
- Lumb, P. B. (1962). The Properties of Decomposed Granite: *Geo- technique*. 12: 226-243.
- Lumb, P. B. (1975) Slope Failures in Hong Kong. *Journal of Engineering Geology*. 8: 31–65.

- Mein, R.G. and Farrell, D.A. (1974). Determination of Wetting front Suction in the Green-Ampt Equation. *Soil Science Society of America, Proceeding*. 38: 872-876.
- Mein, R.G. and Larson, C.L. (1973). Modeling Infiltration during a Steady Rain. *Water Resources Research*. 9(2): 384-394.
- Morgenstern, N. R. and Price, V. E. (1965). The Analysis of the Stability of General Slip Surfaces. *Geotechnique*. 15(1): 79-93.
- Morgenstern, N.R. (1992). The Evaluation of Slope Stability – A 25 Year Perspective. *Proc. Stability and Performance of Slopes and Embankments – II*. Berkeley, California: 1-26.
- Nahlawi, H., Bouazza, A. and Kodikara, J. (2007). Surface Water Infiltration in a 1-Dimensional Soil-Geotextile Column. *Proceedings of the 10th Australia New Zealand Conference on Geomechanics, Brisbane*. 21-24 October 2007, Brisbane, Australia. 1: 368-373.
- Neuman, S.P. (1976). Wetting Front Pressure Head in the Infiltration Model of Green and Ampt. *Water Resources Research*. 12(3): 564-566.
- Ng, C. W. W., Chen, S. Y., and Pang, Y. W. (1999). Parametric Study of the Effects of Rain Infiltration on Unsaturated Slopes. *Rock Soil Mechanics*. 20(1): 1–14.
- Ng, C. W. W. and Pang, Y. W. (2000). Influence of Stress State on Soil Water Characteristics and Slope Stability. *Journal of Geotechnical and Geoenvironmental Engineering, ASCE*. 126(6): 157-166.
- Ng, C. W. W. and Shi, Q. (1998). A Numerical Investigation of the Stability of Unsaturated Soil Slopes Subjected to Transient Seepage. *Comput. Geotech.* 22(1): 1–28.
- Ng, C.W.W., Wang, B. and Tung, Y.K. (2001) Three-Dimensional Numerical Investigation of Groundwater Responses in an Unsaturated Slope Subjected to Various Rainfall Patterns. *Canadian Geotechnical Journal*. 38:1049–1062
- Ng, C.W.W., Zhan, L.T., Bao, C.G., Fredlund, D.G., and Gong, B.W. (2003). Performance of Unsaturated Expansive Soil Slope Subjected to Artificial Rainfall Infiltration. *Géotechnique*. 53(2): 143–157.

- Pradel, D. and Raad, G. (1993). Effect of Permeability on Surficial Stability of Homogeneous Slopes. *Journal of Geotechnical Engineering, ASCE*. 119(2): 315-332.
- Rahardjo, H. and Han, K. K. (1995). Shear Strength of Unsaturated Soils as it Applies to Slope Stability Analysis. *Symposium on Unsaturated Soil Behaviour and Applications*, Nairobi Kenya. 1-31.
- Rahardjo, H., Lee T.T., Leong E. C., and Rezaur R.B. (2004). A Flume for Assessing Flux Boundary Characteristics in Rainfall-Induced Slope Failure Studies. *Geotechnical Testing Journal*. 27(2): 145-153.
- Rahardjo, H., Li X. W., Toll D. G. and Leong E. C. (2001). The Effect of Antecedent Rainfall on Slope Stability. *Journal of Geotechnical and Geological Engineering*. Netherlands. 19: 371-399.
- Roslan, Z. A., Mohd, S. H. (2005). *ROSE Index for Forecasting Landslide Tragedy*. NASEC, UiTM.
- Rousseau, M., Pietro, L.D., Angulo, J.R., Tessier, D. and Cabibel, B. (2004). Preferential Transport of Soil Colloidal Particles Physicochemical Effects on Particle Mobilization. *Vadose Zone Journal*. 3:247-261.
- Stormont, J.C. and Anderson, C.E. (1999) Capillary barrier effect from underlying coarser soil layer. *Journal of Geotechnical and Geoenvironmental Engineering*. 125(8): 641-648.
- Sung, E.C. and Seung, R.L. (2002). Evaluation of Surficial Stability for Homogeneous Slopes Considering Rainfall Characteristics. *Journal of Geotechnical and Geoenvironmental Engineering, ASCE*. 128(9): 756-763.
- Tami, D., Rahardjo, H. and Leong, E.C. (2004). Effects of Hysteresis on Steady-State Infiltration in Unsaturated Slopes. *Journal of Geotechnical and Geoenvironmental Engineering, ASCE*. 130(9): 956-967.
- Terzaghi, K. (1936). The Shear Resistance of Saturated Soils. *Proceedings, 1st International Conference of Soil Mech. Found. Eng.* Cambridge. 1: 54-56

- Terzaghi, K. (1943). *Theoretical Soil Mechanics*. New York: John Wiley & Sons, Inc.
- Toll, D.G., Rahardjo, H. and Leong, E.C. (1999). Landslides in Singapore. *Proc. 2nd International Conference on Landslides, Slope Stability and the Safety of Infra-Structures*. Singapore: 269-276.
- Totoev, Y. Z. and Kleeman, P. W. (1998). An infiltration model to predict suction changes in the soil profile. *Water Resources Research*. 34(7): 1617–1622.
- Trinh, M.T., Rahardjo, H. and Leong, E.C. (2006). Shear Strength and Pore-Water Pressure Characteristics during Constant Water Content Triaxial Tests. *Journal of Geotechnical and Geoenvironmental Engineering, ASCE*. 132(3): 411-419.
- Tsaparas I., Rahardjo, H., Toll D.G. and Leong E.C. (2002). Controlling Parameters for Rainfall-Induced Landslides. *Comput. and Geotech*. 29: 1-27.
- Van Genuchten, M.T. (1980). A closed-form equation for predicting the hydraulic conductivity of unsaturated soils. *Soil Science Society of America Journal*. 44: 892–898.
- Wan, M. and Ruslan, R. (2002). Modeling Landslide using GIS and RS: A case of upper stream of Langat River Basin. *Proceedings, International Conference on Environmental Management: 10 years after Rio*. 22-23 October. Bangi, Malaysia.
- Wang, Z., Tuli, A. and Jury, W.A. (2003). Unstable Flow during Redistribution in Homogeneous Soil. *Vadose Zone Journal*. 2: 52-60.
- Yang, H., Rahardjo, H. and Leong, E.C. (2006). Behavior of Unsaturated Layered Soil Columns during Infiltration. *Journal of Hydrologic Engineering, ASCE*. 11(4): 329-337.
- Yang, H., Rahardjo, H., Wibawa, B. and Leong, E.C. (2004b). A Soil Column Apparatus for Laboratory Infiltration Study. *Geotechnical Testing Journal, ASTM*. 27(4): 1-9.
- Youngs, E.G. (1958). Redistribution of Moisture in Porous Materials after Infiltration. *Soil Science*. 86: 117-125.

- Zêzere, J.L., Trigo, R.M., Trigo, I.F. (2005). Shallow and Deep Landslides Induced by Rainfall in the Lisbon Region (Portugal): Assesement of Relationships with the North Atlantic Oscillation. *Natural Hazards and Earth System Sciences*. 5: 331-344.
- Zhan, T.L.T. and Ng, C.W.W. (2004). Analytical Analysis of Rainfall Infiltration Mechanism in Unsaturated Soils. *International Journal of Geomechanics, ASCE*. 4(4): 273-284
- Zhang, Z., Tao, M. and Morvant, M. (2005). Cohesive Slope Surface Failure and Evaluation. *Journal of Geotechnical and Geoenvironmental Engineering, ASCE*. 131(7): 898-906.
- Zhang, L. L., Fredlund, D. G., Zhang, L. M. and Tang, W. H. (2004). Numerical Study of Soil Conditions under which Matric Suction can be Maintained. *Canadian Geotechnical Journal*. 41(4): 569-582.
- Zhou, J. and Yu, J.L. (2005). Influences Affecting the Soil-Water Characteristic Curve. *Journal of Zhejiang University Science*. 6A(8): 797-804.

## LIST OF RELATED PUBLICATIONS

### *International Refereed Journals*

- i. Gofar, N. and Lee, M.L.. (2008). Extreme Rainfall Characteristics for Surface Slope Stability in the Malaysian Peninsular. *Journal of Assessment and Management of Risk for Engineered Systems and Geohazards (Georisk)*, Taylor and Francis. 2(2): 65-78. doi: [10.1080/1799510802072991](https://doi.org/10.1080/1799510802072991)
- ii. Gofar, N., Lee, M.L. and Kassim, A. (2008) Response of Suction Distribution to Rainfall Infiltration in Soil Slope. *Electronic Journal of Geotechnical Engineering, EJGE*. 13 (E):1 – 13
- iii. Kassim, A., Gofar, N. and Lee, M.L. (2008) Numerical Simulation of Infiltration through Unsaturated Soil Column. *Malaysian Journal of Civil Engineering* 20(2)211-222, Published by Universiti Teknologi Malaysia
- iv. Gofar, N. and Lee, M.L. (2008) PERISI : A Computer Program for Preliminary Evaluation of Rainfall-Induced Slope Instability. (Short Note) *Malaysian Journal of Civil Engineering* 21(2), Published by Universiti Teknologi Malaysia

### *International Conferences*

- i. Gofar, N., Lee, M.L. and Kassim, A. (2007). Stability of Unsaturated Slopes Subjected to Rainfall Infiltration. *Proceeding, The 4<sup>th</sup> International Conference on Disaster Prevention and Rehabilitation*. 10-11 September 2007, Diponegoro University, Semarang, Central Java, Indonesia. 158-167.
- ii. Gofar, N., Lee, M.L. and Kassim, A. (2008). Instrumented Soil Column Model for Rainfall Infiltration Study. *Proceeding, International Conference on Geotechnical and Highway Engineering (GEOTROPIKA 2008)*. 26-27 May 2008, Kuala Lumpur.
- iii. Kassim, A., Gofar, N., and Lee, M.L. (2008). Laboratory Model for Rainfall Infiltration in Layered Soil Slope. *Proceeding, International Conference on Geotechnical and Highway Engineering (GEOTROPIKA 2008)*. 26-27 May 2008, Kuala Lumpur.
- iv. Gofar, N., and Lee, M.L. (2009) Integration of Extreme Rainfall in the Evaluation of Slope Stability. *Proceedings of the 12<sup>th</sup> ISGE Annual Science Meeting*, Bandung, Indonesia. 18-19 November 2008.

- v. Gofar, N., Lee, M.L, and Kassim, A. (2009) Extreme Rainfall Analysis for Slope Stability Evaluation. Paper Presented at International Symposium on Prediction and Simulation Methods for Geohazard Mitigation, IS Kyoto, 25-27 May Gofar, N, Kyoto, Japan